E&G

Quaternary Science Journal

Eiszeitalter und Gegenwart

DEUQUA
DEUTSCHE QUARTÄRVEREINIGUNG

DEUQUA 2016 – TRANSITIONS IN THE QUATERNARY

Guest editors Daniel Wolf and Michael Zech

E&G Quaternary Science Journal

Copernicus Publications
The Innovative Open Access Publisher

Editorial

Margot Böse

Institut für Geographische Wissenschaften, Freie Universität Berlin, Berlin, Germany

Correspondence: Margot Böse (m.boese@fu-berlin.de)

Starting with Issue 2 of Volume 66, *E&G Quaternary Science Journal* will be handled by Copernicus Publications, the renowned open-access publishing house from Göttingen (Germany). This change became necessary because the owner of Geozon Science Media, with whom this journal was successfully transferred into a modern open-access publication, had to resign for private reasons. We thank Geozon Science Media for the cooperation during the last 8 years – a very important time in the transformation process of *E&G Quaternary Science Journal*. Now we look forward to a prosperous collaboration with Copernicus Publications. This new publisher is a pioneer with regard to open access, which is now increasingly encouraged and fostered by public bodies such as the German Science Formation (DFG) and the European Commission. Therefore, the strict open-access philosophy of Copernicus Publications matches perfectly the request of the German Quaternary Association DEUQUA. We will continue to support this policy that we adopted almost a decade ago and further develop the journal in this respect. DEUQUA is a non-profit organisation without any commercial interests; our aim is to assist and support authors in publishing their results of relevant Quaternary research under the best conditions and to promote Quaternary sciences in general.

Copernicus Publications will provide modern online applications that are easier to use and efficient for authors, reviewers, and editors alike. While we intend to promote the journal internationally, with a focus on, but not limited to, central Europe, the option to publish papers in the German language will remain. Indexing through different journal index databases has been initiated. As previously, authors will retain the copyright of their publications, there will be no charge for inclusion of colour figures, and all articles will be made freely accessible via the Internet. Additionally, from now on an English language correction service will be available, and the possibility to link articles with data on public disciplinary or institutional repositories will be established.

All papers will be published article by article after the peer-review process and final acceptance by the editor. DEUQUA members and subscribers will continue to receive a printed version of each journal issue if they wish to do so, and the editorial board will ensure that the journal's layout remains at the high standard achieved during the last decade. Besides scientific papers, express reports and thesis abstracts of recently published doctoral theses will also be included in *E&G Quaternary Science Journal*. DEUQUA field trip guides will be published as special issues.

The continued success of the journal is dependent on our members. Therefore, we hope that you will help us promote the journal, and we invite Quaternary scientists to submit manuscripts to *E&G Quaternary Science Journal*.

^{10}Be depth profiles in glacial sediments on the Swiss Plateau: deposition age, denudation and (pseudo-) inheritance

Lorenz Wüthrich[1,2,3], **Claudio Brändli**[3], **Régis Braucher**[4], **Heinz Veit**[1], **Negar Haghipour**[3], **Carla Terrizzano**[1,2,3], **Marcus Christl**[5], **Christian Gnägi**[1], **and Roland Zech**[1,2,3]

[1]Geographical Institute, University of Bern, 3012 Bern, Switzerland
[2]Oeschger Centre for Climate Change Research, University of Bern, 3012 Bern, Switzerland
[3]Geological Institute, ETH Zurich, 8093 Zurich, Switzerland
[4]Aix-Marseille Université, CNRS–IRD–Collège de France, UMR 34 CEREGE, Technopôle de l'Environnement
Arbois–Méditerranée, BP80, 13545 Aix-en-Provence, France
[5]Laboratory of Ion Beam Physics, ETH Zurich, 8092 Zurich, Switzerland

Correspondence: Lorenz Wüthrich (loeru@live.com)

Abstract: During the Pleistocene, glaciers advanced repeatedly from the Alps onto the Swiss Plateau. Numeric age control for the last glaciation is good and thus the area is well suited to test a method which has so far not been applied to till in Switzerland. In this study, we apply in situ produced cosmogenic ^{10}Be depth profile dating to several till deposits. Three sites lie inside the assumed Last Glacial Maximum (LGM) extent of the Rhône and Aare glaciers (Bern, Deisswil, Steinhof) and two lie outside (Niederbuchsiten, St. Urban). All sites are strongly affected by denudation, and all sites have reached steady state, i.e., the ^{10}Be production is in equilibrium with radioactive decay and denudational losses. Deposition ages can therefore not be well constrained. Assuming constant denudation rates of $5\,\mathrm{cm\,kyr^{-1}}$, total denudation on the order of $100\,\mathrm{cm}$ for sites within the extent of the LGM and up to tens of meters for older moraines are calculated. Denudation events, for example related to periglacial conditions during the LGM, mitigate the need to invoke such massive denudation and could help to explain high ^{10}Be concentrations at great depths, which we here dub "pseudo-inheritance". This term should be used to distinguish conceptually from "true inheritance", i.e., high concentrations derived from the catchment.

Kurzfassung: Die Alpengletscher stiessen während des Pleistozäns wiederholt in das Schweizer Mittelland vor. Da die Vergletscherungsgeschichte des Mittellandes relativ gut untersucht ist, ist die Region gut geeignet um eine Methode zu testen, welche bisher noch nicht an Grundmoränen in der Schweiz angewandt wurde. Für die vorliegende Studie erstellten wir ^{10}Be Tiefenprofile für verschiedene Moränenstandorte im Schweizer Mittelland. Drei der Standorte liegen innerhalb der vermuteten LGM (Letztes Glaziales Maximum) Ausdehnung des Rhone und Aare Gletschers (Bern, Deisswil, Steinhof), zwei ausserhalb (Niederbuchsiten, St. Urban). Sämtliche Profile sind stark durch Denudation beeinflusst und alle Standorte, ausser Bern, sind im Gleichgewicht, das heisst die ^{10}Be Produktion entspricht

dem radioaktiven Zerfall und Verlust durch Denudation. Exakte Depositionsalter können deshalb nicht bestimmt werden. Konstante Denudationsraten können auf ca. 5 cm kyr^{-1} geschätzt werden. Dies ergibt eine totale Denudation von ungefähr 100 cm für die LGM Profile und mehrere Meter bis Dekameter für die älteren Profile. Denudationsereignisse, hingegen, zum Beispiel in Zusammenhang mit periglazialen Bedingungen während des LGMs, erklären niedrige Oberflächenkonzentrationen auf alten Standorten und hohe ^{10}Be Konzentrationen in der Tiefe. In diesem Zusammenhang schlagen wir den Begriff "Pseudo Inheritance" vor, um konzeptionell von "Wahrer Inheritance" zu unterscheiden, welche der Präexposition im Einzugsgebiet geschuldet ist.

1 Introduction

In 1909, Albrecht Penck and Eduard Brückner published their famous and seminal three-volume work *Die Alpen im Eiszeitalter* (Penck and Brückner, 1909). They proposed four ice ages during the Quaternary: Würm, Riss, Mindel and Günz. Although mostly based on field work in the Bavarian and Austrian Alps, Penck and Brückner (1909) also applied their scheme to Switzerland. Apart from minor modifications (Eberl, 1930; Beck, 1933), the assumption that there were four glaciations in the Alps did not undergo big changes for decades. In the early 1980s, research based on palynology (Welten, 1982, 1988) and sedimentology (Schlüchter and Wolfarth-Meyer, 1986; Schlüchter, 1988, 1989b) led to a turnover of the four classical Quaternary ice ages. It was proposed that Alpine glaciers advanced at least 15 times onto the Swiss Plateau (Schlüchter, 2010; Preusser et al., 2011). New nomenclature was also introduced for the Swiss glaciations (Graf, 2009; Preusser et al., 2011; Keller and Krayss, 2011). Würm is now called Birrfeld Glaciation and encompasses marine isotope stages (MIS) 5d to 2, the penultimate glacial was renamed from Riss to Beringen and probably occurred during MIS 6 (Ivy-Ochs et al., 2006b; Graf et al., 2007, 2015), and the most extensive glaciation is now referred to as Möhlin Glaciation (> 300 ka; Graf, 2009; Preusser et al., 2011).

Since the 1960s Middle and Late Quaternary deposits of the Rhône and Aare glaciers (Fig. 1) have been investigated in several studies, focusing on glacial sediments and stratigraphy (Zimmermann, 1963), paleosols (Mailänder and Veit, 2001) and chronology (Ivy-Ochs et al., 2004; Preusser et al., 2007; Preusser, 2009). Although the extent of the Last Glacial Maximum (LGM) is controversial (Bitterli et al., 2011; Bläsi et al., 2015), the references cited above show that the chronology of the last glaciation in Switzerland is in general well established (Preusser et al., 2011). This makes the LGM deposits of the LGM Rhône and Aare glaciers suitable sites to test a method that has so far not been applied on till. In this study, we present one of the first applications of in situ produced ^{10}Be depth profile dating on moraines. In situ produced ^{10}Be is produced at the Earth surface by cosmic radiation, and production decreases exponentially with depth (Gosse and Phillips, 2001). Until now, depth profile dating

has mainly been applied to terraces and alluvial fans (Hidy et al., 2010; Rixhon et al., 2011; Haghipour et al., 2014; Akçar et al., 2014; Delmas et al., 2015; Ruszkiczay-Rüdiger et al., 2016; Claude et al., 2017; Schaller et al., 2009). In order to determine the deposition age of a moraine, one would generally sample large, stable erratic boulders for ^{10}Be surface exposure dating (Heyman et al., 2016). However, boulders on the Swiss Plateau are often either completely destroyed or at least affected by human influence (Akçar et al., 2011). Under such circumstances, depth profile dating might be a promising alternative. Apart from dating, ^{10}Be depth profiles also allow to quantify denudation and inheritance (Braucher et al., 2009; Siame et al., 2004). Our study specifically aims to

i. evaluate the potential of ^{10}Be depth profile dating of moraines,

ii. investigate denudation rates and total denudation, and

iii. quantify inheritance.

2 Material and methods

2.1 Sampling sites and sampling

The research area is situated in the western part of the Swiss Plateau, which lies south of the Jura Mountains, which are built of marine sediments deposited in a shallow shelf ocean of Triassic to Jurassic age (Pfiffner, 2009). The Swiss Plateau is mainly built of clastic sediments deriving from erosion of the Alps during the Cenozoic, called the molasse (Pfiffner, 2009). For the present study we sampled till, which overlays the molasse deposits. The sampling sites are located on lateral moraines (Bern), on the valley floor (Deisswil) or on the top of molasse hills (Steinhof, Niederbuchsiten, St. Urban). Five sites have been selected for depth profile dating (Figs. 1–3). The youngest site considered in the present study is Bern, deposited by the Aare glacier during its retreat (Wüthrich et al., 2017a), followed by Deisswil and Steinhof. Both lie inside the LGM extent of the Rhône Glacier according to Bini et al. (2009). Additionally, we sampled two more depth profiles from till deposits, which are attributed to older glaciations. They are at least 130 kyr old (Preusser et al., 2011; Bitterli et al., 2011) and are situated near Niederbuchsiten and
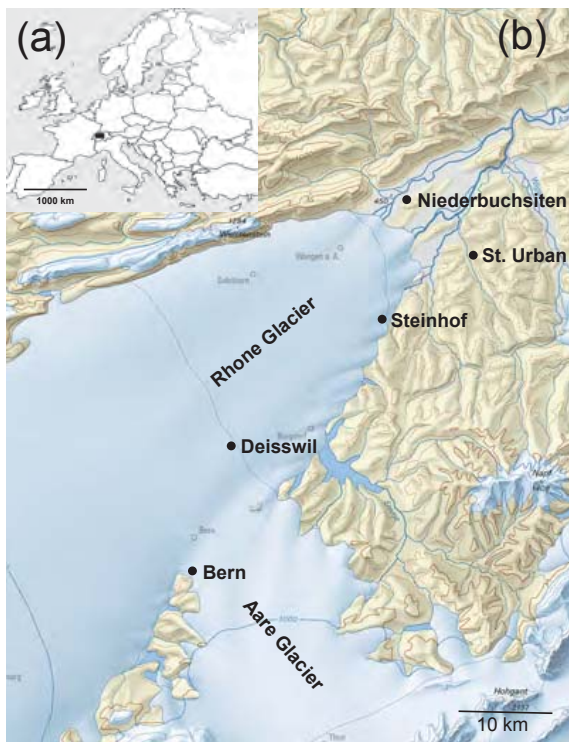
Figure 1. **(a)** Location of the research area in Europe. **(b)** LGM map of the research area modified after Bini et al. (2009). The black dots mark the sample locations (reproduced with permission of Swisstopo, BA15134). The equidistance of the contour lines is 200 m.

Figure 2. Digital elevation models for all sites (source: Federal Office of Topography).

St. Urban. Because of the human influence on the landscape, the selection of these sites was quite challenging. As the profiles in quarry pits are already exposed, they are basically perfect for the application of depth profiles. Unfortunately, an unknown amount of material is often pushed away. In the selected quarry pits, anthropogenic removal during work in the pit was estimated based on both conversations with workers and evidence in the field. Steinhof is the only site in the present work without a quarry pit. The depth profile in this location is rather important because boulders, only several hundred meters away from the sampling site, were dated by Ivy-Ochs et al. (2004). That is why we excavated a trench using a shovel and pickaxe.

2.1.1 Bern

The profile is located in a small quarry pit right on the top of a lateral moraine, which was deposited by the Aare Glacier along the eastern slopes of Gurten mountain. According to Wüthrich et al. (2017a), the glacier retreated 18 ka from this position. The uppermost 30 cm of the sampled profile is decalcified and consists of loamy sand and some coarser clasts. Below is an unweathered, compact till, composed of clasts of diverse lithologies from the catchment of the Aare Glacier. We collected three discrete sediment samples (B1 to B3) at depths of 10, 40 and 165 cm (Table 1).

2.1.2 Deisswil

Inside the extent of the LGM Rhône glacier, a gravel pit near Deisswil exposes several meters of fluvial and fluvioglacial sediments at the base and a 200 cm thick till above. The decalcification depth varies between 140 and 200 cm. Three discrete samples were collected at depths of 50, 80 and 200 cm (DW1 to 3), the lowest one being just below the local decalcification depth of 180 cm.

2.1.3 Steinhof

South of Steinhof, a 2 m deep trench was excavated close to the top of a molasse hill covered by till. According to Ivy-Ochs et al. (2004), who applied surface exposure dating on boulders at Steinhof, the Rhône Glacier reached the site during the global LGM and disappeared ∼ 24 ka. Seven discrete samples down to 190 cm were collected for the ^{10}Be depth profile (SH1 to SH7; Table 1). The sediment changes at 150 cm depth from a sandy loam with almost no pebbles, possibly a water lain till (Dreimanis, 1979), to a diamict (Flint et al., 1960a, b) with unknown thickness but at least 400 cm. The decalcification depth was reached in a drill core at 360 cm depth. The hiatus expressed in the sediments is also confirmed in the XRF data and the grain size analysis (L. Wüthrich, unpublished data).

Table 1. Locations and ^{10}Be concentrations of all samples. The steady-state denudation rate for each depth is used to find out whether the ^{10}Be concentration in the profile is in equilibrium.

Sample name	Altitude (m. a.s.l.)	Latitude (° N)	Longitude (° E)	Surface production rate (^{10}Be atoms a^{-1})	Sample depth (cm) [g cm^{-2}]	Quartz dissolved (g)	^{9}Be carrier added (mg)	^{10}Be / ^{9}Be (10^{-12})	Concentration (10^{4} ^{10}Be atoms g^{-1})	Steady state denudation for ∞ time (cm kyr^{-1})
B1 (Bern)	654	46.922	7.453	7.07	10 [22]	29.3	0.3	0.118 (±0.01)	8.11 (±0.67)	6.59
B2					40 [88]	23.3	0.56	0.033 (±0.006)	2.78 (±0.48)	13.98
B3					165 [363]	8.8	0.32	0.004 (±0.002)	1.01 (±0.46)	13.76
DW1 (Deisswil)	574	47.034	7.465	6.61	50 [110]	2.8	0.31	0.076 (±0.009)	6.21 (±0.78)	5.19
DW2					80 [176]	11.7	0.42	0.08 (±0.01)	4.32 (±0.55)	5.56
DW3					200 [440]	12.7	0.3	0.017 (±0.003)	2.67 (±0.50)	3.80
SH1 (Steinhof)	593	47.155	7.682	6.71	10 [22]	42	0.3	0.16 (±0.008)	7.69 (±0.39)	6.64
SH2					30 [66]	34.2	0.3	0.109 (±0.007)	6.33 (±0.39)	6.43
SH3					60 [132]	31.1	0.38	0.043 (±0.004)	3.53 (±0.34)	8.50
SH4					90 [198]	33.3	0.3	0.045 (±0.005)	2.67 (±0.27)	8.48
SH5					120 [264]	25.1	0.3	0.026 (±0.003)	2.09 (±0.23)	8.47
SH6					150 [330]	23.8	0.3	0.03 (±0.004)	2.51 (±0.30)	5.58
SH7					190 [418]	41.7	0.31	0.034 (±0.004)	1.71 (±0.19)	6.66
NB1 (Niederbuchsiten)	483	47.286	7.77	6.13	30 [66]	44.1	0.3	0.184 (±0.009)	8.27 (±0.41)	1.57
NB2					70 [154]	10.8	0.3	0.031 (±0.004)	5.79 (±0.66)	1.72
NB3					100 [220]	38.9	0.3	0.102 (±0.007)	5.21 (±0.34)	1.58
NB4					150 [330]	47.2	0.3	0.081 (±0.008)	3.44 (±0.32)	2.10
NB5					220 [484]	46.5	0.2	0.096 (±0.007)	2.82 (±0.21)	2.20
U1 (St. Urban)	540	47.21	7.855	6.43	27.5 [60]	35.5	0.35	0.225 (±0.038)	8.79 (±1.5)	4.54
U2					66 [145]	25.3	0.25	0.155 (±0.017)	12.31 (±1.41)	2.04
U3					160 [352]	33.3	0.29	0.168 (±0.017)	9.61 (±1.08)	1.01
U4					380 [836]	51	0.51	0.170 (±0.018)	6.48 (±0.72)	0.43

2.1.4 Niederbuchsiten

The sediment located on top of a molasse hill belongs to the penultimate glaciation (Bitterli et al., 2011) and is thus at least 130 kyr old. The 10 m thick till of the Rhône glacier overlies gravel with a thickness of several decameters. We collected five samples (NB1 to NB5) for depth profile dating from 30, 70, 100, 150 and 220 cm depth (Table 1). The uppermost 20 cm of the profile consists of silty sand. This cover bed may have been deposited during the Younger Dryas (Mailänder and Veit, 2001; Semmel and Terhorst, 2010). The decalcification depth is at 300 cm.

2.1.5 St. Urban

An active quarry near St. Urban exposes freshwater molasse (Gerber and Wanner, 1984) covered by 600 cm of completely decalcified till. The deposit lies outside the extent of the LGM boundaries (Bini et al., 2009) and is thus at least 130 kyr old. We collected four samples down to a depth of 380 cm (U1 to U4; Table 1). The uppermost sample from this site comes from the ∼ 60 cm thick silty top part of the profile. The sediment was probably deposited by the ancient Rhône Glacier.

2.2 Sample preparation and AMS analyses

The depth profile samples were dispersed in Calgon and sieved to 63 to 1000 μm. We followed standard lab procedures to obtain clean quartz and then extract the beryllium (Kohl and Nishiizumi, 1992). The ^{10}Be / ^{9}Be analyses were

conducted with the TANDY accelerator mass spectrometer (AMS) at the Laboratory of Ion Beam Physics, ETH Zurich. The measured ratios were normalized to the ETH Zurich in-house ^{10}Be / ^{9}Be standard S2007N with a nominal ratio of $28.10 \pm 0.76 \times 10^{-12}$ (Christl et al., 2013). Two blanks were processed together with the samples. They had ^{10}Be / ^{9}Be ratios of 0.006×10^{-12}, i.e., mostly more than 10 times smaller than the samples. The blank ratios were subtracted from the samples before calculating exposure and depth profile ages.

2.3 Depth profile calculations

Rock samples from the upper meters of Earth surface, bombarded by secondary particles originated from the cosmic rays, accumulate cosmogenic nuclide; as a result the concentration of these nuclides increase with altitude and latitude at a rate that depends on the local denudation rate. ^{10}Be is one of these in situ produced cosmogenic nuclides with a half-life of 1.387 Ma (Chmeleff et al., 2010; Korschinek et al., 2010). Its concentration reaches equilibrium as soon as the radioactive decay of ^{10}Be is equal to its production. ^{10}Be is produced by neutrogenic spallation and by muogenic interaction, mainly with oxygen (Gosse and Phillips, 2001; Heisinger et al., 2002a, b). In the last years, the application of ^{10}Be depth profiles has become an important method to date unconsolidated sediments (Hidy et al., 2010; Rixhon et al., 2011; Haghipour et al., 2014; Akçar et al., 2014; Delmas et al., 2015; Ruszkiczay-Rüdiger et al., 2016; Claude et al., 2017; Schaller et al., 2009). The advantage of this method is that it allows not only to calculate the age of the
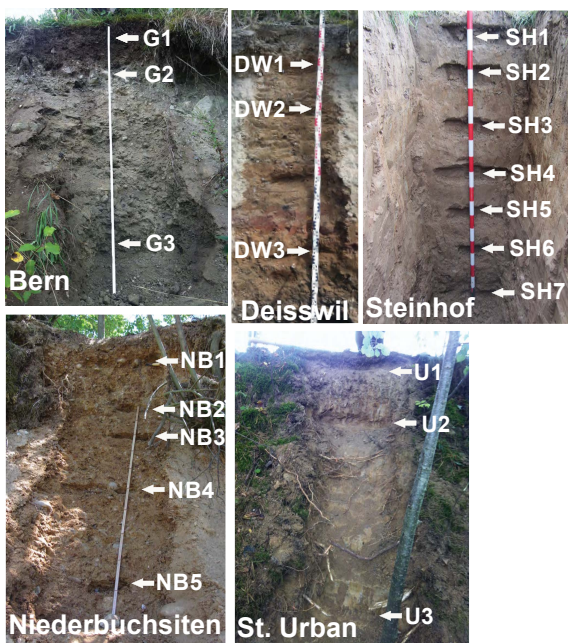
Figure 3. Photographs of the sampled profiles. U4 is not shown but is taken from the same sediment unit at 380 cm depth.

deposit but also denudation rate and the inherited share of ^{10}Be, accumulated in the catchment. As unconsolidated sediments are eroded much faster that boulders, equilibrium between production and decay is reached much faster. Because at the surface the production rate of ^{10}Be is dominated by neutrons and high, the equilibrium is reached quite quickly. Spallogenic production is exceeded by muogenic production at greater depths (Braucher et al., 2003) and it takes longer to reach steady state in deeper parts of the profile. To determine whether a depth profile has reached equilibrium, the time in Eq. (1) is set to infinity and the concentration at each depth is modeled as function of denudation rate:

$$C(z, \varepsilon, t) = \sum_i \frac{P(0)_t}{\frac{\varepsilon \cdot \rho_z}{\Lambda_i} + \lambda} \cdot e^{\left(-\frac{z \cdot \rho_z}{\Lambda_i}\right)} \cdot \left[1 - e^{\left(-t\left(\frac{\varepsilon \cdot \rho_z}{\Lambda_i} + \lambda\right)\right)} \right]$$
$$+ C_{\text{inh}} \cdot e^{-\lambda \cdot t}, \tag{1}$$

where C is concentration (atoms g^{-1}), z is depth (cm), t is time (years), ε is denudation rate (cm a^{-1}), C_{inh} is the inherited concentration (atoms g^{-1}), $P(0)_i$ is the site-specific production rate of ^{10}Be via production pathway i, ρ_z is the cumulative bulk density (g cm^{-3}) and Λ_i is the attenuation length of pathway i (g cm^{-2}). The attenuation length is the depth in a sediment with the density ρ_z at which the production rate is $1/e$, compared to the surface production rate. When modeled steady-state denudation rates increase with depth, equilibrium has not been reached yet. Decreasing denudation rates indicate inheritance and/or complex deposition histories (Delmas et al., 2015; Ruszkiczay-Rüdiger et al., 2016). Constant denudation rates with depth indicate that the

^{10}Be production rate has reached the equilibrium and one can only calculate the minimum deposition age T_{eff} (Lal, 1991), which is the time needed to reach equilibrium with the modeled denudation rate.

$$T_{\text{eff}} = \frac{1}{\lambda + \left(\frac{\rho}{\Lambda}\right) \cdot \varepsilon} \tag{2}$$

Λ is the attenuation length of neutrons (160 g cm^{-2}).

We also used the MATLAB code version 1.2, published by Hidy et al. (2010), to calculate deposition ages, i.e., the time when the glacier has left the area, denudation rates and inheritance for our sites. The code uses a Monte Carlo approach to find solutions for Eq. (1). Apart from the measured ^{10}Be concentrations at specific depths, critical input parameters are the allowed age range (time, t), ranges for denudation rate (cm a^{-1}) and inheritance (atoms g^{-1}), as well as a denudation threshold. We used a reference production rate for neutrogenic spallation of 3.93 atoms g^{-1} a^{-1} (Heyman, 2014) and the scaling model by Lal (1991) and Stone (2000) to calculate the production rate for each site. Because the standard files for calculating muogenic production rate after Heisinger et al. (2002a, b) yield too-high values (Braucher et al., 2003, 2011, 2013; Phillips et al., 2016), we used the .m files provided Ruszkiczay-Rüdiger et al. (2016). Calculations were done until 100 000 solutions were found. No corrections were applied for snow and vegetation cover and/or shielding. For density, the allowed range was between 2.1 and 2.3 g cm^{-3}, i.e., realistic values for till (Schlüchter, 1989a).

3 Results

3.1 Bern

^{10}Be concentrations of the three samples from the Bern decrease with depth and range from 8.1×10^4 atoms g^{-1} at 10 cm depth to 1.0×10^4 atoms g^{-1} at 165 cm depth (Fig. 4, Table 1). Because of the poor fit, no reliable results could be obtained with the Hidy et al. (2010) calculator and also T_{eff} could not be calculated.

3.2 Deisswil

In the Deisswil profile, ^{10}Be concentrations decrease with depth and range from 6.2×10^4 atoms g^{-1} at 50 cm depth to 2.7×10^4 atoms g^{-1} at 200 cm depth (Fig. 4, Table 1). The steady-state denudation rate between the first and second sample does not increase with depth. Between DW2 and DW3 it does. The results from the Monte Carlo simulation did not yield any useful results and are thus not used in the paper. Minimum age T_{eff} for the uppermost two samples is 14 kyr, and calculated steady-state denudation rate is 5.2 cm kyr^{-1} (Table 2).

Table 2. Minimum ages (T_{eff}) and steady-state denudation rates for the profiles, calculated using Excel and the results of the Monte Carlo approach.

Location	Excel solutions		MATLAB solutions			
	T_{eff} (kyr)	Denudation rate (cm kyr^{-1})	Age (kyr) [2σ lower–2σ upper]	Denudation (cm kyr^{-1}) [2σ lower–2σ upper]	Inheritance (10^4 atoms g^{-1}) [2σ lower–2σ upper]	Density (g cm^{-2}) [2σ lower–2σ upper]
Deisswil	14	5.2				
Steinhof	11	6.6	16.3 [12.4–478.7]	6.2 [1.9–6.9]	0 [0–0.9]	2.278 [2.1–2.3]
Niederbuchsiten	16	4.5	21.7 [29.3–975.6]	4.9 [3.7–6.3]	2.2 [1.3–2.9]	2.138 [2.1–2.3]
St. Urban			32.6 [26.6–912.3]	2.8 [1.5–5.7]	7.3 [5.4–7.3]	2.111 [2.1–2.3]
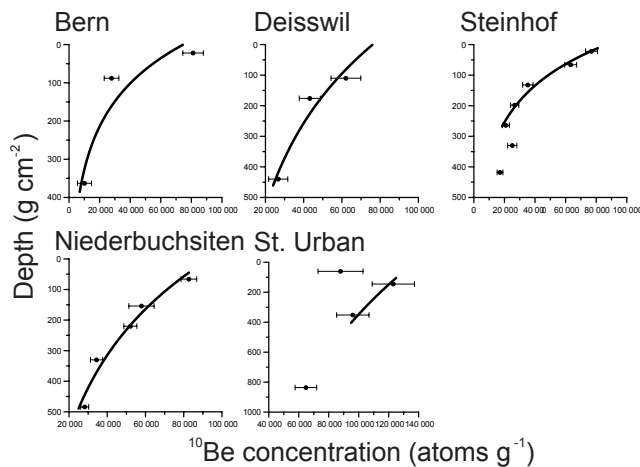
Figure 4. Measured depth profiles with error bars. The trend lines $y = a \cdot \ln(x) + b$, which calculate how the particles are attenuated are shown for the uppermost 200 cm (440 g cm^{-2}), where neutrogenic spallation is the dominant production pathway. The calculated attenuation lengths are 160 g cm^{-2} for Bern, 400 g cm^{-2} for Deisswil, 173 g cm^{-2} for Steinhof, 370 g cm^{-2} for Niederbuchsiten and 835 g cm^{-2} for St. Urban. Values exceeding 160 g cm^{-2} indicate denudational events and/or high denudation rates.

3.3   Steinhof

Concentrations decrease exponentially with depth and range from 7.7×10^4 atoms g^{-1} at 10 cm depth to 2.1×10^4 atoms g^{-1} at 120 cm depth (Fig. 4). The two lowermost samples (150 and 190 cm) have higher concentrations than expected from the exponential trend. Based on that and our sedimentological observations, we suspect that two phases of till deposition may have occurred and that the sediments below 150 cm may have experienced exposure predating the deposition of the uppermost 150 cm of the profile. The two lowermost samples were excluded from further calculations. The profile has reached steady state, with a T_{eff} of 11 kyr and a denudation rate of 6.6 cm kyr^{-1} (Table 2). The most probable Bayesian age, denudation rate and inheritance of the Monte Carlo simulation are 16.3 kyr, 6.2 cm kyr^{-1} and 0, respectively (Table 2).

3.4   Niederbuchsiten

^{10}Be concentrations in the profile near Niederbuchsiten decrease exponentially with depth and range from 8.3×10^4 atoms g^{-1} at 30 cm depth to 2.8×10^4 atoms g^{-1} at 220 cm depth (Fig. 4). The profile is in steady state with a T_{eff} and denudation rate of 16 kyr and 4.5 cm kyr^{-1} (Table 2). The Monte Carlo calculations yield 21.7 kyr, 4.9 cm kyr^{-1} and 2.2×10^4 atoms g^{-1} for age, denudation rate and inheritance, respectively (Table 2).

3.5   St. Urban

Concentrations decrease with depth and range from 12.3×10^4 atoms g^{-1} at 66 cm depth to 6.5×10^4 atoms g^{-1} at 380 cm depth (Fig. 4, Table 1). The uppermost sample from a depth of 27.5 cm has been excluded from the calculations due to its relatively low concentration of 8.8×10^4 atoms g^{-1}, which indicates that the uppermost 60 cm of the profile were deposited as loess cover long after deposition of the underlying till. The profile has reached equilibrium. In fact, steady-state denudations rates decrease with depth, indicating inheritance or a complex deposition history. We have not calculated T_{eff} because of the loess cover. The Monte Carlo calculations yield 32.6 kyr, 2.8 cm kyr^{-1} and 7.3×10^4 atoms g^{-1} for age, denudation rate and inheritance, respectively (Table 2).

4   Discussion

4.1   Ages in chronological context

The ^{10}Be concentrations in all profiles are much lower than what may be expected from the assumed deposition ages of the tills (~ 20 kyr and more). The uppermost samples for all profiles but St. Urban, for example, are within 10 to 50 cm from the surface but have less than 5×10^5 atoms g^{-1}. For comparison, ^{10}Be concentrations from boulder surfaces in that area with an age of ~ 20 kyr are 2 times higher (Ivy-Ochs et al., 2004). This indicates that denudation of the landform surface has led to substantial loss of surface sediments. Ignoring denudation in the depth profile calculations would

lead to an obvious, massive underestimation of the deposition ages. The low values for T_{eff} indicate that equilibrium was reached quite fast due to high denudation rates and/or denudation events.

The minimum deposition ages T_{eff} of 14, 11 and 16 kyr for Deisswil, Steinhof and Niederbuchsiten, respectively, do not provide useful age constraints and only point to high denudation. They do not even exceed the age of the Late Glacial readvances of the Gschnitz Stade in the Alps ~ 16 ka (Ivy-Ochs et al., 2006a; Reitner, 2007; Federici et al., 2012). It is important to emphasize that the ages in this study obtained from the Monte Carlo calculations should not be overinterpreted either: The age ranges are extremely large and, more importantly, all profiles have reached equilibrium. In that sense, no meaningful age can be inferred for any site. The fact that the concentrations in the profiles have reached equilibrium is graphically also illustrated in the denudation rate–age plots (Fig. 5), where the ages go towards infinity and are only restricted by our input parameters given for the Monte Carlo approach. Solutions are found for age ranges spanning several hundreds of thousands of years, and even the 100 best fits (blue dots in Fig. 5) scatter widely and cannot provide useful constraints for the deposition ages of the moraines. However, when equilibrium is reached, denudation rates can be estimated reasonably well, and total denudation since deposition can be inferred if independent age control is available. For this purpose, we here briefly summarize the currently available data and the state of knowledge. All exposure ages have been (re)calculated using the CRONUS web calculator (Marrero et al., 2016) with the time-dependent scaling model by Lifton et al. (2014) and a reference production rate of 3.93 (± 0.1) atoms g^{-1} a^{-1} (Heyman, 2014).

For the Bern site, unpublished ^{10}Be surface exposure ages on three boulders show that the Aare glacier started to retreat 18 ka from this position (Wüthrich et al., 2017a). The Deisswil site must be older than the Bern site based on stratigraphical considerations, but it is younger than Steinhof. The two oldest boulders in Steinhof (out of four) yield exposure ages of 24.4 and 23 kyr (Ivy-Ochs et al., 2004). The deposition age of the boulders in Steinhof has been questioned by Bitterli et al. (2011) and Bläsi et al. (2015) due to the high decalcification depth. At this point, we find that decalcification is also strongly affected by other factors than time – mainly the initial content of carbonates in the sediment, which decreases from west to east (Gasser and Nabholz, 1969) – and that the exposure ages are a good estimate for the deposition age of the moraine at Steinhof.

Schlüchter (1988) suggested the absence of glaciers in the Swiss Alpine Foreland during MIS 6, based on sedimentological and palynological evidence from the sections Thalgut and Meikirch, ~ 15 km south and ~ 10 km north of Bern, respectively.

This conflicts with the classical notion that the penultimate glaciation (i.e., Riss, Beringen, MIS 6) in the Alps was more extensive than the ultimate glaciation (Würm, Birrfeld)
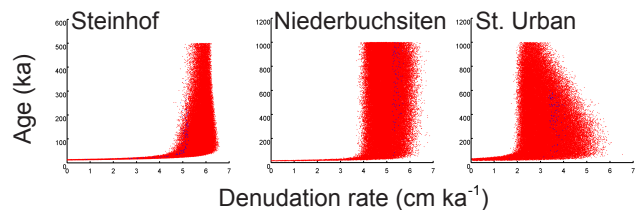

Figure 5. Denudation rate and age plots, acquired using the depth profile calculator by Hidy et al. (2010). Red dots mark all possible solutions and blue dots the 100 best χ^2 fits.

(Doppler et al., 2011; van Husen and Reitner, 2011; Preusser et al., 2011) and implies that the Niederbuchsiten till may have been deposited already during one of the early mid-Pleistocene glaciations. Attempts have been made recently to solve this controversy by applying ^{10}Be surface exposure dating on erratic boulders in the Jura Mountains by Graf et al. (2007, 2015), yet with limited success, as the oldest dated boulders date into MIS 6 but are interpreted to have been deposited much earlier. Various novel dating techniques based on luminescence and cosmogenic nuclides have been applied to sediments in Meikirch (Preusser et al., 2005) and its vicinity (Dehnert et al., 2010), and these studies do suggest that the penultimate glaciation was more extensive than the LGM. In any case, the till at Niederbuchsiten does very likely not document the oldest extensive glaciation, because it overlies fluvioglacial sediments that were deposited after an even earlier glacial advance and the respective denudational event. The till in St. Urban is completely weathered down to its base (~ 4 m) and lies directly on molasse sediments. We can tentatively infer that it is at least MIS 6 in age and likely corresponds to the Möhlin glaciation.

4.2 Denudation rate and total denudation

The results from the Bern site do not allow to calculate age and denudation rate because of the very poor fit between the samples and the trend line (Fig. 4). We speculate that decalcification is responsible for this: decalcification means a loss of material and thus a decrease in thickness and a lowering of the surface. The samples in ^{10}Be depth profile "move" closer together. The other profiles may have been influenced by this process as well but to a lower degree, because the initial calcite content is highest in the sediments of the Aare Glacier and decreases from west to east in the deposits of the Rhône Glacier (Gasser and Nabholz, 1969). Decalcification cannot yet be corrected for and will be ignored in the following discussion.

The steady-state denudation rates of 5.2 and 6.6 cm kyr^{-1} for Deisswil and Steinhof are comparable to the most probable Bayesian denudation rates of 6.2 cm kyr^{-1} for Steinhof. Assuming constant denudation rates of ~ 6 cm kyr^{-1} and exposure ages of ~ 24 kyr for these three sites yields total denudation on the order of 120 cm. Denudation was probably

not constant over time, and another back-of-the-envelope calculation could assume most recent denudation due to anthropogenic activity. As the ^{10}Be production decreases to half of its surface value at ~ 50 cm depth, total denudation would thus be at least on that order of magnitude.

For the Niederbuchsiten site denudation rates between 3.7 and 6.3 cm kyr^{-1} can be modeled (Table 2), yet all best fits are close to the most probable Bayesian denudation rate of 4.9 cm kyr^{-1} and the steady-state denudation of 4.5 cm kyr^{-1} (Fig. 5). Assuming constant denudation on that order of magnitude yields a total denudation of > 6 m in the case that the till was deposited during the Beringen Glaciation (MIS 6). In the case that the till at Niederbuchsiten was deposited during MIS 8, 300 ka or earlier, a total denudation of > 13 m can be calculated. Again, however, constant denudation is unlikely, particularly in view of the old age spanning at least one glacial–interglacial cycle, and we evaluate an alternative more complex scenario: as the ^{10}Be production decreases to 10 % of its surface value at ~ 380 g cm^{-2} (~ 170 cm with a density of 2.2 g cm^{-2}) depth, deposition during MIS 6 and the most recent anthropogenic truncation of the profile on that order of magnitude is one scenario. Also, periglacial solifluction during the LGM may have removed much of the ^{10}Be that accumulated close to the surface since MIS 6. In that case denudation must additionally have been active since the LGM because, like in the case of Steinhof, Deisswil and Bern, the surface ^{10}Be concentration at Niederbuchsiten is only about half of the concentration than one would expect from a stable surface exposed since the LGM.

The denudation rates obtained from the Monte Carlo simulations for St. Urban are between 1.5 and 5.7 cm kyr^{-1} and the most probable Bayesian denudation rate is 2.8 cm kyr^{-1} (Table 2, Fig. 5c). With such denudation rates, one would calculate ~ 4 m total denudation if the till was deposited during the penultimate glaciation and ~ 25 m if the till was deposited 800 ka. Again, several meters of denudation due to intensive periglacial dynamics during the LGM (and possibly earlier) could have played an important role in lowering the ^{10}Be concentrations. For St. Urban, this is most probably the case, because the depth profile can be fitted best with an attenuation length of 835 g cm^{-2} (Fig. 4). Such a high value strongly exceeds the attenuation length of 160 g cm^{-2} related to neutrogenic production (dominant only near the surface) and points to a significant muogenic contribution (1500 g cm^{-2} for slow muons and 4320 g cm^{-2} for fast muons; Braucher et al., 2009, 2013). The attenuation lengths are expressed in the slope (a) of the trend line in Fig. 4. Interestingly, Niederbuchsiten also shows this indication for massive denudation (fitted attenuation lengths of 370 g cm^{-2}), although not to such a degree, whereas Bern and Steinhof do not, consistent with their presumably last glacial age.

We conclude that denudation rates can be reasonably constrained with the help of ^{10}Be depth profiles, and total denudation can be estimated provided that the deposition age
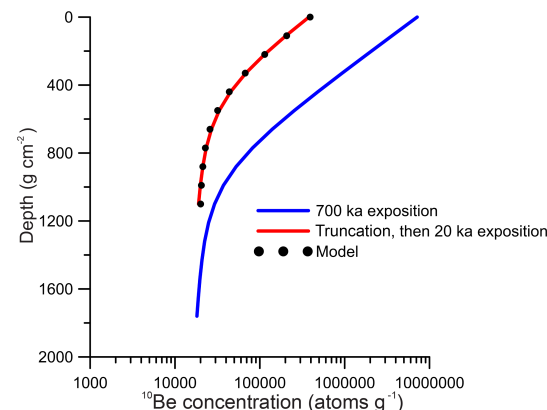

Figure 6. Illustration of "pseudo-inheritance". The plot shows a theoretical profile which was exposed for 700 kyr. Then 3 m were truncated immediately. Afterwards, the profile was again exposed to the cosmic radiation for 20 kyr. We modeled the age (31 kyr) and inheritance (19×10^4 atoms g^{-1}) using excel.

of the parent material is known. This works particularly well for sites not older than the LGM, where constant denudation rates are ~ 5 cm kyr^{-1} and total denudation is on the order of 0.5 to 1 m. For older sites, constant denudation rates can be constrained by the Monte Carlo simulations to 3–5 cm kyr^{-1}. However, the assumption of constant denudation is very likely wrong and would result in several meters of total denudation for MIS 6 sites and even several tens of meters for older sites. Total denudation of even more than 100 m is necessary to explain the ^{10}Be depth profiles in Deckenschotter (Häuselmann et al., 2007; Akçar et al., 2014; Claude et al., 2017). We suggest that denudational events related to periglacial dynamics might play an important role for the denudation history. This would substantially mitigate the need to invoke massive total denudation. It might therefore be a promising endeavor for future studies to modify the Monte Carlo simulations in a way that denudational events can be evaluated.

4.3   Inheritance and "pseudo-inheritance"

The most probable Bayesian inheritance is zero for Steinhof (Table 2) and also low for Bern and Deisswil (Fig. 4), whereas Niederbuchsiten and St. Urban have a much higher inheritance of 2.2×10^4 and 7.3×10^4 atoms g^{-1} (Table 2). This might be a systematic pattern, with less inheritance for the younger sites and more inheritance for the older ones. The pattern might document that the earlier glacial advances eroded a landscape that had accumulated substantial amounts of cosmogenic nuclides near the surface before the onset of the massive glaciations. During the course of the Pleistocene glaciations, the glaciers eroded deeper and deeper and therefore transported and deposited sediments with less inheritance. In the following, however, we elucidate that the high inheritance in Niederbuchsiten and St. Urban may not neces-

sarily reflect "true" inheritance from the catchment but can alternatively be explained with denudation events during the long exposure history of the sites since deposition.

When a site is exposed to cosmic radiation over hundreds of thousands of years, notable amounts of ^{10}Be are produced not only at the surface but also at greater depth, mostly due to muogenic production (Heisinger et al., 2002a, b; Braucher et al., 2003, 2011, 2013). Massive denudation, related for example to periglacial conditions, could truncate the site but still leave considerable amounts of these muogenic ^{10}Be atoms that decrease in concentration with depth with a much smaller slope than ^{10}Be atoms that are produced close to the surface by neutrons. New exposure after the denudational event leads to accumulation of new ^{10}Be, and the concentration in the upper few meters will soon again have the steep slope related to the neutron flux. When age, constant denudation and inheritance are calculated from such a depth profile, the high ^{10}Be concentration at depth is therefore wrongly interpreted as inheritance. We dub the high concentration at depth "pseudo-inheritance" when it is the result of long exposure of the site and massive denudation rather than "true" inheritance from the catchment.

To illustrate the concept of pseudo-inheritance, we create a 800 cm deep depth profile that has experienced a 700 kyr long exposure without denudation. Then we truncate 300 cm in a single event. After that, we allow an exposure of 20 kyr without denudation. In the following, we modeled the concentrations using Excel with unconstrained inheritance and age and zero denudation (Fig. 6). The results yield a best fit age of 31 kyr and an inheritance of 19×10^4 atoms g^{-1}. The young apparent age and high apparent inheritance reflect the denudational loss of the neutron component and the dominance of the muogenic component, respectively. The apparent inheritance is *not* derived from the catchment and should not be confused with "true" inheritance.

5   Conclusions

– Our results show that ^{10}Be depth profiles on the Swiss Plateau reach steady state within a few thousand years and do not provide new robust age control for the timing of Pleistocene glaciation.

– Concentrations of the Niederbuchsiten and St. Urban profiles decrease with a suspiciously low slope, possibly indicating significant muogenic contributions, pre-LGM deposition ages and massive denudation since deposition.

– The ^{10}Be depth profiles can be used to reasonably constrain modeled constant denudation rates to ~ 5 cm kyr^{-1}. Given independent age constraints for the MIS 2 sites, total denudation amounted to ~ 100 cm since deposition. Alternatively, most recent anthropogenic denudation would be on the order of 50 cm to explain the low ^{10}Be concentrations at all three sites.

– For Niederbuchsiten and St. Urban, the ^{10}Be depth profiles also yield denudation rates of ~ 5 cm kyr^{-1}, but the assumption of constant denudation would imply several or even tens of meters of total denudation. Denudation events related to periglacial activity, for example during the LGM, would substantially mitigate the need to invoke massive total denudation. Only a few meters of periglacial denudation during glaciations would be sufficient to explain the low observed ^{10}Be concentrations. Massive denudation and/or denudation events result in relatively high concentrations at depth stemming from muogenic production, and as this may wrongly be interpreted as inheritance, we dub this phenomenon "pseudo-inheritance". Modifications in the depth profile calculations should be made so that denudation events can be included in the Monte Carlo simulations.

We finally conclude that ^{10}Be depth profiles are an innovative tool to quantitatively investigate Earth surface processes. Deposition ages can be inferred for fluvial terraces and moraines, yet ages should always be discussed in context with denudation, which itself is generally poorly constrained. We see great potential for studying denudation histories at specific sites and for whole catchments, where the age of the parent material is known independently. In the future, dating of soft sediments in such a dynamic environment as the Swiss Plateau with high denudation rates can be improved with the combination of samples from shallow depths, with many more samples (than in this study) from greater depths (> 700 g cm^{-2}), which allows us to calculate denudation in steady state from the upper part and better constrained ages from the lower part. Also the combination of several cosmogenic nuclides might help to (i) constrain the timing of denudational events in the past (Fülöp et al., 2015) and (ii) obtain burial ages (Balco and Rovey, 2008).

References

Akçar, N., Ivy-Ochs, S., Kubik, P. W., and Schlüchter, C.: Post-depositional impacts on "Findlinge" (erratic boulders) and their

implications for surface-exposure dating, Swiss J. Geosci., 104, 445–453, https://doi.org/10.1007/s00015-011-0088-7, 2011.

Akçar, N., Ivy-Ochs, S., Alfimov, V., Claude, A., Graf, H. R., Dehnert, A., Kubik, P. W., Rahn, M., Kuhlemann, J., and Schlüchter, C.: The first major incision of the Swiss Deckenschotter landscape, Swiss J. Geosci., 107, 337–347, https://doi.org/10.1007/s00015-014-0176-6, 2014.

Balco, G. and Rovey, C. W.: A isochron method for cosmogenic-nuclide dating of buried soils and sediments, Am. J. Sci., 308, 1083–1114, https://doi.org/10.2475/10.2008.02, 2008.

Beck, P.: Über das schweizerische und europäische. Pliozän und Pleistozän, Eclogae Geol. Helv., 26, 335–437, 1933.

Bini, A., Buonchristiani, J.-F., Couterand, S., Ellwanger D., Felber, M., Florineth, D., Graf, H. R., Keller, O., Kelly, M., Schlüchter, C., and Schöneich, P.: Die Schweiz während des letzteiszeitlichen Maximums (LGM), Bundesamt für Landestopografie, Wabern, 2009.

Bitterli, T., Jordi, H., Gerber, M., Gnaegi, C., and Graf, H. R.: Geologischer Atlas der Schweiz: Blatt 1108: Murgenthal (Erlaeuterungen), Bundesamt für Landestopografie, Wabern, 2011.

Bläsi, H. R., Gygi, R., Gnägi, C., Graf, H. R., Jordan, P., Labscher, H. P., Ledermann, H., Herold, T., Schlanke, S., Burkhalter, R., and Kälin, D.: Geologischer Atlas der Schweiz. Blatt 1107: Balsthal (Erlaeuterungen), Bundesamt für Landestopografie, Wabern, Switzerland, 2015.

Braucher, R., Brown, E. T., Bourlès, D. L., and Colin, F.: In situ produced [10]Be measurements at great depths: implications for production rates by fast muons, Earth Planet. Sc. Lett., 211, 251–258, 2003.

Braucher, R., Del Castillo, P., Siame, L., Hidy, A. J., and Bourles, D. L.: Determination of both exposure time and denudation rate from an in situ-produced [10]Be depth profile: a mathematical proof of uniqueness. Model sensitivity and applications to natural cases, Quat. Geochronol., 4, 56–67, 2009.

Braucher, R., Merchel, S., Borgomano, J., and Bourlès, D. L.: Production of cosmogenic radionuclides at great depth: a multi element approach, Earth Planet. Sc. Lett., 309, 1–9, 2011.

Braucher, R., Bourlès, D., Merchel, S., Vidal Romani, J., Fernandez-Mosquera, D., Marti, K., Léanni, L., Chauvet, F., Arnold, M., Aumaître, G., and Keddadouche, K.: Determination of muon attenuation lengths in depth profiles from in situ produced cosmogenic nuclides, Nucl. Instrum. Meth. B, 294, 484–490, https://doi.org/10.1016/j.nimb.2012.05.023, 2013.

Chmeleff, J., von Blanckenburg, F., Kossert, K., and Jakob, D.: Determination of the [10]Be half-life by multicollector ICP-MS and liquid scintillation counting, Nucl. Instrum. Meth. B, 268, 192–199, 2010.

Christl, M., Vockenhuber, C., Kubik, P. W., Wacker, L., Lachner, J., Alfimov, V., and Synal, H.-A.: The ETH Zurich AMS facilities. Performance parameters and reference materials, Nucl. Instrum. Meth. B, 294, 29–38, https://doi.org/10.1016/j.nimb.2012.03.004, 2013.

Claude, A., Akçar, N., Ivy-Ochs, S., Schlunegger, F., Kubik, P. W., Dehnert, A., Kuhlemann, J., Rahn, M., and Schlüchter, C.: Timing of early Quaternary gravel accumulation in the Swiss Alpine Foreland, Geomorphology, 276, 71–85, https://doi.org/10.1016/j.geomorph.2016.10.016, 2017.

Dehnert, A., Preusser, F., Kramers, J. D., Akcar, N., Kubik, P. W., Reber, R., and Schlüchter, C.: A multi-dating approach applied to

proglacial sediments attributed to the Most Extensive Glaciation of the Swiss Alps, Boreas, 39, 620–632, 2010.

Delmas, M., Braucher, R., Gunnell, Y., Guillou, V., Calvet, M., Bourlès, D., and ASTER Team: Constraints on Pleistocene glaciofluvial terrace age and related soil chronosequence features from vertical [10]Be profiles in the Ariege River catchment (Pyrenees, France), Global Planet. Change, 132, 39–53, 2015.

Doppler, G., Krömer, E., Rögner, K., Wallner, J., Jerz, H., Grottenthaler, W.: Quaternary Stratigraphy of Southern Bavaria, Quaternary Science Journal, 60, 329–365, https://doi.org/10.3285/eg.60.2-3.08, 2011.

Dreimanis, A.: The problem of waterlain tills, in: Moraines and varves, edited by: Schlüchter, C., A.A. Balkema, Rotterdam, the Netherlands, 167–175, 1979.

Eberl, B.: Die Eiszeitfolge im nürdlichen Alpenvorland, ihr Ablauf, ihre Chronologie auf Grund der Aufnahme im Bereich des Lech- und Illergletschers, Benno Filzer, Augsburg, Germany, 1930.

Federici, P. R., Granger, D. E., Ribolini, A., Spagnolo, M., Pappalardo, M., and Cyr, A. J.: Last Glacial Maximum and the Gschnitz stadial in the Maritime Alps according to [10]Be cosmogenic dating, Boreas, 41, 277–291, https://doi.org/10.1111/j.1502-3885.2011.00233.x, 2012.

Flint, R. F., Sanders, J. E., and Rodgers, J.: Diamictite: A substitute term for Symmictite, Geol. Soc. Am. Bull., 71, 1809–1810, 1960a.

Flint, R. F., Sanders, J. E., and Rodgers, J.: Symmictite: A name for nonsorted terrigenous sedimentary rocks that contain a wide range of particle sizes, Geol. Soc. Am. Bull., 71, 507–510, 1960b.

Fülöp, R.-H., Bishop, P., Fabel, D., Cook, G. T., Everest, J., Schnabel, C., Codilean, A. T., and Xu, S.: Quantifying soil loss with in situ [10]Be and ^{14}C depth-profiles, Quat. Geochronol., 27, 78–93, 2015.

Gasser, U. and Nabholz, W.: Zur Sedimentologie der Sandfraktion im Pleistozän des schweizerischen Mittellander, Eclogae Geol. Helv., 62, 467–516, 1969.

Gerber, M. E. and Wanner, J.: Blatt 1128: Langenthal, Schweizerische Geologische Kommission (Geologischen Atlas der Schweiz 1 : 25 000), 1984.

Gosse, J. C. and Phillips, F. M.: Terrestrial in situ cosmogenic nuclides: theory and application, Quaternary Sci. Rev., 20, 1475–1560, https://doi.org/10.1016/S0277-3791(00)00171-2, 2001.

Graf, H. R.: Stratigraphie von Mittel- und Spätpleistozän in der Nordschweiz, Beiträge zur Geologischen Karte der Schweiz 168, Bundesamt für Landestopografie swisstopo, Wabern, 2009.

Graf, A. A., Strasky, S., Ivy-Ochs, S., Akcar, N., Kubik, P. W., Burkhard, M., and Schlüchter, C.: First results of cosmogenic dated pre-Last Glaciation erratics from the Montoz area, Jura Mountains, Switzerland, Quaternary Int., 164165, 43–52, https://doi.org/10.1016/j.quaint.2006.12.022, 2007.

Graf, A. A., Akçar, N., Ivy-Ochs, S., Strasky, S., Kubik, P. W., Christl, M., Burkhard, M., Wieler, R., and Schlüchter, C.: Multiple advances of Alpine glaciers into the Jura Mountains in the Northwestern Switzerland, Swiss J. Geosci., 108, 225–238, https://doi.org/10.1007/s00015-015-0195-y, 2015.

Haghipour, N., Burg, J.-P., Ivy-Ochs, S., Hajdas, I., Kubik, P., and Christl, M.: Correlation of fluvial terraces and temporal steady-state incision on the onshore Makran accretionary wedge in southeastern Iran: Insight from channel profiles and [10]Be expo-

sure dating of strath terraces, Geol. Soc. Am. Bull., 127, 560–583, https://doi.org/10.1130/B31048.1, 2014.

Häuselmann, P., Fiebig, M., Kubik, P. W., and Adrian, H.: A first attempt to date the original "Deckenschotter" of Penck and Brückner with cosmogenic nuclides, From the Swiss Alps to the Crimean Mountains – Alpine Quaternary stratigraphy in a European context, 164–165, 33–42, https://doi.org/10.1016/j.quaint.2006.12.013, 2007.

Heisinger, B., Lal, D., Jull, A. T., Kubik, P., Ivy-Ochs, S., Knie, K., and Nolte, E.: Production of selected cosmogenic radionuclides by muons: 2. Capture of negative muons, Earth Planet. Sc. Lett., 200, 357–369, 2002a.

Heisinger, B., Lal, D., Jull, A. T., Kubik, P., Ivy-Ochs, S., Neumaier, S., Knie, K., Lazarev, V., and Nolte, E.: Production of selected cosmogenic radionuclides by muons: 1. Fast muons, Earth Planet. Sc. Lett., 200, 345–355, 2002b.

Heyman, J.: Paleoglaciation of the Tibetan Plateau and surrounding mountains based on exposure ages and ELA depression estimates, Quaternary Sci. Rev., 91, 30–41, https://doi.org/10.1016/j.quascirev.2014.03.018, 2014.

Heyman, J., Applegate, P. J., Blomdin, R., Gribenski, N., Harbor, J. M., and Stroeven, A. P.: Boulder height – exposure age relationships from a global glacial 10Be compilation, Quat. Geochronol., 34, 1–11, https://doi.org/10.1016/j.quageo.2016.03.002, 2016.

Hidy, A. J., Gosse, J. C., Pederson, J. L., Mattern, J. P., and Finkel, R. C.: A geologically constrained Monte Carlo approach to modeling exposure ages from profiles of cosmogenic nuclides: An example from Lees Ferry, Arizona, Geochem. Geophy. Geosy., 11, Q0AA10, https://doi.org/10.1029/2010GC003084, 2010.

Ivy-Ochs, S., Schäfer, J., Kubik, P. W., Synal, H.-A., Schlüchter, C.: Timing of deglaciation on the northern Alpine foreland (Switzerland), Eclogae Geol. Helv., 97, 47–55, https://doi.org/10.1007/s00015-004-1110-0, 2004.

Ivy-Ochs, S., Kerschner, H., Kubik, P. W., and Schlüchter, C.: Glacier response in the European Alps to Heinrich Event 1 cooling: the Gschnitz stadial, J. Quaternary Sci., 21, 115–130, 2006a.

Ivy-Ochs, S., Kerschner, H., Reuther, A., Maisch, M., Sailer, R., Schäfer, J., Kubik, P. W., Synal, H.-A., and Schlüchter, C.: The timing of glacier advances in the northern European Alps based on surface exposure dating with cosmogenic 10Be, 26Al, 36Cl, and 21Ne, Geol. S. Am. S., 415, 43–60, https://doi.org/10.1130/2006.2415(04), 2006b.

Keller, O. and Krayss, E.: Mittel- und spätpleistozäne Stratigraphie und Morphogenese in Schlüsselregionen der Nordschweiz, E&G Quaternary Sci. J., 59, 88–119, https://doi.org/10.3285/eg.59.1-2.08, 2011.

Kohl, C. and Nishiizumi, K.: Chemical isolation of quartz for measurement of in-situ -produced cosmogenic nuclides, Geochim. Cosmochim. Ac., 56, 3583–3587, https://doi.org/10.1016/0016-7037(92)90401-4, 1992.

Korschinek, G., Bergmaier, A., Faestermann, T., Gerstmann, U. C., Knie, K., Rugel, G., Wallner, A., Dillmann, I., Dollinger, G., Gostomski, C. L. von, Kossert, K., Maiti, M., Poutivtsev, M., and Remmert, A.: A new value for the half-life of 10Be by Heavy-Ion Elastic Recoil Detection and liquid scintillation counting, Nucl. Instrum. Meth. B, 268, 187–191, https://doi.org/10.1016/j.nimb.2009.09.020, 2010.

Lal, D.: Cosmic ray labeling of erosion surfaces: in situ nuclide production rates and erosion models, Earth Planet. Sc. Lett.,

104, 424–439, https://doi.org/10.1016/0012-821X(91)90220-C, 1991.

Lifton, N., Sato, T., and Dunai, T. J.: Scaling in situ cosmogenic nuclide production rates using analytical approximations to atmospheric cosmic-ray fluxes, Earth Planet. Sc. Lett., 386, 149–160, https://doi.org/10.1016/j.epsl.2013.10.052, 2014.

Mailänder, R. and Veit, H.: Periglacial cover- beds on the Swiss Plateau: Indicatords of soil, climate and landscape evolution during the Late Quaternary, CATENA, 45, 251–272, https://doi.org/10.1016/S0341-8162(01)00151-5, 2001.

Marrero, S. M., Phillips, F. M., Borchers, B., Lifton, N., Aumer, R., and Balco, G.: Cosmogenic nuclide systematics and the CRONUScalc program, Quat. Geochronol., 31, 160–187, https://doi.org/10.1016/j.quageo.2015.09.005, 2016.

Penck, A. and Brückner, E.: Die Alpen im Eiszeitalter, 3 Vol., C. H. Tauchnitz, Leipzig, Germany, 1909.

Pfiffner, O. A.: Geologie der Alpen, 1st Edn., Haupt (UTB, 8416), Bern, 2009.

Phillips, F. M., Argento, D. C., Balco, G., Caffee, M. W., Clem, J., Dunai, T. J., Finkel, R., Goehring, B., Gosse, J. C., Hudson, A. M., Jull, A. T., Kelly, M. A., Kurz, M., Lal, D., Lifton, N., Marrero, S. M., Nishiizumi, K., Reedy, R. C., Schaefer, J., Stone, J. O., Swanson, T., and Zreda, M. G.: The CRONUS-Earth Project: A synthesis, Quat. Geochronol., 31, 119–154, https://doi.org/10.1016/j.quageo.2015.09.006, 2016.

Preusser, F.: Towards a chronology of the late Pleistocene in the northern Alpine Foreland, Boreas, 33, 195–210, https://doi.org/10.1111/j.1502-3885.2004.tb01141.x, 2009.

Preusser, F., Drescher-Schneider, R., Fiebig, M., and Schlüchter, C.: Re-interpretation of the Meikirch pollen record, Swiss Alpine Foreland, and implications for Middle Pleistocene chronostratigraphy, J. Quaternary Sci., 20, 607–620, https://doi.org/10.1002/jqs.930, 2005.

Preusser, F., Blei, A., Graf, H., and Schlüchter, C.: Luminescence dating of Würmian (Weichselian) proglacial sediments from Switzerland: methodological aspects and stratigraphical conclusions, Boreas, 36, 130–142, https://doi.org/10.1111/j.1502-3885.2007.tb01187.x, 2007.

Preusser, F., Graf, H. R., Keller, O., Krayss, E., and Schlüchter, C.: Quaternary glaciation history of northern Switzerland, E&G Quaternary Sci. J., 60, 282–305, 2011.

Reitner, J. M.: Glacial dynamics at the beginning of Termination I in the Eastern Alps and their stratigraphic implications, Quaternary Int., 164, 64–84, 2007.

Rixhon, G., Braucher, R., Bourlès, D., Siame, L., Bovy, B., and Demoulin, A.: Quaternary river incision in NE Ardennes (Belgium) – Insights from 10Be/26Al dating of river terraces, Quat. Geochrono., 6, 273–284, https://doi.org/10.1016/j.quageo.2010.11.001, 2011.

Ruszkiczay-Rüdiger, Z., Braucher, R., Novothny, Á., Csillag, G., Fodor, L., Molnár, G., Madarász, B., and ASTER Team: Tectonic and climatic control on terrace formation: Coupling in situ produced 10Be depth profiles and luminescence approach, Danube River, Hungary, Central Europe, Quaternary Sci. Rev., 131, 127–147, 2016.

Schaller, M., Ehlers, T. A., Blüm, J. D., and Kallenberg, M. A.: Quantifying glacial moraine age, denudation and soil mixing with cosmogenic nuclide depth profiles, J. Geophys. Res., 114, F01012, https://doi.org/10.1029/2007JF000921, 2009.

Schlüchter, C.: A non-classical summary of the Quaternary stratigraphy in the northern Alpine foreland of Switzerland, Bulletin de la Société neuchâteloise de géographie, 23, 143–157, 1988.

Schlüchter, C.: Eiszeitliche Lockergesteine- Geologie, Genese und Eigenschaften. Ein Beitrag zu den Beziehungen zwischen fundamentaler und angewandter Eiszeitgeologie, Habilitationsschrift, ETH Zürich, 1989a.

Schlüchter, C.: The most complete quaternary record of the Swiss Alpine Foreland, Palaeogeogr. Palaeocl., 72, 141–146, https://doi.org/10.1016/0031-0182(89)90138-7, 1989b.

Schlüchter, C.: Das Eiszeitalter der Schweiz-. Eine schematische Zusammenfassung, Institut für Geologie der Universität Bern, 2010.

Schlüchter, C. and Wolfarth-Meyer, B.: Till facies varieties of the Western Swiss Alpine Foreland, in: Till and Glaciotectonics, edited by: van der Meer, J. J. M., A.A. Balkema, Rotterdam, the Netherlands, 67–72, 1986.

Semmel, A. and Terhorst, B.: The concept of the Pleistocene periglacial cover beds in central Europe: a review, Quaternary Int., 222, 120–128, 2010.

Siame, L., Bellier, O., Braucher, R., Sébrier, M., Cushing, M., Bourlès, D., Hamelin, B., Baroux, E., de Voogd, B., Raisbeck, G., and Yiou, F.: Local erosion rates versus active tectonics: cosmic ray exposure modelling in Provence (south-east France), Earth Planet. Sc. Lett., 220, 345–364, 2004.

Stone, J. O.: Air pressure and cosmogenic isotope production, J. Geophys. Res.-Sol. Ea., 105, 23753–23759, https://doi.org/10.1029/2000JB900181, 2000.

van Husen, D. and Reitner, J. M.: An outline of the Quaternary stratigraphy of Austria, Eiszeitalter und Gegenwart, 60, 366–387, 2011.

Welten, M.: Pollenanalytische Untersuchungen im jüngeren Quartär des nördlichen Alpenvorlandes der Schweiz, Stämpfli (Beiträge zur geologischen Karte der Schweiz, 156), Bern, 1982.

Welten, M.: Neue pollenanalytische Ergebnisse über das Jüngere Quartär des nördlichen Alpenvorlandes der Schweiz (Mittel- und Jungpleistozän), Stämpfli (Beiträge zur geologischen Karte der Schweiz, 162), Bern, 1988.

Wüthrich, L., Garcia Morabito, E., Zech, J., Gnägi, C., Trauerstein, M., Veit, H., Merchel, S., Scharf, A., Rugel, G., Christl, M., and Zech, R.: ^{10}Be surface exposure dating of the last deglaciation in the Aare Valley, Switzerland, Swiss J. Geosci., submitted, 2017a.

Wüthrich, L., Brändli, C., Braucher, R., Veit, H., Haghipour, N., Terrizzano, C., Christl, M., Gnägi, C., and Zech, R.: Beryllium 10 (^{10}Be) concentrations from till in the western Swiss lowlands, PANGAEA, https://doi.org/10.1594/PANGAEA.884060, 2017b.

Zimmermann, H. W.: Die Eiszeit im westlichen zentralen Mittelland (Schweiz), Separat Abdruck aus den Mitteilungen der Naturforschenden Gesellschaft Solothurn, 21, 10–143, 1963.

Landscape evolution of the northern Alpine Foreland: constructing a temporal framework for early to middle Pleistocene glaciations

Anne Claude[1,a]

[1]Institute of Geological Sciences, University of Bern, Bern, Switzerland
[a]present address: IMP Bautest AG, Oberbuchsiten, Switzerland

Supervisors: Naki Akçar, Susan Ivy-Ochs, Christian Schlüchter, Fritz Schlunegger

The Deckenschotter deposits are believed to represent the oldest Quaternary sediments in the Alpine Foreland and are thus a geoarchive, documenting paleoenvironmental changes during the Quaternary. Lithostratigraphic positions of the Deckenschotter deposits in Switzerland have been extensively studied. However, compared to late Quaternary glaciations, the timing of these accumulations is poorly understood. The investigations related to the dissertation shed light on this timing and hence on the landscape evolution of the northern Alpine Foreland.

The study area is located in the northern Alpine Foreland of Switzerland where seven sites of the Höhere ("higher"; HDS) Deckenschotter, Tiefere ("lower"; TDS) Deckenschotter and Hochterrasse ("higher terrace") were investigated; from east to west, these sites are Irchel (three sites: Wilemer, Steig and Hütz), Stadlerberg, Siglistorf, Rechberg, Ängi, Mandach and Pratteln (Hohle Gasse) (Fig. 1). From each site either sediment samples were collected for dating with cosmogenic ^{10}Be and/or ^{36}Cl depth-profile dating or clasts with quartz-rich lithologies were sampled for isochron burial dating with ^{10}Be and ^{26}Al. At Irchel Steig, the same outcrop was dated using both methods. In addition, detailed investi-

gations of clast fabrics, petrographic compositions and clast morphometries enable the identification of sediment source areas and the interpretation of their transport mechanisms and depositional environments. Finally, coupling the reconstructed chronologies with interpolated vertical height differences between the bedrock underlying the Deckenschotter deposits and the bedrock beneath the modern Rhine River allows for the estimation of post-depositional bedrock incision rates.

Analyses show that the HDS at Wilemer Irchel (Claude et al., 2017c), Stadlerberg (Claude et al., 2017a) and Siglistorf (Akçar et al., 2017) accumulated approximately around 2 Ma ago. Clasts were eroded from the northern Central Alps and brought to the foreland by paleoglaciers (Fig. 2a). In the foreland, glaciers also eroded conglomerates of the Miocene Molasse and transport was furthermore provided by glacial outwash. The influence of mainly the Linth paleoglacier is recognized in the provenance of the sediments. Clasts at the sites Wilemer Irchel, Stadlerberg and Siglistorf were deposited in a glacier-proximal environment. At that time, the Alpine Rhine, originating in the central Eastern Alps, was draining through Lake Constance into the Danube River and finally eastwards into the Black Sea (Fig. 2a). Estimated long-term bedrock incision rates are on the order of 130 ± 60–150 ± 40 m Ma^{-1} for the time interval from 2 Ma until the
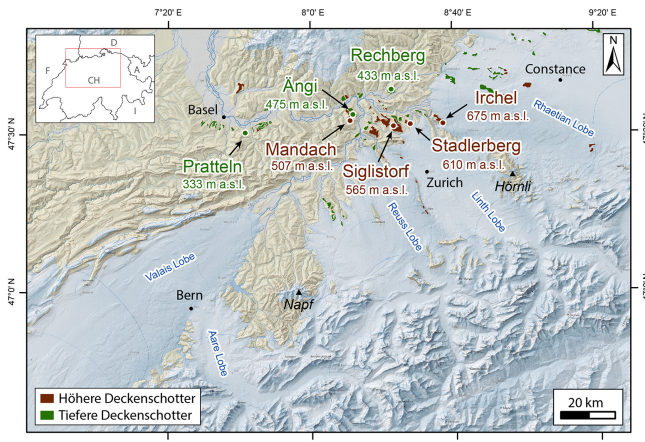
Figure 1. Extension of the Valais, Aare, Reuss, Linth and Rhaetian loves during the last Glacial Maximum (from Bini et al., 2009); location of the study sites Irchel, Stadlerberg, Siglistorf, Rechberg, Ängi, Mandach and Pratteln and distribution of the Deckenschotter deposits in the northern Alpine Foreland (© Federal Office of Topography, swisstopo). Figure modified from Claude et al. (2017a).

present. The landscape prior to 2 Ma was a low-relief landscape with smoother hillslopes than at present.

A second phase of gravel accumulation, the TDS at Irchel Steig and Hütz, Rechberg, Ängi and Mandach occurred at around 1 Ma, coinciding with the Mid-Pleistocene Revolution (MPR; Akçar et al., 2014; Claude et al., 2017c). At this time, sediments were eroded from both the northern Central and central Eastern Alps and brought to the Alpine Foreland by the Rheatian, Linth and Reuss paleoglaciers (Fig. 2b). Additionally, to the material derived directly from the Alps, all these deposits contain erosional products that were reworked from the Miocene Molasse. Similar to the older HDS deposits, the younger 1 Ma deposits were also transported as bedload in rivers in a proximal glaciofluvial system. After the Mid-Pleistocene Revolution, accelerated bedrock incision rates between 170 ± 80 and 340 ± 110 m Ma^{-1} were estimated. Higher rates suggest that a landscape with a more pronounced topographic relief developed compared to the early Pleistocene. These high rates might be the result of the Alpine Rhine draining westwards into the Upper Rhine Valley. As a consequence, the Danube River lost its Alpine catchment, and the discharge, the sediment flux and the erosional capacity increased within the Rhine River. Accordingly, we conclude that the principal driver of the accelerated incision rates in the Alpine Foreland was the climatic signal around the MPR along with a reorganization of the Alpine Rhine and that tectonics likely had only a minor influence.

In the area between Basel and Rheinfelden, the boundaries between the different terrace levels are not always clear. Here, both HDS and TDS deposits occur between elevations of 360 and 390 m a.s.l. At the site Pratteln (Hohle Gasse) a multi-isotope approach using cosmogenic ^{10}Be
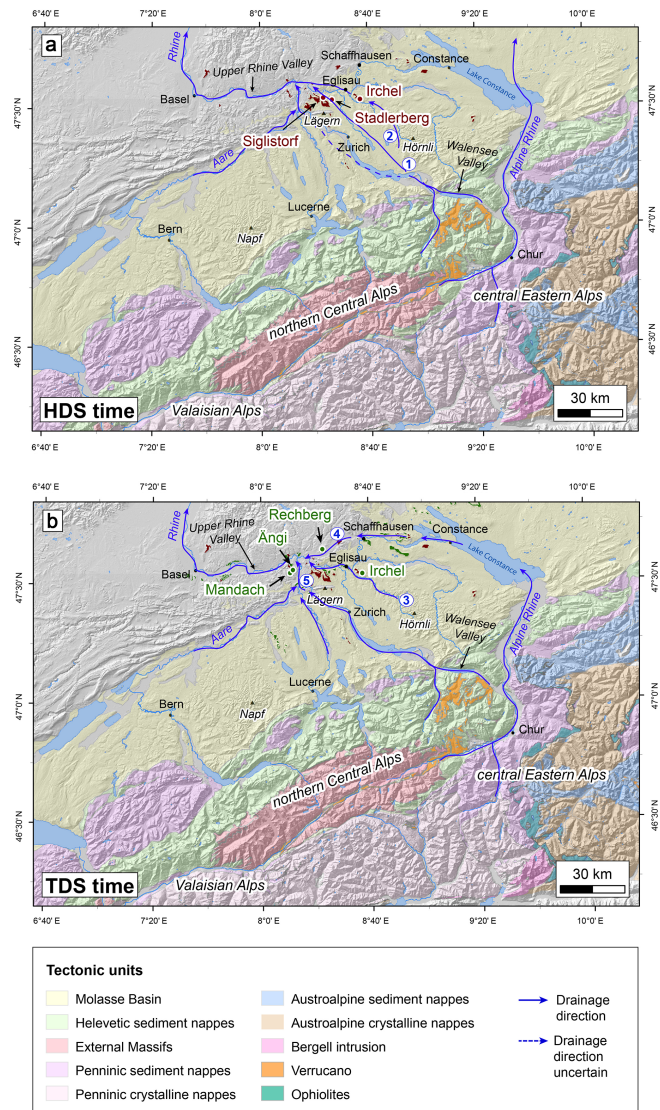
Figure 2. Map showing the tectonic units (© Federal Office of Topography, swisstopo) with possible source areas of the clasts at the study sites. The blue lines mark the evolution of the drainage network in the northern Alpine Foreland during the Pleistocene (Claude et al., 2017c). **(a)** Drainage network during the time of HDS accumulation. **(b)** Drainage network during the time of TDS accumulation.

and ^{36}Cl yielded an age of ca. 270 ka for this site (Claude et al., 2017b). Our findings revealed that this site should be assigned to the morphostratigraphic unit Hochterrasse rather than TDS. The location of this site ca. 40 km downstream of the confluence of the Aare with the Rhine River (Fig. 1) makes it impossible to distinguish whether the western and/or Central Alps contributed more material to the study site. Compared to the older Deckenschotter deposits, the gravels in Pratteln were deposited in a distal glaciofluvial environment in a high-concentration braided river system.

This work shows that great progress was made in cosmogenic nuclide dating using both depth-profile and isochron burial dating methods and that both methods are suitable to date such old sediments. In addition, this study helps to understand the past landscape evolution of the northern Swiss Alpine Foreland, which is of utmost importance for the planning of deep geological repositories that will be located in the Alpine Foreland. As many radionuclides in the waste have long half-life times, the on-site fluvial and glacial erosion of the future 1 Ma is a key issue with respect to long-term safety of the waste repository. Hence, this study is not only a direct input for research on Quaternary geology but also an input for the environmental safety of deep geological repositories for radioactive waste.

Competing interests. The author declares that she has no conflict of interest.

References

Akçar, N., Ivy-Ochs, S., Alfimov, V., Claude, A., Graf, H. R., Dehnert, A., Kubik, P. W., Rahn, M., Kuhlemann, J., and Schlüchter, C.: The first major incision of the Swiss Deckenschotter landscape, Swiss J. Geosci., 107, 337–347, 2014.

Akçar, N., Ivy-Ochs, S., Alfimov, V., Schlunegger, F., Claude, A., Reber, R., Christl, M., Vockenhuber, C., Dehnert, A., Rahn, M., and Schlüchter, C.: Isochron-burial dating of glaciofluvial deposits: primary results from the Alps, Earth Surf. Proc. Land., 42, 2414–2425, https://doi.org/10.1002/esp.4201, 2017.

Bini, A., Buonchristiani, J.-F., Couterand, S., Ellwanger, D., Felber, M., Florineth, D., Graf, H. R., Keller, O., Kelly, M., Schlüchter, C., and Schoeneich, P.: Switzerland during the Last Glacial Maximum (LGM), 1 : 500 000, Federal Office of Topography, swisstopo, Wabern, Switzerland, 2009.

Claude, A., Akçar, N., Ivy-Ochs, S., Schlunegger, F., Kubik, P. W., Dehnert, A., Kuhlemann, J., Rahn, M., and Schlüchter, C.: Timing of early Quaternary gravel accumulation in the Swiss Alpine Foreland, Geomorphology, 276, 71–85, 2017a.

Claude, A., Akçar, N., Ivy-Ochs, S., Schlunegger, F., Rentzel, P., Pümpin, C., Tikhomirov, D., Kubik, P. W., Vockenhuber, C., Dehnert, A., Rahn, M., and Schlüchter, C.: Chronology of Quaternary terrace deposits at the locality Hohle Gasse (Pratteln, NW Switzerland), Swiss J. Geosci., 110, 793–809, https://doi.org/10.1007/s00015-017-0278-z, 2017b.

Claude, A., Akçar, N., Ivy-Ochs, S., Schlunegger, F., Kubik, P. W., Christl, M., Vockenhuber, C., Kuhlemann, J., Rahn, M., and Schlüchter, C.: Changes in landscape evolution patterns in the northern Alpine Foreland during the Mid-Pleistocene Revolution, GSA Bulletin, in review, 2017c.

Palaeoenvironments during MIS 3 and MIS 2 inferred from lacustrine intercalations in the loess–palaeosol sequence at Bobingen (southern Germany)

Christoph Mayr[1,2,3], **Renate Matzke-Karasz**[2,3], **Philipp Stojakowits**[4], **Sally E. Lowick**[5], **Bernd Zolitschka**[6], **Tanja Heigl**[2], **Richard Mollath**[1], **Marian Theuerkauf**[1], **Marc-Oliver Weckend**[2], **Rupert Bäumler**[1], and **Hans-Joachim Gregor**[7]

[1]Institute of Geography, Friedrich-Alexander-Universität Erlangen-Nürnberg,
Wetterkreuz 15, 91058 Erlangen, Germany
[2]Palaeontology and Geobiology, Earth and Environmental Sciences,
Ludwig-Maximilians-Universität München, 80333 München, Germany
[3]GeoBio-Center, Ludwig-Maximilians-Universität München, 80333 München, Germany
[4]Institute of Geography, Universität Augsburg, Alter Postweg 118, 86135 Augsburg, Germany
[5]Institute for Geological Sciences, Universität Bern, Baltzerstrasse 1 + 3, 3012 Bern, Switzerland
[6]Universität Bremen, Institute of Geography, Geomorphology and Polar Research (GEOPOLAR),
Celsiusstr. 2, 28359 Bremen, Germany
[7]Daxerstr. 21, 81240 Olching, Germany

Correspondence: Christoph Mayr (christoph.mayr@fau.de)

Abstract: Recently exposed loess–palaeosol sequences in the northern Alpine foreland close to Bobingen (southern Germany) were investigated with a multi-proxy approach combining isotopic, geochemical, lithological, and micropalaeontological methods. Luminescence ages date the sections into the Middle and Upper Würmian periods corresponding to Marine Isotope Stages 3 and 2. A gleyic soil horizon at the base was dated to 45 ka and provided a palynoflora dominated by Poaceae, Cyperaceae, and *Pinus*, as well as frequent aquatic taxa. Lacustrine conditions prevailed after the gley formation until 30 ka, providing a comparatively diverse lacustrine fauna dominated by aquatic gastropods and the ostracod species *Candona candida*. At the transition to the Upper Würm, climatic conditions became harsh, indicated by accelerated deposition of more coarse-grained loess, organic geochemical indicators, and scarceness of biotic remains. Two tundra-gley horizons in the Upper Würm point to short phases of climatic amelioration with higher humidity also evidenced by reoccurrence of ostracod and aquatic gastropod remains. We propose that these climatic ameliorations were coincident with the Greenland interstadials 4 and 2.

Kurzfassung: Unlängst bei Bobingen (Bayern) im nördlichen Voralpenland aufgeschlossene Löß-Paläoboden-Sequenzen wurden mit einem Multi-Proxy-Ansatz untersucht, der mikropaläontologische, geochemische, lithologische und isotopische Methoden umfasste. Mit Hilfe von Lumineszenz-Datierungen wurden die Profile in das Mittlere und Obere Würm, entsprechend dem marinen Isotopenstadium (MIS) 3 und 2, datiert. Ein gleyartiger Horizont an der Basis datierte auf 45 ka und lieferte eine Pollenflora, die von Poaceae, Cyperaceae und *Pinus*, aber auch häufigen aquatischen Taxa dominiert wird. Lakustrine Verhältnisse herrschten nach der Bildung des Gleys bis 30 ka. Diese Ablagerungen lieferten eine vergleichsweise artenreiche lakustrine Fauna, in der aquatische Gastropoden und die Ostracodenart *Candona candida* vorherrschen. Am Übergang zum Oberen Würm setzten strengere klimatische Bedingungen ein, die sich durch vermehrte Ablagerung von grobkörnigerem Löß, weitgehendes Fehlen von biotischen Resten und in den organisch-geochemischen Indikatoren zeigen. Zwei Tundragley-Horizonte im Oberen Würm deuten auf kurze Phasen mit milderem Klima hin, wobei in diesen die Wiederkehr von Ostracoden und aquatischen Gastropoden auch auf höhere Feuchtigkeit hinweist. Diese Phasen kurzfristiger Klimaverbesserung entsprechen wahrscheinlich den Grönland-Interstadialen 4 und 2.

1 Introduction

Despite a long research history, starting with Penck (1882) and Penck and Brückner (1901–1909), large gaps still exist in our knowledge of glacial palaeoenvironments in the northern Alpine foreland mainly due to the fragmentary and discontinuous preservation of natural climate archives in this region. In particular, sedimentary records of the last glacial period, the Würm, often have numerous hiatuses caused by subsequent glaciofluvial erosion in the Alps and their foreland (Doppler et al., 2011). Recent studies of speleothems and inner-Alpine lacustrine sequences (Moseley et al., 2014; Heiri et al., 2014, and references therein) have substantially enlarged our knowledge of regional Würmian climate and environments. Loess sequences provide another archive of Quaternary palaeoenvironments in southern Germany, which has been investigated chronostratigraphically and sedimentologically in detail since the 1950s (e.g. Brunnacker, 1953). Typical successions of palaeosoils and loess (loess–palaeosol sequences, LPS) from central Europe were described and allowed us to establish a pedo- and lithostratigraphic framework (Zöller and Semmel, 2001; Terhorst et al., 2015). However, incomplete preservation due to hiatuses hamper the comparison of LPS from central Europe and require compilations of loess stratigraphies from multiple sites (Lehmkuhl et al., 2016). In the last decade, multi-proxy investigations provided new insights into palaeoenvironmental conditions during the last glacial period in the western European loess belt (Antoine et al., 2009, 2013). Here, we present a recently exposed LPS close to the town of Bobingen in the northern Alpine foreland of southern Germany. Although the stratigraphy of adjacent profiles was investigated in detail previously, the new section is exceptional due to the occurrence of lacustrine intercalations in the loess sequence. Thus, the Bobingen site provides one of the very few lacustrine

records in a loess landscape of Middle Würmian age in the Northern Alps and their foreland (Starnberger et al., 2009; Heiri et al., 2014). Additionally, multi-proxy approaches for palaeoenvironmental reconstruction were not yet frequently applied to these LPS in the northern Alpine foreland, despite the fact that they provide valuable new insights to their interpretation (e.g. Antoine et al., 2013). Detailed micropalaeontological, isotopic, and geochemical methods were combined at the Bobingen site. Together with new optically stimulated luminescence (OSL) dates, this multi-proxy approach aims to shed new light on the palaeoclimate and palaeoenvironment during the Middle and Upper Würm in the northern foreland of the Alps.

2 Site description

The main terraces alongside the river Lech are a classical area of loess research in southern Germany for more than two decades (Aktas and Frechen, 1991; Schreiber and Müller, 1991; Bibus, 1995). They are subdivided into three areas locally called (from north to south) Rain, Langweid, and Augsburg high terraces (Schaefer, 1957; Scheuenpflug, 1979). The uppermost gravel units forming these terraces were dated to the penultimate Rissian glaciation in the Augsburg high terrace corresponding to Marine Isotope Stage (MIS) 6 (Frechen, 1999). Recent luminescence dating extends the ages for the basal unit of these gravel deposits to MIS 7 and older in the Langweid and Rain high terraces, whereas the age span for the top gravel unit was confirmed (Schielein et al., 2015). Previous studies described the lithological and pedogenic features of the loess sequence on the Augsburg high terrace and provided the first luminescence ages, placing it in the Würm (Becker-Haumann and Frechen, 1997; Frechen, 1999).

The new site studied here was exposed in a gravel pit close to Bobingen (48.277° N, 10.852° E; 521 m a.s.l.) and

is situated on the Augsburg high terrace (Fig. 1). On this terrace, glaciofluvial gravel and sand deposits are covered by a locally preserved and then prominent reddish ("rubified") palaeosoil and around 5 m of loessic sediments exposed in gravel pits of the company Lauter Sand Kies Beton GmbH east of Bobingen (Fig. 2). Previous OSL dating in a gravel pit a few hundreds of metres west of the outcrops described here suggested Mid-Würmian age of the loess deposits and Rissian age for the gravel deposit, while the rubified palaeosoil was attributed to the Eemian (Becker-Haumann and Frechen, 1997). The locality recently came into the focus of research again because of the discovery of megamammal teeth and bone fragments (*Coelodonta antiquitatis*, *Elephas primigenius*, *Equus ferus*) in the loessic deposits and channel fillings cut into the underlying gravel deposits (Gregor, 2012). In the course of these findings, the loess sections were reinvestigated, leading to the discovery of lacustrine deposits with aquatic gastropods, ostracods, and micromammal remains in an area named Gewanne II (Fig. 2). A detailed description of the stratigraphic succession, its fossil content, and facies is the topic of this study.

3 Material and methods

3.1 Sampling and fieldwork

The loess sections in the gravel pit at Bobingen were studied and sampled between the years 2011 and 2013. The investigated sections were 3 to 60 m apart from each other (Fig. 3). Sections I and II were sampled in 2011 for micropalaeontological and isotopic analyses; section IV was analysed in 2012 for XRF, grain-size, bulk geochemical, and pollen analyses; and section III was sampled in 2013 for OSL dating. The sections were linked using sedimentological and pedogenic marker layers (Fig. 3). The colour of the samples was determined using the Munsell Soil Color Charts at the fresh outcrops (Munsell Color, 2000).

3.2 Grain size and carbonate contents

About 10 to 20 g of each sample was weighed for grain-size determination. Carbonate content was removed prior to analysis with 10 % HCl. Decalcification could have changed the original grain-size composition of clastic components. However, this was unavoidable as carbonate particles were partly of pedogenic and biogenic origin. After decalcification, samples were repeatedly suspended with deionized water and centrifuged until achieving a neutral pH. Then they were dried at 105 °C. The decalcified samples were dispersed in 80 mL $Na_4P_2O_7$ solution (0.1 %) and shaken overnight. Afterwards, the coarse grain-size fractions were separated with a nested column of sieves with mesh widths of 2000, 630, 200, and 63 µm. Coarse fractions were determined by the weight of the sieve residues after drying. Silt and clay fractions (< 63 µm) were collected, resuspended,
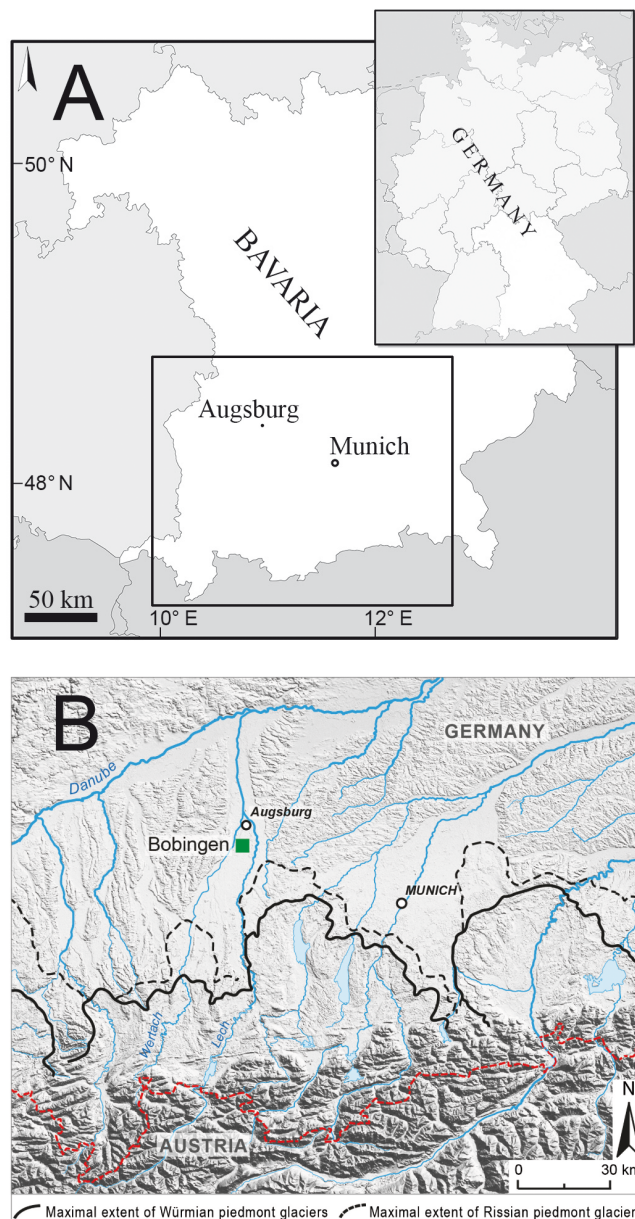
Figure 1. (a) Maps of Germany and Bavaria; the box indicates the inset shown in panel **(b)**. **(b)** Research area in the southern Bavarian Alpine foreland showing the maximal extents of Würmian and Rissian piedmont glaciers and the location of Bobingen. Base map modified from Scilands GmbH. The red line indicates the German–Austrian border.

and analysed using an X-ray absorption-based particle-size analyser (SediGraph III plus, Micrometrics).

The carbonate content of the samples was determined by measuring the partial pressure of CO_2 evolved in a closed volume after having added 6N HCl (25 %) in excess to 0.70 g of the homogenized sample. For these analyses a sealed container was used, described as *Karbonat-Bombe* (Müller and Gastner, 1971).
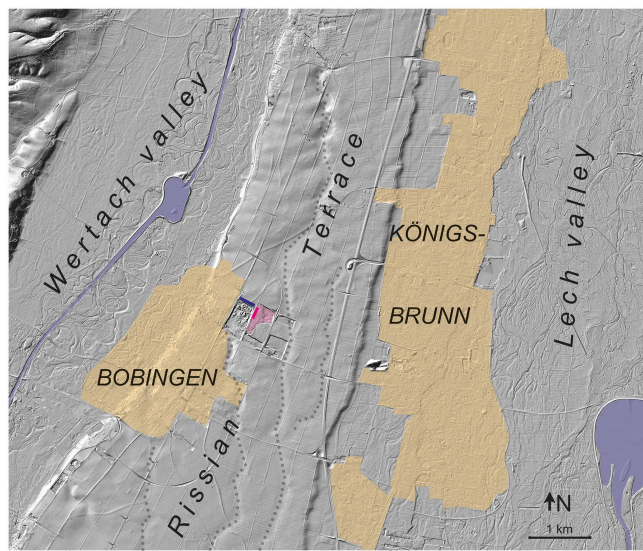
Figure 2. Digital elevation model (geographic basic data: Bayerische Vermessungsverwaltung) of the area around Bobingen showing the Rissian terrace surrounded by the lower terraces of the River Wertach to the west and the River Lech to the east. The present courses of these rivers are outlined in blue and the settlements of Bobingen and Königsbrunn in beige. The position of the investigated gravel pit and the loess profile are indicated by the pink area and line (Gewanne II), respectively. The blue line indicates the position of the profiles presented in Becker-Haumann and Frechen (1997). Dotted lines highlight inactive fluvial channels on the Rissian terrace, presumably originating from before the Last Glacial (Würmian) Maximum.

3.3 Organic geochemistry

A representative mixed sample from each unit of section I was homogenized with a mortar and pestle. An aliquot of 2–50 mg of the homogenized sample was weighed in tin capsules for determination of total carbon (TC) and nitrogen (TN) content. About 50–60 mg of another aliquot was weighed into a silver capsule and decalcified with 5 % and subsequently 20 % HCl at 70 °C on a heating plate for total organic carbon (TOC) contents and organic carbon isotope ratios ($\delta^{13}C_{org}$). The capsules were combusted in a continuous helium flow in an elemental analyser (NC2500, Carlo Erba) linked to an isotope-ratio mass spectrometer (DeltaPlus, Thermo-Finnigan). The carbon and nitrogen mass percentages were calculated from sample-peak areas using the elemental standards atropine and cyclohexanone-2,4-dinitrophenylhydrazone for calibration. Low TOC and TN contents were accounted for by calibrating with appropriately low weights of the standards. Total inorganic carbon (TIC) was calculated as difference between TC and TOC. All element content values are reported in % relative to dry mass. TOC / TN ratios are given as molar ratios. $\delta^{13}C_{org}$ values are given in ‰ according to the formula $\delta^{13}C = (R_{sample}/R_{standard} - 1) \times 1000$, where R is the isotope

ratio ($^{13}C / ^{12}C$) and Vienna Pee Dee Belemnite (VPDB) represents the international standard. The precision of the analyses calculated from lab standards routinely analysed together with the samples was better than 0.2 ‰ for $\delta^{13}C_{org}$ analyses and about 5 % for the TN and TOC determinations.

3.4 Palaeobiological methods (palynology, ostracods, gastropods)

About 1000–10 000 cm^3, depending on the microfossil content, of sediment from all lithological units was taken from sections I and II for micropalaeontological studies. The air-dried samples were dispersed in deionized water for 24 h and the suspension was sieved with tap water through sieves with mesh widths of 500 and 100 µm. If the suspension was incomplete, the dispersion procedure was repeated. Finally the sieve residues were rinsed with deionized water and dried for 74 h at 40 °C. The fossil remains, in particular molluscs and ostracods, were selected from the different size fractions using reflected-light microscopes (Leica MS 5 and Leica MZ6). For taxonomic identification of molluscs Zettler and Glöer (2006), Boschi (2011), Glöer and Meier-Brook (2003), Ložek (1964), and Welter-Schultes (2012) were used. Ostracods were identified using Fuhrmann (2012), Griffiths et al. (1993), Griffiths and Holmes (2000), and Meisch (2000). The classification of secondary carbonates followed Barta (2011) and Koeniger et al. (2014).

For pollen analyses only the lowest part of section IV was suitable, as it was deposited under reducing conditions indicated by darkish and bluish-grey colours in contrast to the overlying strata. The loessic upper part of the section was not investigated as oxic conditions commonly prevent the conservation of sufficient amounts of pollen (Moore et al., 1991). The pollen samples were taken from a sediment monolith of 52 cm length subsampled in the laboratory at 2 cm intervals. Each subsample contained 5 cm^3. The samples were first sieved to get the grain fraction smaller than 150 µm. Afterwards, they were treated with warm NaOH to deflocculate clays, with $ZnCl_2$ to remove silicates by heavy liquid separation, and finally by acetolysis following standard procedures (Faegri and Iversen, 1989; Moore et al., 1991). Pollen grains were identified at magnifications of 400 and 1000 by comparison with the pollen reference collection at the Department of Geography (University of Augsburg), the pollen key of Beug (2004), and primary literature for specific taxa (Clarke et al., 2001; Blackmore et al., 2003).

3.5 XRF scanning

For XRF scanning air-dried samples, each covering 10 cm of stratigraphic height in sediment section IV, were homogenized using a planetary mill (Pulverisette 5, Fritsch). Thereafter, 1 cm^3 of the powdered samples was filled
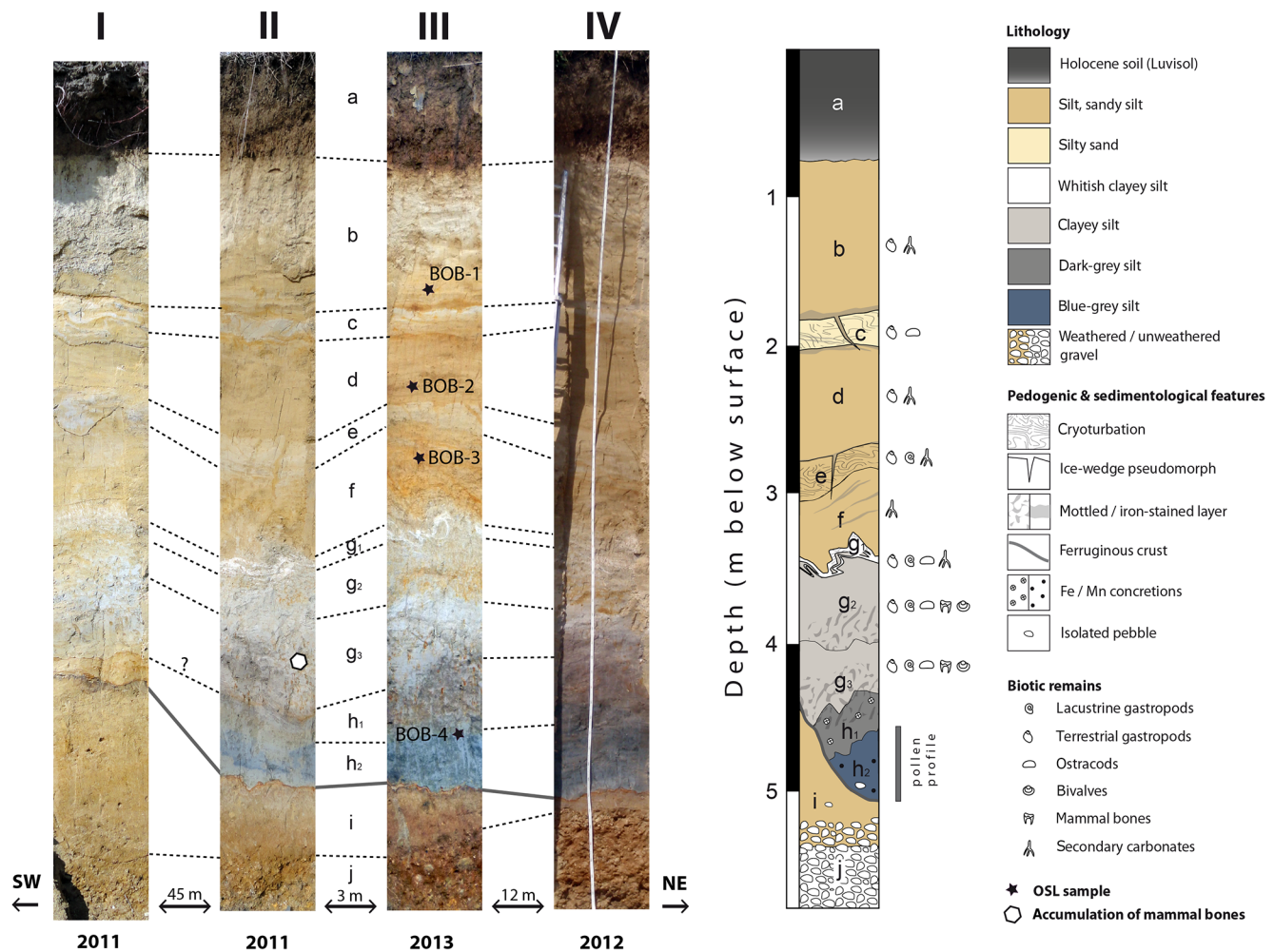
Figure 3. Photographs of the four loess sections I to IV sampled in the years 2011 to 2013 in Bobingen. The idealized composite profile summarizes the main sedimentological and palaeontological features observed. The positions of the OSL samples (labelled BOB-1 to BOB-4) are indicated in III and the position of accumulated micromammal bones in II. Sedimentary and pedogenic units are labelled a to j.

into sample cups and compacted manually. Samples were mounted equidistantly in a tray and analysed with an XRF core scanner (ITRAX, Cox Analytics) equipped with a Mo tube (Ohlendorf, 2017). Each sample was analysed at a constant exposure time of 100 s and a power setting of 30 kV and 20 mA. The XRF core scanner produces single dispersive energy spectra for each point measured. Unlike for conventional XRF measurements, instrumental calibrations are not routine. Counts of elements Al to U in the periodic system were registered and calculated by mathematical fitting of peak area integrals for the measured spectra using the software Q-Spec (Croudace et al., 2006). Here, we only present the good-quality elemental records obtained for K, Ca, Fe, and Ti. These elements appear to be most indicative for the pedogenic and sedimentological processes of interest. Problems with elemental scattering can occur with variations in water content and grain size (both excluded here as all samples were dried and ground before analyses) and content

of organic matter. To take care of such matrix effects as well as of sample inhomogeneity, all values (given in counts per second: cps) were normalized by dividing them with the respective coherent radiation (coh).

3.6 OSL dating

Four samples, labelled BOB-1 to BOB-4 from top to bottom, were taken for OSL dating with aluminium tubes (35 cm length, inner diameter 5 cm) from section III. All sample preparations and measurements were conducted at the Institute for Geological Sciences of the University of Bern. The outer layers of the OSL samples that may have been exposed to daylight were removed and all further work was carried out under subdued orange light in the laboratory. Samples underwent fine-grain preparation, where grains were treated with 32 % HCl to remove carbonates, 30 % hydrogen peroxide to remove any organic component, and

sodium oxalate to prevent aggregation of grains. To isolate the polymineral fine-grain fraction (4–11 μm), samples were settled in Atterberg cylinders utilizing Stokes' law. To obtain a quartz fraction, a portion of the polymineral fraction was immersed in 31 % hydrofluorosilicic acid for 10 days, followed by rinsing with 32 % HCl to remove fluorides. Grains were settled in acetone on stainless steel discs. All measurements were made on automated Risø TL/OSL DA-20 readers, fitted with an EMI 9235QA photomultiplier tube. Optical stimulation of quartz (OSL) was performed at 90 % power using blue LEDs (470 ± 30 nm; ∼ 41 and 48 mW cm^{-2} maximum power), and the OSL signal was detected through 7.5 mm of a Hoya U-340 transmission filter. For each sample, 400–500 g of material from the surrounding sediment was used for dose rate calculations, and the specific activities of U, Th, and K were determined using high-resolution gamma spectrometry (Preusser and Kasper, 2001). No evidence for radioactive disequilibrium in the uranium decay chain was found using the approach described by Zander et al. (2007).

Water contents were determined on fresh samples. About 20 % was added to these values to account for possible desiccation due to short time exposure of the outcrop. All estimated dose (D_e) measurements were made using a modified version of the single aliquot regenerative (SAR) dose protocol (Murray and Wintle, 2000; described in Table 1). Dose recovery and preheat tests were conducted using temperatures from 220 to 280 °C (Fig. 4a) in order to identify the appropriate temperature at which D_e was seen to be independent. A preheat temperature of 260 °C was chosen for all quartz measurements. This was held for 10 s and also applied to all test doses. For dose recovery tests, a laboratory dose of ∼ 150 Gy was given, and all samples were able to recover the dose within 10 % of unity for all temperatures (Fig. 4b). Recycling ratios confirmed the ability of the measurement sequence to correct for any change in sensitivity of the sample over time (Wintle and Murray, 2000). Recuperation of the signal following a zero regenerative dose was monitored, and this did not exceed 5 % of the natural signal for most aliquots. The response of the quartz fraction to IR stimulation was used to detect any feldspar contamination by determining a reverse IR depletion ratio (Duller, 2003). IR stimulation for 100 s at 50 °C was inserted before all measurements, but prior to that for the second recycle point. The IR depletion ratio remained above 0.90 for all aliquots and confirmed that the quartz signal does not suffer adverse effects from feldspar contamination. Mean D_e values were calculated using the Central Age Model (Galbraith et al., 1999).

An example of the OSL decay curve for sample BOB-1 is shown in Fig. 5, and confirms that the quartz signal displayed a rapid decay, indicating that it is dominated by the fast component. Quartz D_e values were determined using the first 0.4 s of the OSL decay curve and subtraction of a late background calculated using the last 40 s of a 60 s

Table 1. SAR protocol modified from Murray and Wintle (2003) applied to the fine-grained quartz fraction of all samples. L is the stimulation of the natural signal (n) and regeneration doses (x); T is the subsequent test dose.

Step	Treatment	Observed
1	Give dose[a]	
2	Preheat 260 °C for 10 s	
3[b]	IR stimulation for 100 s at 50 °C	
4	Blue stimulation for 60 s at 125 °C	L_n or L_x
5	Give test dose	
6	Preheat 260 °C for 10 s	
7	Blue stimulation for 60 s at 125 °C	T_n or T_x
8	IR stimulation for 100 s at 50 °C	
9	Return to 1	

[a] For L_n this is 0. [b] Not applied for second recycle point.
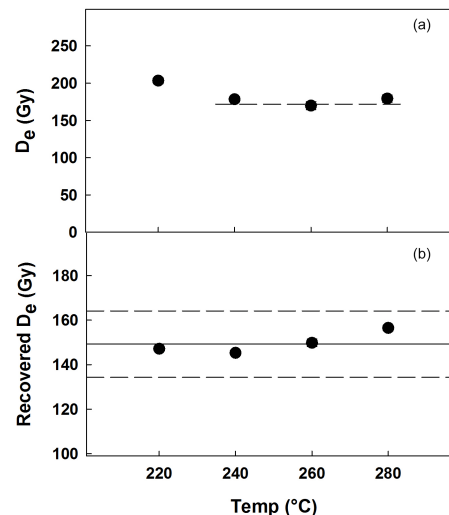
Figure 4. Preheat (**a**) and dose recovery (**b**) tests applied to BOB-4. For the dose recovery test, a regenerative dose of ∼ 150 Gy was applied. Dashed lines represent 10 % errors.

stimulation. The quartz OSL dose response fit best to a saturating exponential function, which was used to determine D_e values.

4 Results

4.1 Stratigraphy and lithology

Although the lithological features changed along the southwest–northeast-oriented transect of the sequence, several sedimentary and pedogenic units could be unambiguously traced through the sections and were labelled a to j (Fig. 3). Unit a represents the Holocene soil that developed above the Würmian loess. The 80 cm thick soil c is a Luvisol (*Parabraunerde* according to German soil classification) characterized by a Bt horizon. Below the
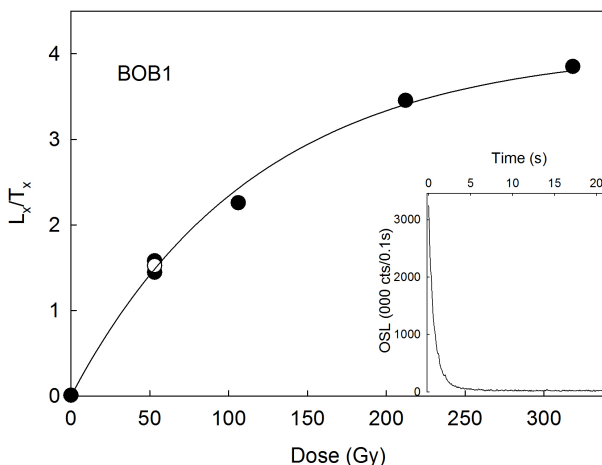
Figure 5. Dose response curve for sample BOB-1 together with the decay curve of a natural signal (inset). Empty circle indicates the recycle dose point. This behaviour is representative for all samples.

Holocene soil, a succession of alternating yellowish silty to pale-ochre silty-sandy loess horizons (b–f in Fig. 3) is exposed. The uppermost of these horizons (b) consists of 100–120 cm thick yellowish-ochre sandy silt (Munsell soil colour 2.5 Y6/4) and contains a few gastropod remains and secondary carbonates. The secondary carbonates were classified as combined hypocoatings and carbonate coatings. The underlying horizon c consists of leached yellowish-grey silty sand (2.5 Y6/3), which is sandwiched by iron-stained layers. It contains very few gastropods and ostracods. The thickness of layer c is 15–20 cm and ice wedge pseudomorphs of a few decimetre length cut through it from its surface. The wavy structure of this horizon points to cryoturbation. Horizon d is 60–80 cm thick and consists of yellowish-ochre sandy silt (2.5 Y6/4). It contains hypocoatings and a few gastropods. The 20–30 cm thick horizon e below resembles horizon c in colour (2.5 Y6/3) and sedimentary features. It consists of leached brownish grey silt, shows evidences of cryoturbation, and contains a combined form of hypocoatings and carbonate coatings (Fig. 9r), gastropods, as well as ice wedge pseudomorphs. Horizon f is a yellowish-ochre (2.5 Y6/4), 40–60 cm thick silt that partially shows weak stratification caused by iron staining. Except for combined hypocoatings and carbonate coatings no macroscopic biotic remains were found. A comparatively high fossil content characterizes horizon g with a thickness of about 1 m. It can be subdivided into three layers (g_1, g_2, and g_3 from top to bottom), differing in colour, but all three contain a comparatively diverse ostracod and lacustrine mollusc fauna in addition to terrestrial gastropods. The topmost layer g_1 is a pale-white (2.5 Y8/2) silt, strongly deformed by cryoturbation. It contains earthworm biospheroids (Fig. 9s) and few hypocoatings. Unit g_2 consists of greyish-brownish silt with mottled colouration (2.5 Y5/6

and 2.5 Y5/1). Unit g_3 consist of light-grey silt (2.5 Y6/2 and 2.5 Y6/4).

Unit h is characterized by absence of macroscopic biotic remains, low carbonate and clay contents, and a predominance of the medium-sized silt fraction (6.3–20 μm). It has a thickness of about 70 cm and was subdivided into an upper dark-grey (2.5 Y5/3) layer with rust stains (h_1) and a lower bluish-grey (4/5 GY) part (h_2) in the northern sections (II–IV; Fig. 3). The lower limit of h_2 is a ferruginous crust with an ascending position from north to south. In the southernmost section I the grey colour disappears completely due to oxidation and horizon h cannot be distinguished optically from the basal layer i. In other sections (II–IV), the basal layer i consists of brownish silt (7.5 YR 4/4) above the basal brown loamy weathered gravel (layer j, 7.5 YR 4/4).

4.2 OSL dating and age model

D_e values and ages are reported together with dosimetric data in Table 2. All aliquots measured passed the performance criteria, and the rapid decay of stimulation curves confirmed the identification of the fast component. When determining D_e values from quartz OSL signals, Wintle and Murray (2006) state that the calculation of uncertainties may become problematic above 2D0 (a value used to characterize 85 % saturation of the signal). 2D0 was calculated by fitting dose response curves to a single saturating exponential and values ranged between 2 and 300 Gy. All OSL ages were in stratigraphic agreement and provided ages between 20 and 50 kiloyears (ka). D_e values remained below 150 Gy and do not fall in a region for which methodological problems have been reported (Chapot et al., 2012; Lai, 2010; Lowick et al., 2010; Timar et al., 2010). Therefore these ages are considered reliable.

4.3 Organic geochemistry

The TC content varied between 0.2 and 0.3 % in the lower units h to j (Fig. 6), gradually increased from unit g_3 (1.5 %) to g_1 (6.4 %), and remained at a higher level (between 6.6 and 7.4 %) in the upper units. The TIC contents are only slightly less than TC values, indicating that most of the carbon is of carbonate origin and TOC contributes only a minor amount. The TOC contents were between 0.1 and 0.4 % in the lower part and around 0.1 % in the upper part of the section. TN correlates with TOC and TN values were between 0.01 to 0.02 % in the upper (units b to g_1) and between 0.04 and 0.06 % in the lower part (units g_2 to j). Unit g_3 had the highest TOC (0.4 %) and TN (0.06 %) contents. The $\delta^{13}C_{org}$ values also show a twofold pattern. The lower part of the section has values between −26.1 ‰ (unit h) and −24.0 ‰ (unit g_1). The values in the upper part are around −23.4 ‰ (units d and e). TOC / TN values were rather low and varied between 4 (units i, j) and 9 (unit g_3).

Table 2. Information about dosimetry, water content, D_e values, and calculated ages.

Sample	Sediment depth (cm)	Lithological unit	Grain size (µm)	N^b	Radionuclide concentration (Bq kg^{-1})[a]			Dose rate (Gy ka^{-1})	Water (%)	D_e (Gy)	Age (ka)[c]
					^{266}Ra	^{232}Th	^{40}K				
BOB-1	200	b	4–11	7	26.9 ± 0.4	18.8 ± 0.8	209.9 ± 5.3	1.7 ± 0.2	15	39.8 ± 0.4	23.1 ± 2.7
BOB-2	295	d	4–11	6	26.4 ± 0.3	16.4 ± 0.3	167.2 ± 5.7	1.5 ± 0.2	15	43.5 ± 1.2	28.5 ± 3.5
BOB-3	345	f	4–11	7	29.0 ± 0.6	19.6 ± 0.5	196.0 ± 3.0	1.6 ± 0.2	25	46.3 ± 1.1	29.6 ± 3.8
BOB-4	545	h$_1$/h$_2$	4–11	7	45.5 ± 0.9	47.7 ± 0.7	451.8 ± 5.2	2.8 ± 0.3	35	124.4 ± 1.9	45.2 ± 5.4

[a] Concentrations were converted to infinite matrix dose using the standard conversion factors of Adamiec and Aitken (1998). Cosmic radiation contribution was calculated using the present-day sample burial depth following Prescott and Hutton (1994), and attenuation factors were taken from Mejdahl (1987). [b] N is the number of individual aliquots contributing to the D_e value. [c] Errors on OSL ages represent 1 standard error.
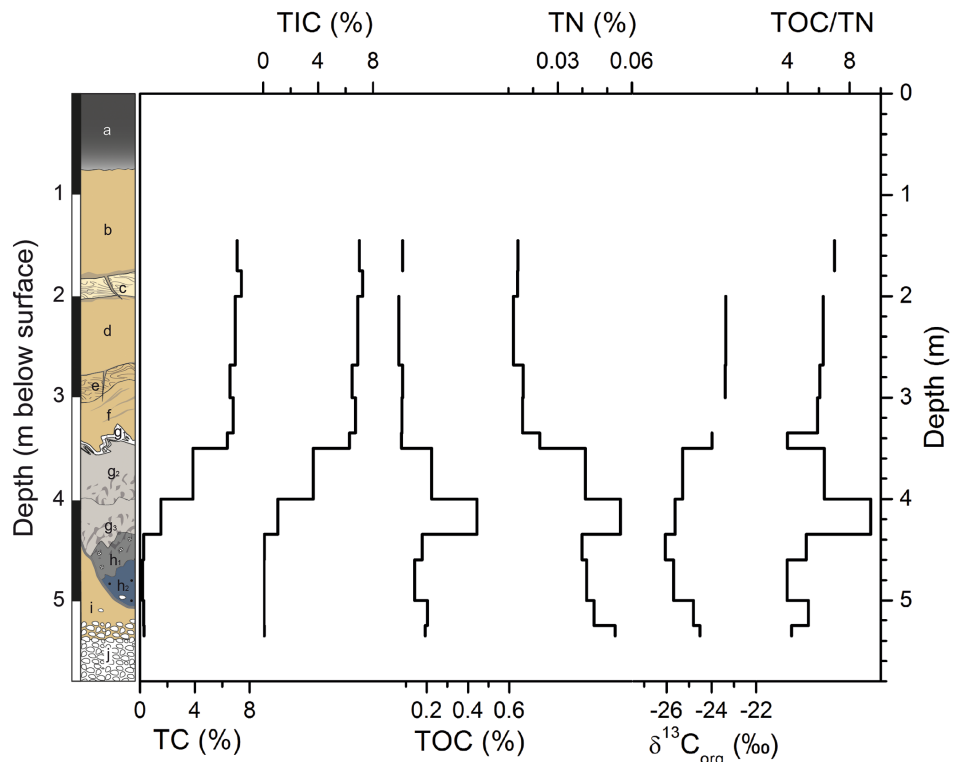
Figure 6. Organic geochemistry and isotope data from section I. Missing values are indicated by gaps.

4.4　Inorganic geochemistry and grain-size distribution

Results of carbonate-content, XRF, and grain-size analyses are shown in Fig. 6. An intense decalcification, represented by low carbonate contents (1–3 %) and low Ca counts, characterizes the modern Luvisol (unit a), whereas Ti, K, and Fe contents are relatively high. In contrast, the underlying units b to g$_2$ show high carbonate contents (42–56 %) and Ca counts in agreement with the high TIC contents recorded in section I (Fig. 6), while Fe, K, and Ti decrease in these units. Below layer g$_3$ the carbonate content drops to 10 % and subsequently further decreases until values of around 1 % are reached in horizon i. Decreased Ca and increased Ti, K, and Fe contents accompany the drop of carbonate values starting

at the base of g$_3$. In the basal gravel these trends reverse again and Ti, K, and Fe decrease while Ca increases (Fig. 7).

The grain-size distribution of the section shows increased clay content in the modern Luvisol (Fig. 7). In the underlying loess units the sand fraction increases and reaches maximum values in unit c. Below this unit, the sand fraction gradually decreases and reaches low values in unit g$_3$ to h$_2$. Unit g$_3$ is also characterized by a high amount of clay, while the underlying units h$_1$ and h$_2$ contain almost exclusively silt. The sand and clay fractions increase again in unit i and towards the top of unit j. Finally, the coarse sand fraction as well as the clay fraction are increasing in unit j.
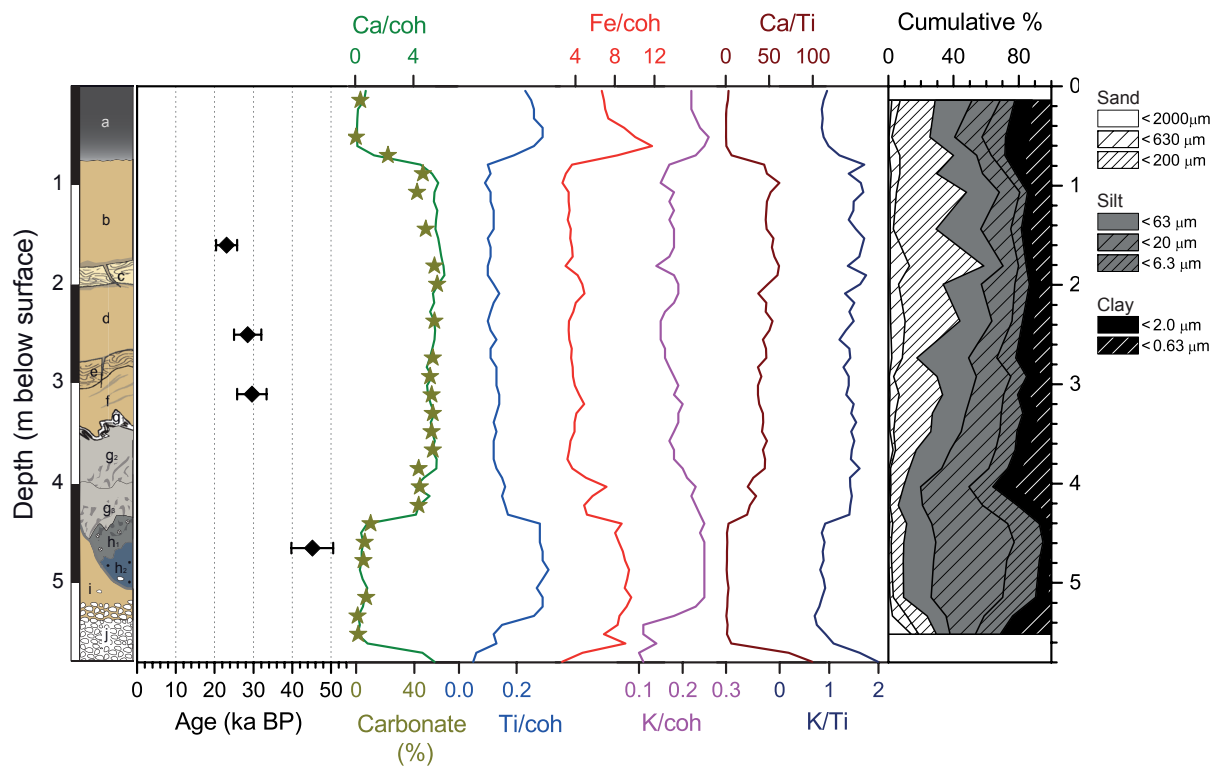
Figure 7. Element contents, grain-size distribution, and carbonate contents from section IV. The relative element contents derived from XRF analyses were divided by values of coherent radiation (coh) to account for matrix effects. Ages are interpolated from section III. Carbonate contents (stars) are plotted on top of the Ca curve to demonstrate the high accordance of both datasets.

4.5 Vegetation record

The pollen profile comprises the lithological unit h_2 and the lowermost part of h_1. Grass taxa (Poaceae, Cyperaceae) dominate most of the pollen profile (Fig. 8). Among the arboreal pollen, *Pinus* is most abundant. The other arboreal taxon, *Betula*, occurs regularly, while *Picea*, *Alnus*, *Corylus*, and *Salix* as well as *Hippophaë*, *Ephedra distachya*-type, and *E. fragilis*-type were found only sporadically. Towards the top of the profile *Juniperus*, together with *Pinus* and *Betula*, becomes more frequent. Increased values of Cichorioideae in some stratigraphic levels are probably related to selective preservation of this resistant pollen type. The herbs *Artemisia*, *Thalictrum*, Brassicaceae, and Chenopodiaceae occur discontinuously throughout the profile. Aquatic macrophytes are represented by abundant pollen of the *Ranunculus aquatilis* group in the lower part of the profile peaking in unit h_2, which is in accordance with the distribution of the chlorococcalean green algae *Pediastrum* and *Botryococcus*. All these aquatic taxa decrease towards the top. A single find of a seed of the *Ranunculus aquatilis* group from unit g_3 (Fig. 9p) may indicate the presence of aquatic macrophytes also at a later time. Other aquatic macrophytes represented in the pollen record are *Myriophyllum spicatum* and *M. alterniflorum*. The pollen concentrations are very low in the whole profile and vary

between 11 and 100 pollen grains in the sample volume of $5\,cm^3$.

4.6 Faunal remains

The results of screening for microfossils are listed in Table 3. Secondary carbonates were evident in all loessic units in the upper part of the profile except for unit c but were lacking in the layers below g_2. Bivalves (Fig. 9a–d) only occurred in g_2 and g_3. Gastropods (Fig. 9e–o) were present in two groups of layers: an upper part including c, d, and e and a lower part comprising g_1, g_2, and g_3. Ostracods (Fig. 10) were found in layers c, g_1, g_2, and g_3. Overall, the microfossil yield was low for most of the horizons, except for units g_2 and g_3, which provided enough specimens for statistical analyses. In all other layers, less than 30 specimens were found from each organism group; therefore these were not statistically evaluated. Bivalves were represented by *Pisidium hibernicum*. While in the upper part the gastropod assemblages consisted of a single species only (*Succinella oblonga*), the assemblages in the lower part were more diverse and included mainly aquatic species. The dominant gastropod taxon in g_2 and g_3 is *Gyraulus acronicus* with 78 and 60 %, respectively. The second- and third-most common species are *Radix labiata* and *Valvata piscinalis alpestris*
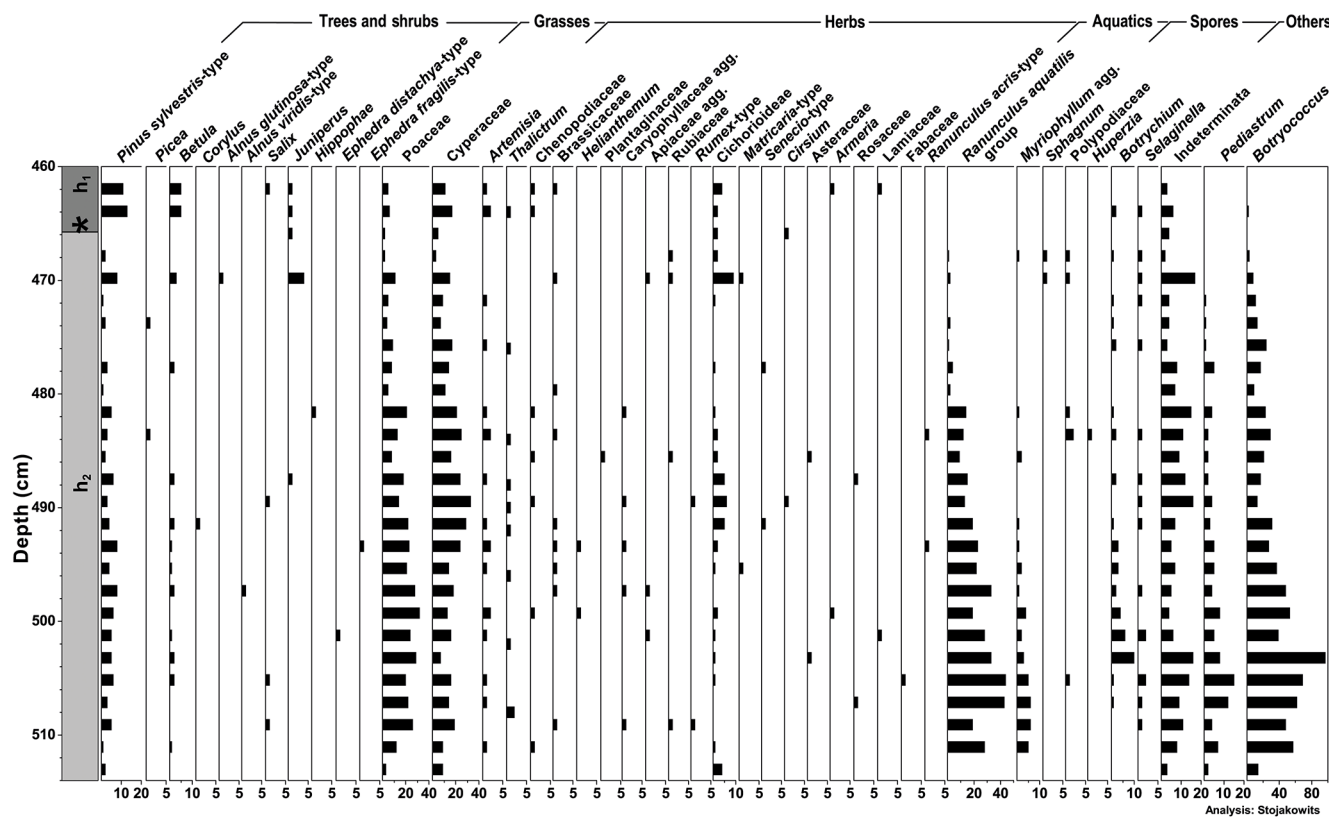
Figure 8. Pollen diagram of the monolith taken from unit h_2 and the base of h_1 in section IV showing the counted values from $5\,cm^3$ of sediment. The asterisk marks the position of the OSL sample BOB-4. The landscape was characterized by open tundra-like vegetation with steppe elements and groups of shrubs.

in both units. In unit g_3 *Succinella oblonga* is present with 5.5 % while it is almost absent in g_2 (0.8 %). Limacidae and *Anisus spirorbis* occur in both units with less than 1 %. The ostracod assemblages in units g_2 and g_3 are mainly composed of *Candona candida* with 82 and 92 %, respectively. In unit g_2 *Limnocytherina sanctipatricii* is the second-most dominating species (13 %) and in unit g_3 *Cyclocypris ovum* (4 %). As a further taxon *Pseudocandona* sp. occurs with minor percentages in both units (Fig. 8).

Bones of micromammals were found in units g_2 and especially in g_3. Three teeth of the species *Lemmus lemmus* were identifiable (Fig. 9q). A fragment of a megamammal tooth found in unit g_3 in section III most likely belonged to an equid.

5   Discussion

5.1   Chrono-, bio-, and lithostratigraphic framework

The uppermost part of the gravel deposits in the gravel pit directly adjacent to the NW to our sites at Bobingen provided OSL ages of 152 ± 18 and 160 ± 53 ka typical for the penultimate Rissian glaciation (Frechen, 1999). The palaeosoil remnants indicated by layer j in our profiles

are corresponding to a Bt horizon described previously as remnants of a truncated brown forest soil (layer B in Frechen, 1999). It was suggested to be of Eemian age (Bibus, 1995; Becker-Haumann and Frechen, 1997). Our luminescence data cannot directly contribute to the question whether a sedimentation gap exists in the Bobingen LPS and whether the Lower Würm is entirely missing. A Lower Würmian hiatus, however, is likely, considering the small amount of sediment that, if sedimentation were continuous, would have been deposited from the brownish relic soil (unit j), attributed to an age of the end of the Eemian at 119 ka (Rasmussen et al., 2014) until the layer containing our lowermost OSL date. This OSL date is at the transition of unit h_1/h_2 and provides an age of 45.2 ± 5.4 ka. The Middle Würm lasted from 74 to 30 ka (Preusser, 2004) and includes MIS 3 (59–29 ka; Voelker et al., 2002). Thus, the base of unit h_2 is of Middle Würmian age.

Schielein and Schellmann (2016) recently mapped the Quaternary deposits in the Lech and Wertach valleys around Bobingen. They dated a LPS succession similar to the one described here located about 30 m west of it in an adjacent gravel pit. Their infrared stimulated luminescence (IRSL) age for a layer corresponding to units h_1/h_2 is 47 ± 5 ka and,

Table 3. Semi-quantitative distribution of faunal remains in sections I and II.

Taxon	Abundance*												
Unit	b	c	d	e	f	g_1	g_2	g_3	h_1	h_2	i_1	i_2	j
Gastropods													
Succinella oblonga	0	2	1	2	0	2	1	2	0	0	0	0	0
Anisus spirorbis	0	0	0	0	0	0	1	1	0	0	0	0	0
*Gyraulus acronicus*s	0	0	0	1	0	0	2	2	0	0	0	0	0
Radix labiata	0	0	0	0	0	1	2	2	0	0	0	0	0
Valvata piscinalis alpestris	0	0	0	0	0	0	2	2	0	0	0	0	0
Limacidae	0	0	0	0	0	0	1	1	0	0	0	0	0
Ostracods													
Candona candida	0	2	0	0	0	1	2	2	0	0	0	0	0
Cyclocypris ovum	0	0	0	0	0	0	1	1	0	0	0	0	0
Limnocytherina sanctipatricii	0	2	0	0	0	0	2	1	0	0	0	0	0
Pseudocandona sp.	0	0	0	0	0	0	1	1	0	0	0	0	0
Bivalves													
Pisidium hibernicum	0	0	0	0	0	0	1	1	0	0	0	0	0
Mammals													
Lemmus lemmus	0	0	0	0	0	0	1	2	0	0	0	0	0
Equus sp.	0	0	0	0	0	0	0	1	0	0	0	0	0

* Abundance categories listed are absent ("0", $N = 0$), rare ("1", $0 < N \leq 4$), and frequent ("2", $N > 4$). The number of specimens (N) is related to a sediment volume of about $1000\,\mathrm{cm}^3$.

thus, excellently matches our dating result. The underlying stratum, corresponding to unit i in our section, was thicker and more structured there. It provided an IRSL date of 59 ± 9 ka reaffirming the Middle Würmian age of the lower part of the LPS section (Schielein and Schellmann, 2016).

The almost complete lack of clay during the deposition of unit h_1 and h_2 may point to changing morphodynamic conditions during that time possibly related to higher wind speed or higher availability of clastic material from local (i.e. proximity of Wertach and Lech valleys) or regional sources. The palynological data of unit h_2 and the base of h_1 confirm the lack of Early Würmian strata and thus a hiatus. The Early Würm of the Füramoos pollen record from the northern Alpine foreland contains a markedly higher amount of *Picea* and *Pinus* pollen (Müller et al., 2003) than our pollen record. Thus, the units h_1 and h_2 were definitely deposited after the Early Würm. These units are also decalcified (Fig. 7) and thus indicate soil formation. A relative increase in Ti and Fe is contrasted by a decrease in Ca in these units. Ti is not affected by varying redox conditions (Haug et al., 2001) and increases with the concentration of weathering-resistant minerals. The similarity of Fe and Ti records (Fig. 7) suggests weathering as a predominant process for the enrichment of Fe in our sections. In contrast, Ca is removed by pedogenesis due to elution and decalcification, making the Ca / Ti ratio a primary weathering proxy (Fischer et al., 2012). However, Ca can also be re-precipitated as

secondary carbonates. K is an element that is also easily eluted, and thus the K / Ti ratio serves as an additional weathering proxy (Fischer et al., 2012). The similar courses of K / Ti and Ca / Ti (Fig. 7) confirm these considerations. As a consequence, the low K / Ti and Ca / Ti ratios of units h_1, h_2, and i indicate similarly strong weathering as in the modern soil (unit a) as a result of pedogenesis. The greyish-bluish colour preserved in units h_2 to g_2 in sections II, III, and IV, but not in section I, points to a gleyic soil horizon formed under water-saturated conditions. The frequently occurring aquatic palynomorphs in the pollen record of this layer support this interpretation. The absence of reduced features at the base of section I is likely related to secondary oxidation indicated by the ferruginous crust irregularly intersecting the bases of the sections (Fig. 3).

Bibus (1995) assigned a rubiginous, silty loam exposed at an adjacent loess section at Bobingen to the Böckingen soil. This horizon had approximately the same stratigraphic position as units h_1 and h_2 and was overlain by a loamy horizon with an olive tint that was attributed to the Lohne soil (Bibus, 1995). However, neither attributions was documented by independent dating methods at that time. Indeed, the age of h_1 and h_2 is approximately time-equivalent to the so-called Böckingen soil, originally described as a cambic soil horizon from the Neckar area in southern Germany (Bibus, 2002). The Böckingen soil was dated with luminescence methods to ca. 45 ka in southern Germany and Austria (Frechen, 1999;
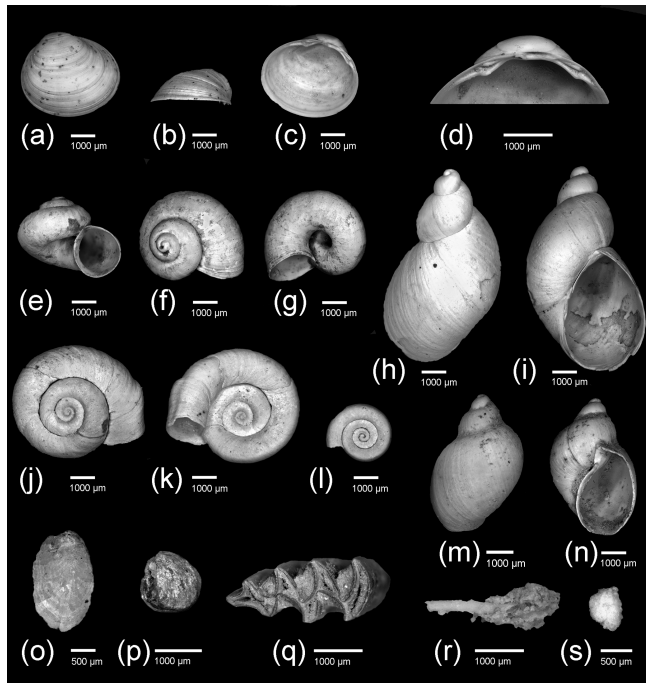
Figure 9. Bivalves, gastropods, and other fossil remains extracted from e (**h, i, r**), g$_1$ (**s**), g$_2$ (**l**), and g$_3$ (**a–g, j, k, m–q**). All fossils are from section II except (**s**) (section I). (**a–d**) *Pisidium hibernicum*: right valve exterior (**a**), lateral (**b**), interior (**c**), and hinge area (**d**). (**e–f**) *Valvata piscinalis alpestris*. (**h, i**) *Succinella oblonga*. (**j, k**) *Gyraulus acronicus*. (**l**) *Anisus spirorbis*. (**m, n**) *Radix labiata*. (**o**) Limacidae indet. (**p**) Seed of *Ranunculus aquatilis*. (**q**) *Lemmus lemmus*. (**r**) Example of secondary carbonates: partly exposed carbonate coating inside hypocoating. (**s**) Earthworm biospheroid. Scale bars for (**o, s**): 500 µm and for (**a–n, p–r**) 1000 µm.

Figure 10. Scanning electron micrographs of ostracod species extracted from section II (g2 and g3). (**a, b**) *Candona candida*: right valve exterior (**a**) and interior (**b**). (**c, d**) *Pseudocandona* sp.: right valve exterior (**c**) and interior (**d**). (**e, f**) *Cyclocypris ovum*: left valve exterior (**e**) and interior (**f**). (**g, h**) *Limnocytherina sanctipatricii*: male left valve exterior (**g**) and female right valve exterior (**h**). Scale bars 100 µm.

Terhorst et al., 2002, 2015) and is considered to be time-equivalent to the Hengelo interstadial in northern Germany (Frechen 1999). However, the pedogenic features of a cambic soil horizon, in particular a brownish pigmentation, are not fulfilled for the units h$_1$ and h$_2$ in our profile. Instead gleyic features dominate both units. The 32 to 28 ka old Lohne soil is overlying the Böckingen soil in many loess sections in central Europe (Terhorst et al., 2015). In this context it should be mentioned that according to new data the Lohne soil probably evolved during several Greenland Interstadials. Nevertheless, it is still a valuable pedostratigraphic marker (Sauer et al., 2016). It is possible that units g$_3$ to g$_1$ are time-equivalent to this soil, but, as outlined below, they are not primarily pedogenic but of lacustrine origin at our site.

The OSL date of 29.6 ± 3.8 ka in the centre of unit f indicates that this unit was deposited around or shortly after the transition from the Middle to the Upper Würm. The age of unit d is only about 1 kyr younger than that of unit f when the average values of age determinations without error margins are considered. This would indicate that the sedimentation rate in the upper part of the section had

increased substantially due to enhanced loess deposition. The uppermost age of unit b (23.1 ka) is centred in the Last Glacial Maximum (LGM, 26.5–18.5 ka; Clark et al., 2009; Wirsig et al., 2016). Accordingly, full glacial conditions persisted during the deposition of unit b. In the area around Regensburg, about 120 km northeast of Bobingen, the accumulation of loess ended in the Oldest Dryas at 16.5 ka based on luminescence dating (Buch and Zöller, 1990).

5.2 Palaeoenvironmental reconstruction

5.2.1 Middle Würm

As outlined above, the Middle Würm covers MIS 3 and is represented by the units j to f in our sections. The pollen spectra from units h$_1$ and the base of h$_2$ point to an open tundra-like vegetation consisting of steppe elements (e.g. *Artemisia*, Chenopodiaceae, *Helianthemum*, *Thalictrum*), Poaceae, some Cyperaceae, and many herbs. At some places

shrub formations consisting of *Juniperus*, *Salix*, and probably a few pine (*Pinus sylvestris*) and birch (*Betula*) trees occurred in the further surroundings. The open vegetation, which grew under relatively cold climatic conditions, is also indicated by *Botrychium* and *Selaginella selaginoides* as well as by low pollen concentrations. Water plants (*Ranunculus aquatilis* group, *Myriophyllum spicatum*, and *M. alterniflorum*) and Cyperaceae dominated the local vegetation and have grown at the edges of a stagnant water body or a slow-flowing stream. These strata might reflect a climatic change related to short-term warming events commonly known as Dansgaard–Oeschger events or Greenland interstadials (GI) from the Greenland ice cores. Twenty-five of these warming events are known for the last glacial period (Rasmussen et al., 2014). Temperature increases of up to 15 °C in a few centuries were reconstructed during MIS 3 for these warm phases in Greenland (Huber et al., 2006). The most likely corresponding equivalent for the warm phase reflected in the pollen record of Bobingen is the relatively long period of warm events that started with GI-14 at 54.2 ka and lasted until GI-12 at 44.3 ka (Rasmussen et al., 2014).

The stagnant water body already present in units h_1 and h_2 persisted or even extended during the sedimentation of g_3 and g_2, as aquatic faunal remains indicate. In units g_3 and g_2, the sphaeriid bivalve *Pisidium hibernicum* points to a lentic water body (Zettler and Glöer, 2006). This palaearctic species has been described as titanoeuryplastic (Meier-Brook, 1975).

Aquatic gastropods (*Gyraulus acronicus*, *Radix labiata*, *Valvata piscinalis alpestris*) occur frequently in units g_3 and g_2. The Holarctic species *Gyraulus acronicus* presently inhabits lakes, ponds, swamps, and pools (Ložek, 1964; Glöer and Meier-Brook, 2003). *Anisus spirorbis* is present in small stagnant temporary water bodies and swamps, whereas *Radix labiata* additionally occurs in slowly flowing water bodies (Glöer and Meier-Brook, 2003). The boreal-Alpine gastropod *Valvata piscinalis alpestris* is common in larger ponds and streams with muddy sediment (Ložek, 1964). The aquatic gastropod fauna is complemented by remains of terrestrial Limacidae and by the species *Succinella oblonga*. Both taxa are euryoecious. Limacidae occur in warm and wet vegetation-covered habitats with open areas like humid grasslands, open forests, swamps, and brooks (Ložek, 1964; Danukalova et al., 2015). *Succinella oblonga* is a "damp species" that inhabits wet places with sparse vegetation such as humid grasslands and swampy areas (Ložek, 1990; Moine et al., 2005).

Ostracods also confirm the existence of a water body during the deposition of units g_3 and g_2 and to a lesser extent in unit g_1. The ostracod species *Candona candida* is nowadays common in habitats with a broad range of pH and salinity (Meisch, 2000). The species is oligothermophilic and typical for stagnant water bodies with lower temperatures, often influenced by cold groundwater inflows (Absolon, 1973; Fuhrmann, 2012). In the sedimentary context, its

valves are predominantly found in lake marls and to a lesser extent in brook, spring, and peat deposits (Absolon, 1973). The ostracod *Limnocytherina sanctipatricii*, a cold-stenothermal form, is typical for deeper lakes (Absolon, 1973), where it lives in depths up to 250 m (Löffler, 1969) and less frequently in smaller permanent water bodies such as swampy ponds and small creeks (Meisch, 2000). In central Europe, it presently prefers the cooler profundal areas of lakes but is supposed to have inhabited shallower stagnant water bodies during the last glacial period (Fuhrmann, 2012). *Cyclocypris ovum* is a rather euryoecious species that is reported frequently from the littoral zones of lakes and less from temporary pools and springs (Meisch, 2000). The species prefers permanent and stagnant water bodies with cool water temperature (Fuhrmann, 2012).

All three ostracod species have been previously identified from lacustrine sediments of southern Germany as typical members of Würmian ostracod assemblages, the so-called *candida* fauna (Absolon, 1973). Absolon grouped roughly a dozen species (with *Cyclocypris ovum* and *L. sanctipatricii* being two of them) around *Candona candida* as the leading elements in these assemblages. This *candida* fauna was opposed to the so-called *cordata* fauna, referring to the thermoeuryplastic species *Metacypris cordata* and its accompanying species, typical for the warmer Holocene climate and related higher productivity in lakes. The shift from *candida* fauna to *cordata* fauna has ever since been recorded as indicative for the transition from the last glacial period to the Holocene in central Europe (Günther, 1986; Griffiths and Holmes, 2000; Meisch, 2000).

The ostracods in the Middle Würmian lacustrine deposits at Bobingen, although not rich in species, represent a typical last glacial lacustrine fauna. It points to the presence of a small but persistent stagnant water body, which possibly developed in an inactive fluvial channel or in patterned ground during comparatively mild and humid periods of the Würm. Fluvial channels are recognizable by slight topographic differences in the digital elevation model (Fig. 2) and were outlined as polygenetic valley fillings of Pleistocene to Holocene age by Schielein and Schellmann (2016). Their south–north orientation and their position on the surface of the Rissian high terrace imply that they were formed before the LGM. Already Bibus (1995) mentioned that the gravel pit of Bobingen is located close to a former, now refilled, depression.

The organic carbon content of typical glacial loess deposits in northwestern Europe is less than 0.1 %. Thus, TOC values of the Middle Würmian strata are above average and similarly high as reported for interstadial palaeosoils of the same age at the Czech loess site Dolní Věstonice (Antoine et al., 2013). Thus, the increased TOC values peaking around unit g_3 could indicate organic carbon accumulation during a period of climatic amelioration in the Middle Würm. Alternatively, the higher TOC values were caused by better preservation conditions of organic matter under

waterlogged conditions (Zech et al., 2013). The $\delta^{13}C_{org}$ values are another indicator for climatic changes during loess deposition. $\delta^{13}C_{org}$ values between -26 and $-23\,\%o$ were recorded from European loess deposits. During periods of higher organic carbon deposition lower values were recorded (Antoine et al., 2013), a pattern similar to our record (Fig. 6). Apparently wetter and milder periods led to higher productivity and organic carbon deposition in combination with lower $\delta^{13}C_{org}$ values. Indicators of permafrost occur, especially towards the end of the Middle Würmian deposits, when TOC values decrease and $\delta^{13}C_{org}$ values increase. In particular, unit g_1 is heavily affected by cryoturbation that has occurred during or shortly after deposition.

In summary, the Bobingen profile contains a diverse lacustrine Middle Würmian faunal assemblage that indicates a relatively mild climate. It represents one of the very few lacustrine records of Middle Würmian age in the Northern Alps and their foreland (Heiri et al., 2014).

5.2.2 Upper Würm

The Upper Würm approximately corresponds to MIS 2 and comprises the units f to b. The stagnant water body persisted until shortly before the end of the Middle Würm. In unit f, dated at around 30 ka, no lacustrine zoological indicators are found anymore and a typical loess deposition started. However, a few findings of *Gyraulus acronicus* in unit e and of the ostracod taxa *Candona candida* and *Limnocytherina sanctipatricii* in unit c indicate the return of stagnant water bodies during these short episodes directly before 29 and 23 ka BP, respectively. Since the species *L. sanctipatricii* is restricted to stagnant and permanent water bodies (no resting eggs), an influx of live specimens from and by rivers of nearby valleys can be excluded. A redeposition of dead and fossil material from putative nearby stagnant water bodies is highly unlikely due to the presence of juvenile and adult valves in our samples (lack of sorting effects) and the high quality of preservation. The bleaching of horizons e and c was the result of redoximorphic processes under permanent waterlogging (Terhorst et al., 2014). Such horizons were commonly interpreted as tundra-gley soils, Gelic Gleysols, or Cryosols (Frechen, 1999; Antoine et al., 2009; Terhorst et al., 2014; Lehmkuhl et al., 2016). Regionally they are also called *Nassböden*, and up to six of these horizons were reported as Erbenheim soils in western Germany (Semmel, 1968; Lehmkuhl et al., 2016). The presence of sporadic lacustrine ostracod and gastropod species in these layers at the Bobingen site, in conjunction with pedogenic features such as bleaching (Fig. 3), could indicate warmer climatic conditions. This interpretation is in agreement with observations at the Nussloch site in southwestern Germany. Incipient soil formation combined with reduced aeolian sediment deposition at that site was related to climatic ameliorations equivalent to the short Greenland interstadials (Antoine et al., 2009). GI-4 and GI-

2 at 28.9 and 23.3 ka, respectively, are possible candidates for the warming events observed in our record. However, age uncertainties do not allow a definite correlation. Other GIs than the ones mentioned may not be recorded in our Upper Würmian record because of hiatuses or inadequate temporal resolution, issues which also challenge the interpretation of other loess sections (e.g. Lehmkuhl et al., 2016). Ice wedge pseudomorphs cutting through units c and e indicate sudden cooling under periglacial conditions soon after deposition of these layers.

6 Conclusions

In summary, the Bobingen outcrop contains a Middle and Late Würmian LPS intercalated by lacustrine layers. A gleyic soil developed during MIS 3 around 45 ka and provided a tundra-like palynoflora dominated by steppe elements, a few shrubs, as well as pine and birch. A stagnant water body persisted in this environment until shortly before 30 ka. This stagnant water body hosted submerged and floating aquatic macrophytes and a cool, temperate but not diverse ostracod and gastropod fauna. The environmental setting changed during the transition to the Upper Würm (MIS 2) when the water body disappeared and the gastropod fauna was reduced to a single terrestrial species (*Succinella oblonga*). However, two short milder episodes, represented by units e and c, are indicated by tundra-gleyic features and the reoccurrence of lacustrine species. These relatively warmer periods are presumably related to warming events reported from Greenland ice cores, most likely to GI-4 and GI-2, respectively, based on OSL dates.

References

Absolon, A.: Ostracoden aus einigen Profilen spät- und postglazialer Karbonatablagerungen in Mitteleuropa, Mitteilungen der Bayerischen Staatssammlung für Paläontologie und historische Geologie, 13, 47–94, 1973.

Adamiec, G. and Aitken, M.: Dose-rate conversion factors: update, Ancient TL, 16, 37–50, 1998.

Aktas, A. and Frechen, M.: Mittel- bis jungpleistozäne Sedimente der Hochterrasse in der nördlichen Iller-Lech-Platte, Geologisches Institut der Universität zu Köln, Sonderveröffentlichungen, 82, 19–41, 1991.

Antoine, P., Rousseau, D.-D., Moine, O., Kunesch, S., Hatté, C., Land, A., Tissoux, H., and Zöller, L.: Rapid and cyclic aeolian deposition during the Last Glacial in European loess: a high-resolution record from Nussloch, Germany, Quaternary Sci. Rev., 28, 2955–2973, 2009.

Antoine, P., Rousseau, D.-D., Degeai, J.-P., Moine, O., Lagroix, F., Kreutzer, S., Fuchs, M., Hatté, C., Gauthier, C., Svoboda, J., and Lisá, L.: High-resolution record of the environmental response to climatic variations during the Last Interglacial-Glacial cycle in Central Europe: the loess-palaeosol sequence of Dolní-Vestonice (Czech Republic), Quaternary Sci. Rev., 67, 17–38, 2013.

Barta, G.: Secondary carbonates in loess-paleosoil sequences: a general review, Cent. Eur. J. Geosci., 3, 129–146, 2011.

Becker-Haumann, R. and Frechen, M.: Vergleichende Lumineszenz-Datierungen mit IRSL und TL am Deckschichtenprofil Bobingen/Lechtal, Z. Geol. Wissenschaft., 25, 617–633, 1997.

Beug, H.-J.: Leitfaden der Pollenbestimmung für Mitteleuropa und angrenzende Gebiete, Pfeil, München, Germany, 542 pp., 2004.

Bibus, E.: Äolische Deckschichten, Paläoböden und Mindestalter der Terrassen in der Iller-Lech-Platte, Geologica Bavarica, 99, 135–164, 1995.

Bibus, E.: Zum Quartär im mittleren Neckarraum: Reliefentwicklung, Löß/Paläobodensequenzen, Paläoklima, Tübinger Geographische Arbeiten D, 8, 1–236, 2002.

Blackmore, S., Steinmann, J. A. J., Hoen, P. P., and Punt, W.: The Northwest European Pollen Flora, 65. Betulaceae and Corylaceae, Rev. Palaeobot. Palyno., 123, 71–98, 2003.

Boschi, C.: Die Schneckenfauna der Schweiz. Ein umfassendes Bild- und Bestimmungsbuch, Haupt, Bern/Stuttgart/Wien, 624 pp., 2011.

Brunnacker, K.: Der würmzeitliche Löß in Bayern, Geologica Bavarica, 19, 258–265, 1953.

Buch, M. and Zöller, L.: Gliederung und Thermolumineszenz-Chronologie der Würmlösse im Raum Regensburg, E&G Quaternary Sci. J., 40, 63–84, 1990.

Chapot, M. S., Roberts, H. M., Duller, G. A. T., and Lai, Z. P.: A comparison of natural- and laboratory-generated dose response curves for quartz optically stimulated luminescence signals from Chinese Loess, Radiat. Meas., 47, 1045–1052, 2012.

Clark, P., Dyke, A. S., Shakun, J. D., Carlson, A. E., Clark, J., Wohlfarth, B., Mitrovica, J. X., Hostetler, S. W., and Marshall McCabe, A.: The last glacial maximum, Science, 325, 710–714, 2009.

Clarke, G. C. S., Punt, W., and Hoen, P. P.: The Northwest European Pollen Flora, 51. Ranunculaceae, Rev. Palaeobot. Palyno., 69, 117–271, 2001.

Croudace, I. W., Rindby, A., and Rothwell, R. G.: ITRAX: description and evaluation of a new multi-function X-ray core scanner, in: New Techniques in Sediment Core Analysis, edited by: Rothwell, R. G., Special Publications, Geological Society, London, UK, 51–63, 2006.

Danukalova, G., Osipova, E., Khenzikhenova, F., and Sato, T.: The molluscs record: A tool for reconstruction of the Late Pleistocene (MIS 3) palaeoenvironment of the Bol'shoj Naryn site area (Fore-Baikal region, Eastern Siberia, Russia), Quatern. Int., 355, 24–33, 2015.

Doppler, G., Kroemer, E., Rögner, K., Wallner, J., Jerz, H., and Grottenthaler, W.: Quaternary Stratigraphy of Southern Bavaria, E&G Quaternary Sci. J., 60, 329–365, 2011.

Duller, G. A. T.: Distinguishing quartz and feldspar in single grain luminescence measurements, Radiat. Meas., 37, 161–165, 2003.

Faegri, K. and Iversen, J.: Textbook of Pollen Analysis, John Wiley and Sons, Chichester, UK, 328 pp., 1989.

Fischer, P., Hilgers, A., Protze, J., Kels, H., Lehmkuhl, F., and Gerlach, R.: Formation and geochronology of last interglacial to lower Weichselian loess/palaeosol sequences – case studies from the Lower Rhine Embayment, Germany, E&G Quaternary Sci. J., 61, 48–63, 2012.

Frechen, M.: Upper Pleistocene loess stratigraphy in Southern Germany, Quat. Geochronol., 18, 243–269, 1999.

Fuhrmann, R.: Atlas quartärer und rezenter Ostrakoden Mitteldeutschlands, Altenburger Naturwissenschaftliche Forschungen, 15, 1–320, 2012.

Galbraith, R. F., Roberts, R. G., Laslett, G. M., Yoshida, H., and Olley, J. M.: Optical dating of single grains of quartz from Jinmium rock shelter, northern Australia. Part I: experimental design and statistical models, Archaeometry, 41, 339–364, 1999.

Glöer, P. and Meier-Brook, C.: Süsswassermollusken – Ein Bestimmungsschlüssel für die Bundesrepublik Deutschland, Deutscher Jugendbund für Naturbeobachtung, Hamburg, Germany, 134 pp., 2003.

Gregor H.-J.: Die Eiszeit in Bobingen. Neue Funde und Ergebnisse aus Kiesgruben der Fa. Lauter (Landkreis Augsburg, Bayern), Documenta Naturae, 191, 1–155, 2012.

Griffiths, H. I. and Holmes, J. A.: Non-marine ostracods and Quaternary palaeoenvironments, Quaternary Research Association, Technical guide, 8, 1–179, 2000.

Griffiths, H. I., Rouse, A., and Evans, J. G.: Processing freshwater ostracodes from archaeological deposits, with a key to the valves of the major British genera, Circaea, 10, 53–62, 1993.

Günther, J.: Ostracod fauna of Duvensee, an ancient lake in Northern Germany, Hydrobiologia, 143, 411–416, 1986.

Haug, G., Hughen, K. A., Sigman, D. M., Peterson, L. C., and Röhl, U.: Southward migration of the Intertropical Convergence Zone through the Holocene, Science, 293, 1304–1308, 2001.

Heiri, O., Koinig, K., Spötl, C., Barrett, S., Brauer, A., Drescher-Schneider, R., Gaar, D., Ivy-Ochs, S., Kerschner, H., Luetscher, M., Moran, A., Nicolussi, K., Preusser, F., Schmidt, R., Schoeneich, P., Schwörer, C., Sprafke, T., Terhorst, B., and Tinner, W.: Palaeoclimate records 60–8 ka in the Austrian and

Swiss Alps and their forelands, Quaternary Sci. Rev., 106, 186–205, 2014.

Huber, C., Leuenberger, M., Spahni, R., Flückiger, J., Schwander, J., Stocker, T.F., Johnsen, S., Landais, A., and Jouzel, J.: Isotope calibrated Greenland temperature record over Marine Isotope Stage 3 and its relation to CH$_4$, Earth Planet. Sc. Lett., 243, 504–519, 2006.

Koeniger, P., Barta, G., Thiel, C., Bajnóczi, B., Novothny, Á., Horváth, E., Techmer, A., and Frechen, M.: Stable isotope composition of bulk and secondary carbonates from the Quaternary loess-paleosol sequence in Süttö, Hungary, Quatern. Int., 319, 38–49, 2014.

Lai, Z.: Chronology and the upper dating limit for loess samples from Luochuan section in the Chinese Loess Plateau using quartz OSL SAR protocol, J. Asian Earth Sci., 37, 176–185, 2010.

Lehmkuhl, F., Zens, J., Krauß, L., Schulte, P., and Kels, H.: Loess-paleosol sequences at the northern European loess belt in Germany: Distribution, geomorphology and stratigraphy, Quaternary Sci. Rev., 153, 11–30, 2016.

Löffler, H.: Recent and subfossil distribution of *Cytherissa lacustris* (Ostracoda) in Lake Constance, Mitteilungen – Internationale Vereinigung für theoretische und angewandte Limnologie, 17, 240–251, 1969.

Lowick, S. E., Preusser, F., Pini, R., and Ravazzi, C.: Underestimation of fine grain quartz OSL dating towards the Eemian: Comparison with palynostratigraphy from Azzano Decimo, northeastern Italy, Quat. Geochronol., 5, 583–590, 2010.

Ložek, V.: Quartärmollusken der Tschechoslowakei, Rozpravy ústredního ústavu geologického, 31, 1–374, 1964.

Ložek, V.: Molluscs in loess, their paleoecological significance and role in geochronology – principles and methods, Quatern. Int., 7/8, 71–79, 1990.

Mayr, C., Matzke-Karasz, R., Stojakowits, P., Lowick, S. E., Zolitschka, B., Heigl, T., Mollath, R., Theuerkauf, M., Weckend, M.-O., Bäumler, R., and Gregor, H.-J.: Würmian loess section, Bobingen (Germany): pollen, XRF, geochemical data, PANGAEA, https://doi.org/10.1594/PANGAEA.884265, 2017.

Meier-Brook, C.: Der ökologische Indikatorwert mitteleuropäischer Pisidium-Arten (Mollusca, Eulamellibranchiata), Eiszeitalter und Gegenwart, 26, 190–195, 1975.

Meisch, C.: Freshwater Ostracoda of Western and Central Europe, in: Süsswasserfauna von Mitteleuropa, edited by: Schwoerbel, J. and Zwick, P., vol. 8/3, 1–522, Spektrum Akademischer Verlag, Heidelberg, Germany, 2000.

Mejdahl, V.: Internal radioactivity in quartz and feldspar grains, Ancient TL, 5, 10–17, 1987.

Moine, O., Rousseau, D.-D., and Antoine, P.: Terrestrial molluscan records of Weichselian Lower to Middle Pleniglacial climatic changes from the Nussloch loess series (Rhine Valley, Germany): the impact of local factors, Boreas, 34, 363–380, 2005.

Moore, P. D., Webb, J. A., and Collinson, M.: Pollen Analysis, Blackwell, London, UK, 216 pp., 1991.

Moseley, G. E., Spötl, C., Svensson, A., Cheng, H., Brandstätter, S., and Lawrence Edwards, R.: Multi-speleothem record reveals tightly coupled climate between central Europe and Greenland during marine Isotope Stage 3, Geology, 42, 1043–1046, 2014.

Müller, G. and Gastner, M.: The "Karbonat-Bombe", a simple device for the determination of the carbonate content in sediments, soils and other materials, Neues Jahrbuch für Mineralogie/Monatshefte, 10, 466–469, 1971.

Müller, U. C., Pross, J., and Bibus, E.: Vegetation response to rapid climatic change in Central Europe during the past 140 000 yr based on evidence from the Füramoos pollen record, Quaternary Res., 59, 235–245, 2003.

Munsell Color: Munsell Soil Color Charts, Grand Rapids, USA, 2000.

Murray, A. S. and Wintle, A. G.: Luminescence dating of quartz using an improved single-aliquot regenerative-dose protocol, Radiat. Meas., 32, 57–73, 2000.

Murray, A. S. and Wintle, A. G.: The single aliquot regenerative dose protocol: potential for improvements in reliability, Radiat. Meas., 37, 377–381, 2003.

Ohlendorf, C.: A sample carrier for measuring discrete powdered samples with an ITRAX XRF core scanner, X-Ray Spectrom., 47, 58–62, 2017.

Penck, A.: Die Vergletscherung der Deutschen Alpen, Johann Ambrosius Barth, Leipzig, Germany, 483 pp., 1882.

Penck, A. and Brückner, E.: Die Alpen im Eiszeitalter, Tauchnitz, Leipzig, Germany, 1149 pp., 1901–1909.

Prescott, J. R. and Hutton, J. T.: Cosmic ray contributions to dose rates for luminescence and ESR dating: Large depths and long-term time variations, Radiat. Meas., 23, 497–500, 1994.

Preusser, F.: Towards a chronology of the Late Pleistocene in the northern Alpine Foreland, Boreas, 33, 195–210, 2004.

Preusser, F. and Kasper, H. U.: Comparison of dose rate determination using high-resolution gamma spectrometry and inductively coupled plasma-mass spectrometry, Ancient TL, 19, 17–21, 2001.

Rasmussen, S. O., Bigler, M., Blockley, S., Blunier, T., Buchardt, B., Clausen, H., Cvijanovic, I., Dahl-Jensen, D., Johnsen, S., Fischer, H., Gkinis, V., Guillevic, M., Hoek, W., Lowe, J., Pedro, J., Popp, T., Seierstad, I., Steffensen, J., Svensson, A., Vallelonga, P., Vinther, B., Walker, M., Wheatley, J. J., and Winstrup, M.: A stratigraphic framework for abrupt climatic changes during the Last Glacial period based on three synchronized Greenland ice-core records: refining and extending the INTIMATE event stratigraphy, Quaternary Sci. Rev., 106, 14–28, 2014.

Sauer, D., Kadereit, A., Kühn, P., Kösel, M., Miller, C., Shinonaga, T., Kreutzer, S., Herrmann, L., Fleck, W., Starkovich, B., and Stahr, K.: The loess-palaeosol sequence of Datthausen, SW/Germany: Characteristics, chronology, and implications for the use of the Lohne Soil as a marker soil, Catena, 146, 10–29, 2016.

Schaefer, I.: Geologische Karte von Augsburg und Umgebung 1 : 50 000 mit Erläuterungen, Bayerisches Geologisches Landesamt, München, Germany, 92 pp., 1957.

Scheuenpflug, L.: Die risseiszeitliche Hochterrasse des Lechs nördlich Augsburg und die Schmutter (Bayerisch Schwaben), Heidelberger Geographische Arbeiten, 49, 194–209, 1979.

Schielein, P. and Schellmann, G.: Erläuterungen zur quartärgeologischen Karte 1 : 25 000 des Wertachtals auf Blatt 7730 Großaitingen – Kartierungsergebnisse aus den Jahren 2014 und 2015, Bamberger Geographische Schriften, Sonderfolge, 12, 329–356, 2016.

Schielein, P., Schellmann, G., Lomax, J., Preusser, F., and Fiebig, M.: Chronostratigraphy of the *Hochterrassen* in the lower Lech

valley (Northern Alpine Foreland), E&G Quaternary Sci. J., 64, 15–28, 2015.

Schreiber, U. and Müller, D.: Mittel- und jungpleistozäne Ablagerungen zwischen Augsburg und Landsberg (Lech), Geologisches Institut der Universität Köln, Sonderveröffentlichungen, 82, 265–282, 1991.

Semmel, A.: Studien über den Verlauf jungpleistozäner Formung in Hessen, Frankfurter Geographische Hefte, 45, 1–133, 1968.

Starnberger, R., Terhorst, B., Rähle, W., Peticzka, R., and Haas, J. N.: Palaeoecology of Quaternary periglacial environments during OIS-2 in the forefields of the Salzach Glacier (Upper Austria), Quatern. Int., 198, 51–61, 2009.

Terhorst, B., Frechen, M., and Reitner, J.: Chronostratigraphische Ergebnisse aus Lößprofilen der Inn- und Traunhochterrassen in Oberösterreich, Z. Geomorphol. Supp., 127, 213–232, 2002.

Terhorst, B., Kühn, P., Damm, B., Hambach, U., Meyer-Hintze, S., and Sedov, S.: Paleoenvironmental fluctuations as recorded in the loess-paleosol sequence of the Upper Paleolithic site Krems-Wachtberg, Quatern. Int., 351, 67–82, 2014.

Terhorst, B., Sedov, S., Sprafke, T., Peticzka, R., Meyer-Heintze, S., Kühn, P., and Solleiro Rebolledo, E.: Austrian MIS 3/2 loess-palaeosol records – Key sites along a west-east transect, Palaeogeogr. Palaeocl., 418, 43–56, 2015.

Timar, A., Vandenberghe, D., Panaiotu, E. C., Panaiotu, C. G., Necula, C., Cosma, C., and Van den Haute, P.: Optical dating of Romanian loess using fine-grained quartz, Quat. Geochronol., 5, 143–148, 2010.

Voelker, A. H. L. and workshop participants: Global distribution of centennial-scale records for Marine Isotope Stage (MIS) 3: a database, Quaternary Sci. Rev., 21, 1185–1212, 2002.

Welter-Schultes, F.: European non-marine molluscs, a guide for species identification, Planet Poster Edition, Göttingen, Germany, 760 pp., 2012.

Wintle, A. G. and Murray, A. S.: Quartz OSL: Effects of thermal treatment and their relevance to laboratory dating procedures, Radiat. Meas., 32, 387–400, 2000.

Wintle, A. G. and Murray, A. S.: A review of quartz optically stimulated luminescence characteristics and their relevance in single-aliquot regeneration dating protocols, Radiat. Meas., 41, 369–391, 2006.

Wirsig, C., Zasadni, J., Christl, M., Akçar, N., and Ivy-Ochs, S.: Dating the onset of LGM ice surface lowering in the High Alps, Quaternary Sci. Rev., 143, 37–50, 2016.

Zander, A., Degering, D., Preusser, F., Kasper, H. U., and Brückner, H.: Optically stimulated luminescence dating of sublittoral and intertidal sediments from Dubai, UAE: Radioactive disequilibria in the uranium decay series, Quat. Geochronol., 2, 123–128, 2007.

Zech, M., Krause, T., Meszner, S., and Faust, D.: Incorrect when uncorrected: Reconstructing vegetation history using n-alkane biomarkers in loess-paleosol sequences – A case study from the Saxonian loess region, Germany, Quatern. Int., 296, 108–116, 2013.

Zettler, M. L. and Glöer, P.: Zur Ökologie und Morphologie der Sphaeriidae der Norddeutschen Tiefebene, Heldia, 6, 1–61, 2006.

Zöller, L. and Semmel, A.: 175 years of loess research in Germany – long records and "unconformities", Earth-Sci. Rev., 54, 19–28, 2001.

E&G Open Access Quaternary Science Journal

Late Quaternary climate and environmental reconstruction based on leaf wax analyses in the loess sequence of Möhlin, Switzerland

Lorenz Wüthrich[1,2], **Marcel Bliedtner**[1,2], **Imke Kathrin Schäfer**[1,2], **Jana Zech**[1], **Fatemeh Shajari**[3], **Dorian Gaar**[2,4], **Frank Preusser**[5], **Gary Salazar**[2,6], **Sönke Szidat**[2,6], and **Roland Zech**[1,2]

[1]Geographical Institute, University of Bern, Bern, Switzerland
[2]Oeschger Centre for Climate Change Research, University of Bern, Bern, Switzerland
[3]Geo and Environmental Engineering, Technical University of Munich, Munich, Germany
[4]Institute of Geology, University of Bern, Bern, Switzerland
[5]Institute of Earth and Environmental Sciences, University of Freiburg, Freiburg, Germany
[6]Department of Chemistry and Biochemistry, University of Bern, Bern, Switzerland

Correspondence: Lorenz Wüthrich (loeru@live.com)

Abstract: We present the results of leaf wax analyses (long-chain n-alkanes) from the 6.8 m deep loess sequence of Möhlin, Switzerland, spanning the last $\sim$ 70 kyr. Leaf waxes are well preserved and occur in sufficient amounts only down to 0.4 m and below 1.8 m depth, so no paleoenvironmental reconstructions can be done for marine isotope stage (MIS) 2.

Compound-specific $\delta^2 H_{wax}$ analyses yielded similar values for late MIS 3 compared to the uppermost samples, indicating that various effects (e.g., more negative values due to lower temperatures, more positive values due to an enriched moisture source) cancel each other out. A pronounced $\sim$ 30 ‰ shift towards more negative values probably reflects more humid conditions before $\sim$ 32 ka. Radiocarbon dating of the n-alkanes corroborates the stratigraphic integrity of leaf waxes and their potential for dating loess–paleosol sequences (LPS) back to $\sim$ 30 ka.

Kurzfassung: Wir präsentieren die Ergebnisse von Blattwachsanalysen (langkettige n-Alkane) aus einer 6.8 m mächtigen Löss-Sequenz bei Möhlin, Schweiz, welche bis etwa 70 ka zurückreicht. Nur bis 0.4 m Tiefe und unterhalb von 1.8 m sind die Blattwachse gut und in ausreichender Menge erhalten, so dass Aussagen bezüglich der Umweltbedingungen während der marinen Isotopenstufe (MIS) 2 nicht gemacht werden können. Die Muster der n-Alkane zeigen für alle Proben einen dominanten Input von Gras-Alkanen, jedoch ist es nur anhand der n-Alkane nicht möglich, die Existenz von Koniferen vor allem während des MIS 3 auszuschliessen. Komponenten-spezifische $\delta^2 H_{wax}$ Analysen zeigen für MIS 3 ähnliche Werte wie für die obersten Proben aus der Sequenz. Offensichtlich heben sich mehrere Effekte gegenseitig auf (z.B. negativere Werte aufgrund niedrigerer Temperatur, positivere Werte aufgrund angereicherter Feuchtigkeitsquellen). Ein auffälliger $\sim$ 30 ‰ Wechsel zu negativeren Werten

zeigt vermutlich feuchtere Bedingungen vor ∼ 32 ka an. Komponenten-spezifische Radiokohlenstoff-Datierungen bestätigen die stratigraphische Integrität der Blattwachse und untermauern ihr Potential für die Datierung von Löss-Paläoboden Sequenzen bis etwa 30 ka.

1   Introduction

Vast parts of Switzerland were repeatedly covered by glaciers (Graf, 2009). This explains the lack of widespread thick loess deposits as they exist, for example, in southeastern Germany, southeastern and eastern Europe (Haase et al., 2007). Nevertheless, there are a few sites in Switzerland where loess has been found (Gouda, 1962; Preusser et al., 2011; Gaar and Preusser, 2017), and they might have potential for paleoenvironmental reconstruction. One of these sites is the Möhliner Feld in northwestern Switzerland (Fig. 1). Until recently, there was a subdued ridge considered to be a terminal moraine of the most extensive glaciation (MEG; > 300 ka) in the Swiss Alps (Gutzwiler, 1894; Penck and Brückner, 1909; Keller and Krayss, 2011). However, the ridge cannot be linked to the MEG, because till containing Alpine material is only found 30 m below the surface and covered by gravel and loess (Preusser et al., 2011; Gaar and Preusser, 2017). While the till can be attributed to the MEG, although no numerical age control is available, the ridge has to be interpreted as a loess dune, not as a moraine, as it consists of loess (Gaar and Preusser, 2017). The dune might have been deposited by strong winds, called the "Möhlin jet". The jet nowadays mostly occurs in winter, when the air fills up the Swiss Plateau and overflows the eastern Jura Mountains. This results in a dry wind with a speed of up to 10 m s^{-1} (Schüepp, 1982; Müller, 2001; Gaar and Preusser, 2017). In 2011, a rotary drill core was recovered from the ridge, consisting entirely of loess sediment down to 6.8 m depth. According to luminescence dating (OSL and IR50), most of the loess was deposited during marine isotope stage (MIS) 2 and late MIS 3, while the lowermost part of the sequence probably dates back to MIS 4 (Gaar and Preusser, 2017).

For the present study, we analyzed long-chain n-alkanes, i.e., leaf waxes, in the drill core from Möhlin in order to evaluate their potential for paleovegetation reconstruction. Moreover, we applied compound-specific δ^2H analyses on the most abundant n-alkanes (n-C$_{29}$ and n-C$_{31}$) to reconstruct paleoclimate and hydrology. In addition, we performed radiocarbon dating on some n-alkane samples to test the stratigraphic integrity of the leaf waxes.

2   Leaf waxes – a novel tool in Quaternary research

Long-chain n-alkanes ($> n$-C$_{25}$) are produced by higher terrestrial plants (de Bary, 1871; Eglinton and Hamilton, 1963, 1967; Kunst, 2003; Shepherd and Wynne Griffiths, 2006; Samuels et al., 2008). They are straight, saturated
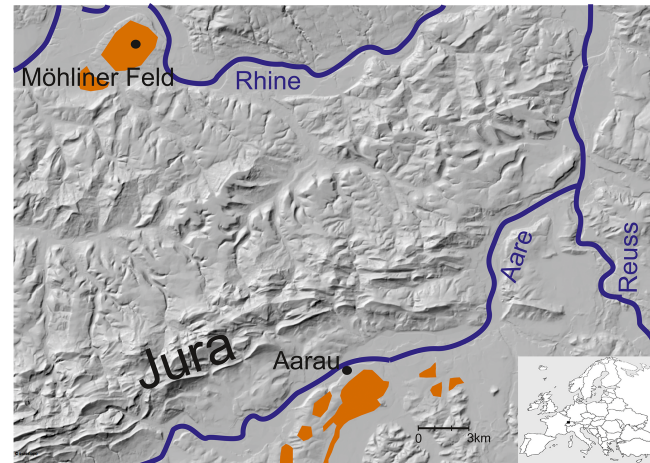

Figure 1. Research area. Orange fields mark loess deposits, drawn after Gouda (1962). Source hillshade: Federal Office of Topography.

carbon–hydrogen chains (C$_n$H$_{2n+2}$), stable over geological timescales (Eglinton and Eglinton, 2008; Schimmelmann et al., 2006) and thus preserved in various sedimentary archives. Their homologue pattern depends on the type of vegetation (Cranwell, 1973; Marseille et al., 1999; Schwark et al., 2002) and can provide information about whether deciduous trees or grasses were dominant in the research area, whereas deciduous trees produce mainly n-C$_{27}$ and grasses predominantly n-C$_{31}$ and n-C$_{33}$ (Zech et al., 2010; Schäfer et al., 2016b; Schwark et al., 2002). Although controversy exists as to whether this approach can be used universally to reconstruct paleovegetation (Bush and McInerney, 2013; Wang et al., 2015), there is good evidence that leaf wax patterns can be used on a local (Schwark et al., 2002) and regional (Schäfer et al., 2016a) scale in Europe. Schwark et al. (2002) investigated n-alkanes in a lake in southern Germany and found a remarkable accordance of pollen records and n-alkanes. Schäfer et al. (2016a) measured leaf wax patterns along a transect from southern to northern Europe in grasslands, deciduous forests and coniferous forests. They analyzed samples from litter and two depths of the uppermost soil horizon. The results of the Schäfer et al. (2016a) study are that (1) the chain lengths correlate significantly along the transect with the grassland and deciduous vegetation, (2) n-alkanes from conifer forests show the understorey and (3) a correction for degradation of the n-alkanes is needed to get reliable information about the vegetation. n-Alkane patterns are thus a particularly valuable tool for the reconstruction of

paleovegetation when pollen are absent, which is often the case in loess–paleosol sequences (LPS).

The compound-specific isotopic composition of n-alkanes (δ^2H_{wax}) is increasingly used as a tool for the reconstruction of past climate conditions. Liu and Huang (2005) measured δ^2H_{wax} in a Chinese loess–paleosol sequence and showed that it recorded past climate changes. In principle, δ^2H_{wax} reflects the isotopic composition of precipitation (δ^2H_{precip}) (Sachse et al., 2012), which in turn depends on (and is thus a proxy for) climate (temperature, precipitation amount, evaporation) and geographical location (latitude, altitude, continentality, moisture source) (Dansgaard, 1964). Additional factors that need to be taken into account when interpreting δ^2H_{wax} records are biosynthetic fractionation, evapotranspirative enrichment, vegetation period, degradation and type of vegetation (Sessions et al., 1999; Sachse et al., 2006; M. Zech et al., 2011, 2015; Kahmen et al., 2013; Gao et al., 2014; Hepp et al., 2015; Tipple et al., 2013). Evapotranspiration leads to an enrichment, depending mainly on relative humidity (M. Zech et al., 2013; Farquhar et al., 2007). Biosynthetic fractionation is often assumed to be $\sim 160\%$ (Sachse et al., 2012).

Compound-specific radiocarbon analyses on sedimentary n-alkanes is a new tool in geochronology (Häggi et al., 2014; Haas et al., 2017; Zech et al., 2017). It allows us to test the synsedimentary nature, and thus the stratigraphic integrity of leaf waxes, and can complement other dating methods, for example based on luminescence.

3 Material and methods

The drill core from Möhlin is described in detail in Gaar and Preusser (2017). In brief, the core consists of loess down to 6.8 m but is decalcified and overprinted by pedogenesis down to 1.6 m depth and from 5.9 to 6.2 m. We sampled the core in continuous 20 cm intervals for leaf wax analyses.

3.1 Leaf wax analyses

Approximately 40 g of each sample was extracted with an accelerated solvent extractor using dichloromethane / methanol (9/1). The total lipid extract was dried and passed over pipette columns with an aminopropyl-coated silica gel as the stationary phase. Nonpolar compounds, including n-alkanes, were eluted with hexane and then spiked with 5α-androstane. The long-chain n-alkanes (nC_{25}–nC_{35}) were analyzed using a GC-FID (gas chromatography–flame ionization detector) at the Department of Soil Science at TUM-Weihenstephan, Freising, Germany. The Thermo Scientific Trace 1310 was equipped with a Zebron ZB-5HT column and operated in splitless injection mode. The He carrier gas flow was set constantly to $1.2\,\mathrm{mL\,min^{-1}}$, and the GC temperature was first held at $50\,°C$ for 1 min, ramped to $250\,°C$ at $30\,°C\,min^{-1}$ and then to $340\,°C$ at $7\,°C\,min^{-1}$, and held for 11 min.

The most abundant n-alkanes, nC_{29} and nC_{31}, were later targeted at the Geographical Institute, University of Bern, for compound-specific δ^2H analyses. Using an IsoPrime 100 mass spectrometer, coupled to an Agilent 7890A GC via a GC5 pyrolysis–combustion interface operating in pyrolysis mode with a Cr (ChromeHD) reactor at $1000\,°C$. Each sample was measured three times. Precision of the measurements was checked by analyzing a standard n-alkane mixture with known isotopic composition twice every six runs. The H_3+ factor was 3.4 and stable. The results are given in delta notation (δ^2H) versus Vienna Standard Mean Ocean Water (VS-MOW).

3.2 n-Alkane patterns

The total n-alkane concentration ($\mu g\,g^{-1}$ dry weight, A_{tot}) is here defined as the sum of nC_{25} to nC_{35}. The odd-over-even predominance (OEP; Eq. 1) was calculated after Hoefs et al. (2002) and is an indicator for degradation: values smaller than 5 are considered to be strongly degraded (Zech et al., 2010; Schäfer et al., 2016a) and must thus be interpreted with care.

$$OEP = \frac{nC_{27} + nC_{29} + nC_{31} + nC_{33}}{nC_{26} + nC_{28} + nC_{30} + nC_{32}} \quad (1)$$

Changes in the average chain length (ACL; Eq. 2) of the measured n-alkanes indicate whether deciduous trees and shrubs (shorter ACL) or grasses and herbs (longer ACL) were the dominant plant type (Poynter et al., 1989).

$$ACL = \frac{27 \cdot nC_{27} + 29 \cdot nC_{29} + 31 \cdot nC_{31} + 33 \cdot nC_{33}}{nC_{27} + nC_{29} + nC_{31} + nC_{33}} \quad (2)$$

Because degradation can influence the ACL, one needs to correct for those effects (Zech et al., 2010). We performed a correction after Schäfer et al. (2016a) (Eq. 3–6), which results in the semi-quantitative %grass content for the samples.

$$Tree\,endmember = 0.09 \cdot \ln(OEP) + 0.66 \quad (3)$$

$$Grass\,endmember = -0.17 \cdot \ln(OEP) + 0.75 \quad (4)$$

$$Ratio = \frac{n-C_{31} + n-C_{33}}{n-C_{27} + n-C_{31} + n-C_{33}} \quad (5)$$

$$\%Grass = \frac{ratio - tree\,endmember}{grass\,endmember - tree\,endmember} \quad (6)$$

3.3 Radiocarbon dating

For radiocarbon analyses of the n-alkanes, four samples were selected and the nonpolar fraction passed over two pipette columns filled with $AgNO_3$ impregnated silica gel and zeolite, respectively. The zeolite was dissolved in HF, and the purified n-alkanes were recovered via liquid–liquid extraction with n-hexane. Finally, the purified n-alkanes were transferred with dichloromethane into tin capsules. The ^{14}C measurements were performed on the MICADAS accelerator mass spectrometer, coupled to an element analyzer (Ruff

et al., 2010; Salazar et al., 2015), at the LARA AMS Laboratory, University of Bern (Szidat et al., 2014). ^{14}C results are reported as fraction modern carbon (F^{14}C) and were corrected for constant and blank contamination (Salazar et al., 2015; Haas et al., 2017). The blank contamination was $0.4\,\mu g\,C$ for a single tin capsule with a F^{14}C value of 0.734 ± 0.19. The calibrated radiocarbon ages were calculated using OxCal (Ramsey, 2009) and IntCal13 (Reimer et al., 2013).

4 Results

Most samples from Möhlin are characterized by a dominance of odd, long-chain ($> nC_{25}$) n-alkanes typical for leaf waxes; additionally, other compounds and an unresolved matrix complex occur in variable amounts (Fig. 2).

However, samples from 0.4 to 1.6 m depth have very low concentrations and quantification of the target compounds is difficult. Total n-alkane concentrations for these samples can only be estimated as $< 0.4\,\mu g\,g^{-1}$, and the OEP values are less than 5, indicating enhanced degradation. These samples are therefore not plotted in Fig. 3. All other data are illustrated in Fig. 3, Table 1 and the supplement table (Wüthrich et al., 2017b).

The two uppermost samples have n-alkane concentrations of 1.2 and $0.4\,\mu g\,g^{-1}$, OEP values of 8.3 and 7.5, and ACL values of 30.1, respectively. Samples from depths of 1.6 to 6.8 m have highly variable n-alkane concentrations, ranging from 1 to $5.3\,\mu g\,g^{-1}$. Their OEP values range from 9.9 to 18.6, and their ACL is between 30.5 and 31.1. The uppermost two samples and the samples below 1.6 m depth had sufficient amounts of nC_{29} and nC_{31} for compound-specific δ^2H analyses. $\delta^2 H_{wax}$ values range from -215.1 to $-143.5\,\permil$ and from -210.4 to $-146.9\,\permil$, respectively. Down-core patterns are very similar and correlate well with an R value of 0.68.

All four samples selected and purified for radiocarbon dating yielded sufficient carbon masses for AMS analyses (Table 4.1). Fraction modern (F^{14}C) ranges from 0.023 to 0.055, yielding calibrated 2σ ages between 26.4 and 38.0 cal kyr BP. As we did measure the whole n-alkane fraction and not single compounds, a contamination of post-sedimentary, especially short-chain and even-numbered, n-alkanes is possible, leading to too-young ages. But as three samples are in very good agreement with the ages published by Gaar and Preusser (2017), a contamination can most probably be excluded for the uppermost three samples.

5 Discussion

5.1 Chronology

The uppermost IR50 (infrared stimulated luminescence at 50°) and OSL (optically stimulated luminescence) ages from Gaar and Preusser (2017) suggest that at least the up-
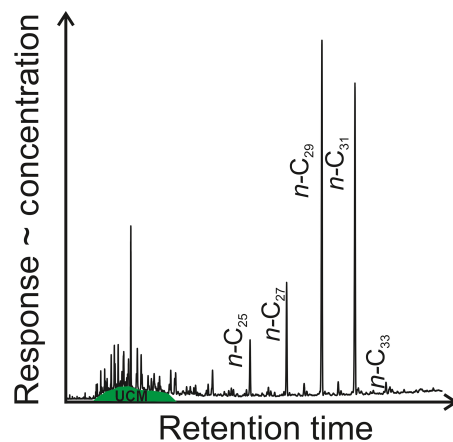

Figure 2. Example of a chromatogram (M13 from 2.4 m depth), showing the unresolved matrix complex (green) and the n-alkane compounds produced in leafs.

per ~ 1 m of Möhlin sequence was deposited ~ 19 ka, i.e., MIS 2, and just before final deglaciation of the Swiss Plateau (Wirsig et al., 2016; Wüthrich et al., 2017a). Soil formation and decalcification down to 1.6 m depth must have occurred during the Late Glacial and Holocene. The next three IR50 and OSL ages from depths of 3.4 to 5 m document rapid sedimentation between 34 and 31 ka, i.e., late MIS 3. Our radiocarbon ages from depths of 2.0 and 3.4 m are slightly younger (26.4 to 30.0 cal kyr BP) but are in reasonable agreement in view of the limitations and uncertainties related to both the luminescence and the radiocarbon dating methods. The radiocarbon age from 5.8 m depth is 31.7 to 38.0 cal kyr BP and with only 0.023 F^{14}C even closer to the lower limit of radiocarbon dating. Nevertheless, the age is also in good agreement with the OSL and IR50 ages of 31.0 and 41 kyr, respectively, from the same depth, so all of these ages document rapid loess accumulation during late MIS 3 (Fig. 3).

The weak paleosol preserved between 5.9 and 6.2 m depth must have developed earlier although probably still during MIS 3, because it developed into loess deposited during MIS 4 based on OSL and IR50 ages of 68.1 and 58.1 kyr, respectively. Our radiocarbon age from 6.8 m depth is only 28.7–32.2 cal kyr BP and very likely underestimates the real sedimentation age of the loess at this depth. The F^{14}C of the sample is only 0.038 and the smallest amounts of contamination (in the lab or from other compounds) can readily explain the discrepancy between the luminescence and radiocarbon ages. Another possibility might be incorporation of root-derived n-alkanes by roots from plants growing after deposition, as suggested, for example, by Gocke et al. (2014). But a post-sedimentary production of roots can most probably be excluded, as shown by Häggi et al. (2014), Zech et al. (2017) and Haas et al. (2017).

In general, our radiocarbon results are in reasonable agreement with the ages of Gaar and Preusser (2017) and corrob-

Table 1. Radiocarbon data and ages for the four selected samples.

Sample label	Sample code	Carbon mass (µg)	$F^{14}C$	Age range (2σ) (cal kyr BP)
M11	BE-3951.1.1	54	0.0547 ± 0.0040	26.4–28.7
M18	BE-3952.1.1	42	0.0486 ± 0.0040	27.4–30.0
M31	BE-3953.1.1	80	0.0229 ± 0.0037	31.7–38.0
M36	BE-3954.1.1	88	0.0378 ± 0.0038	28.7–32.2
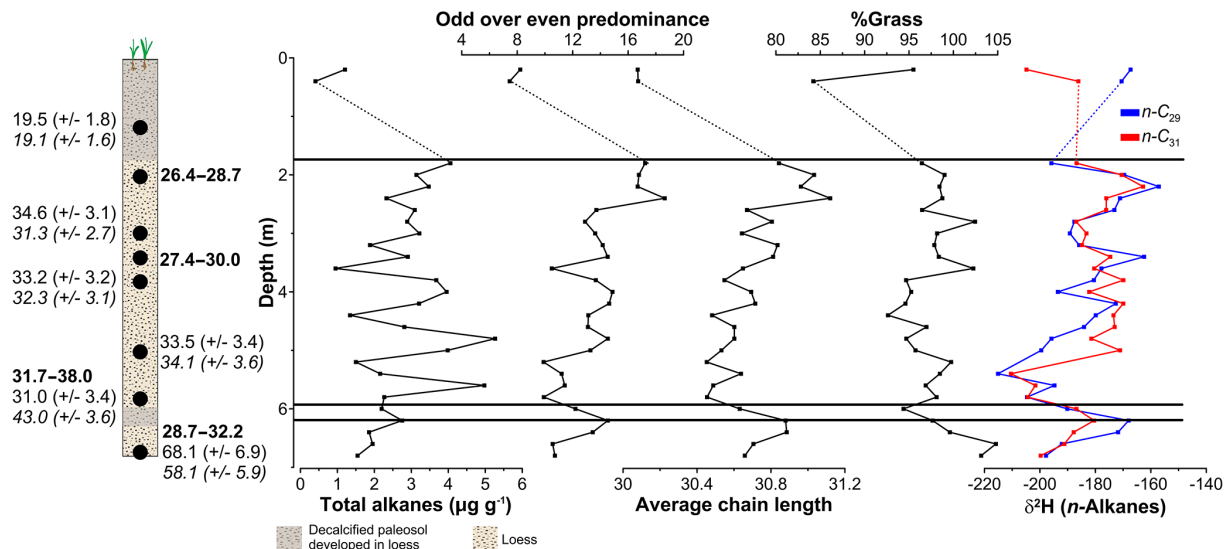
Figure 3. n-Alkane dates for the Möhlin loess sequence. OSL and IR50 (italic) ages have previously been published in Gaar and Preusser (2017); radiocarbon ages are given in bold letters.

orate that radiocarbon analyses of n-alkanes are a promising new tool for dating LPS back to ~ 30 ka (Häggi et al., 2014; Haas et al., 2017; Zech et al., 2017). Moreover, the stratigraphic integrity and synsedimentary nature of the long-chain n-alkanes could be confirmed for the uppermost 6 m.

The OSL, IR50 (Gaar and Preusser, 2017) and our radiocarbon ages show that the major part of the sequence was developed between 35 and 30 kyr and that older deposits are probably influenced by erosion. The paleosol might show a hiatus. Our interpretation is thus mainly valid for the time between 35 and 30 ka, when the rapid loess accumulation occurred.

5.2 Paleovegetation

The uppermost two samples from depths of 0.2 and 0.4 m have a relatively low ACL compared to most other samples from the profile. This indicates more input of n-alkanes from deciduous trees and shrubs; however, concentrations are also lower, and lower OEP values show enhanced degradation (Fig. 4). The plot also illustrates that changes in the alkane ratio (the same is true for the ACL) are partly an artefact of degradation. However, the sample from 0.4 m depth plots furthest below the grass endmember, which is numerically

expressed as lowest %grass (Fig. 3). This possibly reflects the remnant leaf wax signal from the natural potential vegetation at Möhlin during the Holocene, i.e., mainly deciduous trees, whereas the site is used today as grassland.

While the n-alkanes between 0.6 and 1.6 m are strongly degraded and too low in concentration to robustly infer any paleoenvironmental conditions during MIS 2, high concentrations and good preservation allow this for the rest of the sequence. The positive trend in the ACL from depths of ~ 6 to 2 m indicates an increase of grass-derived n-alkane input during late MIS 3. However, the observed trend in ACL is probably an artefact of degradation. This is illustrated in the endmember again (Fig. 4), in which all these samples plot very close to the grass endmember. Accordingly, %grass (Fig. 3) does not show much of a trend and no major vegetation changes seem to be documented in the n-alkane patterns for the lower part of the profile between 1.8 and 6.8 m depth, i.e., during MIS 4 and MIS 3. This example shows that it is imperative to not over-interpret ACL and to account for degradation, even when preservation is generally good.

Our results suggest that the n-alkanes preserved at Möhlin during MIS 3 and possibly MIS 4 were mainly produced by grasses and herbs and that deciduous trees and shrubs
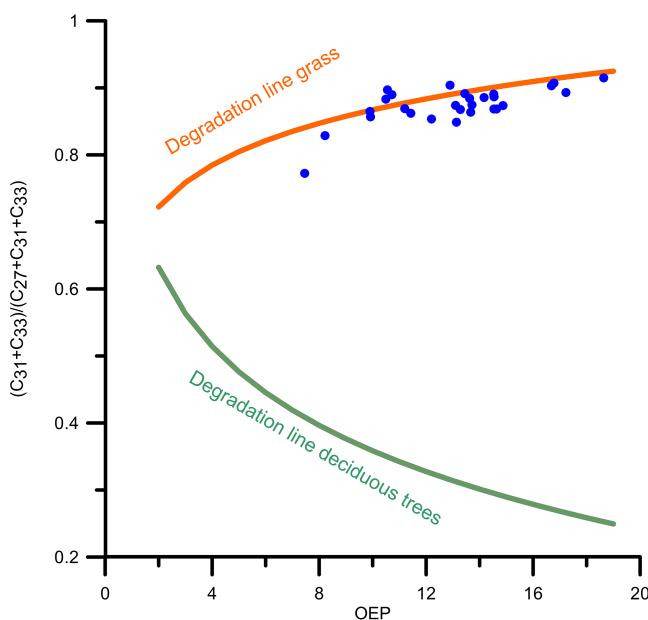
Figure 4. Endmember plot after Schäfer et al. (2016a). Our samples from Möhlin are plotted in blue.

played a minor role, if any. Based on n-alkanes only, however, one cannot rule out that conifer trees grew at the research site. n-Alkane concentrations in conifer needles are mostly about an order of magnitude lower than in deciduous trees or grass, with the exception of *Juniperus*. Hence n-alkane proxy records are quite insensitive for detecting conifer vegetation (Diefendorf et al., 2011; Tarasov et al., 2013; Schäfer et al., 2016b). Open conifer forest during parts of MIS 3 have been reported from peat sequences at Gossau (Schlüchter et al., 1987; Preusser et al., 2003) and Niederwenigen (Drescher-Schneider et al., 2007), both located a few dozen kilometers to the east of Möhlin. Similar vegetation may have prevailed at Möhlin, with the long-chain n-alkanes having only recorded thinly recorded grasses, i.e., the understory of the open conifer forest.

5.3   Paleoclimatology

The δ^2H_{wax} values from the uppermost two samples (ranging from -167 to $-205‰$; Fig. 3) are perfectly in the range observed in topsoil samples from central Europe (Schäfer et al., unpublished data) and in agreement with what can be expected based on theoretical considerations. Assuming a constant metabolic fractionation of $-160‰$, $\delta^2H_{leaf water}$ for the uppermost two samples ranges from -8.7 to $-53.4‰$. This is close but tends to be a little bit higher than today's δ^2H_{precip} in Möhlin, which has a value of $\sim -40‰$ in summer (Bowen et al., 2005; Bowen, 2008). As spring and possibly also winter precipitation, which is more depleted than summer precipitation, may have been used by the plants as well, some evapotranspirative enrichment certainly occurred.

The δ^2H_{wax} values below 1.8 m depth are relatively constant around $-180‰$, i.e., similar to the values from the uppermost two samples. Most conspicuously, a sudden drop occurs just below 5 m depth to values as low as $-215‰$ (Fig. 3). δ^2H_{wax} then increases again in the lowermost meter of the Möhlin sequence. The observed δ^2H_{wax} pattern strongly resembles the pattern from the LPS Bobingen, Germany, 200 km northeast of Möhlin (R. Zech et al., 2015). Here, n-alkanes are $\sim -200‰$ in sediments dated to latest MIS 3 (~ 30 ka) and MIS 2, and values drop to $< -220‰$ below, before they increase again in the lowest part of the profile dated to ~ 45 ka.

Overall, we are therefore confident that the δ^2H_{wax} record from Möhlin is a local signal but also carries valuable regional information about paleoclimate changes. Interpretation in terms of changes in δ^2H_{precip} and evapotranspirative enrichment is, however, very challenging because disentangling these two major controls is not yet possible. To the best of our knowledge, there are no independent continuous records of δ^2H_{precip} in Europe during the last glacial. Luetscher et al. (2015) presented a $\delta^{18}O$ record from a northern Alpine speleothem, but it overlaps only slightly with ours and shows very little variation from 30 to 15 ka ($\sim 1‰$ $\delta^{18}O$, which is equivalent to $\sim 8‰$ δ^2H). The only long continuous isotope records spanning the last 40 to 60 kyr currently come from an LPS in Crvenka, Serbia (R. Zech et al., 2013), which shows not much more than $10‰$ variability, and from marine cores offshore Portugal (Abreu et al., 2003) and in the Mediterranean Sea (Frigola et al., 2008). The marine $\delta^{18}O$ records (measured on foraminifera) show a minor trend towards more enriched values (corresponding to a δ^2H trend $< 10‰$) from ~ 60 to 20 ka. Afterwards, during the last glacial termination and the Holocene, values become much more negative ($\sim 20‰$ δ^2H). A comparison of these records suggests the following hypotheses: the sudden enrichment in δ^2H_{wax} after 32 kyr does not reflect a sudden change in the source, i.e., the North Atlantic. It might therefore document a sudden onset of more arid conditions and enhanced evapotranspiration.

The interpretation of the uppermost two samples is trickier: on one hand, the elevated δ^2H_{wax} of nC_{29} in the uppermost two samples in Möhlin might document even more arid conditions than during MIS 3, because they do not show the more negative source values and thus may have experienced even more evapotranspirative enrichment, possibly caused by elevated temperatures and similar precipitation compared to MIS 3. On the other hand, δ^2H_{wax} of nC_{31} is much more negative than nC_{29}. The reason for this might be different sources of nC_{29} and nC_{31}. It makes a difference whether the alkanes are produced by grasses or deciduous trees: grasses produce their n-alkanes mainly in the intercalary meristem and are thus much less influenced by evaporative enrichment than deciduous trees and shrubs (Kahmen et al., 2013), which produce their n-alkanes mostly at leaf flush (Tipple et al., 2013) and are thus much more influenced by relative hu-

midity. Nevertheless, grasses produce also n-alkanes in their leafs (Gao et al., 2012) and also show evaporative enrichment to some degree. In older publications, it has been stated that nC$_{29}$ is mainly produced by deciduous trees (Cranwell, 1973; Zech et al., 2010); the publication of Schäfer et al. (2016a) shows that both nC$_{29}$ and nC$_{31}$ are more or less equally produced by grasses and shrubs. However, relative to nC$_{31}$, Schäfer et al. (2016b) state that deciduous trees produce more nC$_{29}$. Thus the elevated amount of deciduous trees, recorded in the uppermost two samples, might show evaporative enrichment in nC$_{29}$. Also different biosynthetic fractionation of different plants might be a possible influence on the different values (e.g., Gao et al., 2014). As δ^2H$_{\text{wax}}$ values of shrubs, trees and grasses are quite similar (Sachse et al., 2012), we think that evapotranspirative enrichment plays a more important role.

However, it is unclear how changes in atmospheric circulation, and thus source areas, have changed in the past and to which degree a temperature effect at the site of precipitation may have been relevant. If such a temperature effect was relevant on glacial–interglacial timescales and if the isotope record offshore Portugal reasonably reflected changes in the source signal, both effects would have canceled each other out explain the similar δ^2H$_{\text{precip}}$ and δ^2H$_{\text{wax}}$ values during the Holocene and the late MIS 3. Drawing robust paleoclimatological conclusions from δ^2H$_{\text{wax}}$ records thus remains very difficult and independent δ^2H$_{\text{precip}}$ records are needed to reconstruct changes in paleohumidity and evapotranspirative enrichment.

Last but not least, the OEP might also be influenced by climatic conditions: during MIS 3 it is lowest, when δ^2H$_{\text{wax}}$ also has its lowest values. Higher humidity, expressed in lower δ^2H$_{\text{wax}}$ values, might allow higher microbial activity and thus an enhanced degradation, which leads to a lower OEP.

6 Conclusions

Our investigations of long-chain n-alkanes from the Möhlin sequence reveal that they are well preserved and occur in sufficient amounts in the uppermost samples down to 0.4 m depth, as well as from 1.8 to 5.8 m depth, to use them for the reconstruction of paleovegetation and paleoclimate and for radiocarbon dating. From 0.6 to 1.6 m depth, concentrations are very low, probably related to Holocene pedogenesis and priming.

The n-alkane pattern of the uppermost samples reflects today's grassy vegetation and possibly some leaf wax remnants of the natural deciduous forests that prevailed during most of the Holocene. No major vegetation changes are detected below 1.8 m depth. All samples indicate a dominant input of grass-derived leaf waxes and negligible contributions from deciduous trees and shrubs.

Compound-specific δ^2H analyses have yielded values for the uppermost samples that one can expect from today's isotopic composition of the precipitation, the metabolic fractionation and some evapotranspirative enrichment. The δ^2H$_{\text{wax}}$ values from 1.8 to 5 m depth, i.e., during late MIS 3, are not much different from today's values, which might document that the source effect (more positive source water in the North Atlantic during the glacial) and the temperature effect (more negative precipitation during glacial times) cancel each other out. However, we cannot exclude that changes in evapotranspirative enrichment or in atmospheric circulation and thus source areas were also relevant. Independent records of δ^2H$_{\text{precip}}$ would be necessary to quantitatively derive robust paleoclimatic information, particularly relative humidity and evapotranspirative enrichment. A very interesting feature in the δ^2H$_{\text{wax}}$ pattern from Möhlin is a sudden shift of $\sim 30\,\%o$ towards more negative values below 5 m depth. This shift is also observed in another LPS in the northern Alpine foreland and therefore probably a regional phenomenon. It might document a major change in paleohydrology, namely a shift from more humid to more dry conditions at ~ 32 ka. Nevertheless, independent δ^2H$_{\text{precip}}$ records are needed for more robust paleoclimatic reconstructions.

Radiocarbon dating of the n-alkanes have yielded ages in reasonable agreement with published OSL and IR50 ages, although ages of ~ 30 kyr are close to the limit of radiocarbon dating of the n-alkanes. The synsedimentary nature and stratigraphic integrity of long-chain n-alkanes are thus corroborated, highlighting the great potential of this new tool for dating loess–paleosol sequences. The chronology of the Möhlin sequence shows that loess accumulation occurred during MIS 4 and started again ~ 34 ka, well before the onset of MIS 2.

Overall, our study shows the great potential of leaf wax analyses in LPS. More high-resolution records of leaf wax patterns and compound-specific δ^2H, complemented by larger numbers of radiocarbon dating, would be useful to investigate the regional variability of respective proxy patterns. Ideally, such studies should be accompanied by other sedimentological, paleopedological and geochemical methods. Provenance analyses at Möhlin, for example, might help to investigate the proposed changes in wind direction and loess sources. Other leaf wax compounds, such as long-chain n-carboxylic acids or n-alkanols, or other biomarkers in general, could be used to corroborate and refine the vegetation reconstruction. Most importantly, the lack of independent ^{2}H$_{\text{precip}}$ records currently limits the possibility to robustly reconstruct past changes in relative humidity and evapotranspirative enrichment. A particularly promising path for future work is to further develop the biomarker-based "paleohygrometer", which is based on a coupled δ^2H$_{\text{wax}}$ and δ^{18}O$_{\text{sugar}}$ approach. It allows us to disentangle changes in evapotranspiration and δ^2H$_{\text{precip}}$ and has successfully been tested in topsoils (Tuthorn et al., 2015) and applied to organic-rich archives (M. Zech et al., 2013; Hepp et al., 2015).

98   L. Wüthrich et al.: Late Quaternary climate and environmental reconstruction

References

Abreu, L. de, Shackleton, N. J., Schönfeld, J., Hall, M., and Chapman, M.: Millennial-scale oceanic climate variability off the Western Iberian margin during the last two glacial periods, Mar. Geol., 196, 1–20, https://doi.org/10.1016/S0025-3227(03)00046-X, 2003.

Bowen, G. J. (Ed.): The Online Isotopes in Precipitation Calculator, The GNIP Database, available at: http://www.waterisotopes.org (last access: 17 August 2017), 2008.

Bowen, G. J., Wassenaar, L. I., and Hobson, K. A.: Global application of stable hydrogen and oxygen isotopes to wildlife forensics, Oecologia, 143, 337–348, https://doi.org/10.1007/s00442-004-1813-y, 2005.

Bush, R. T. and McInerney, F. A.: Leaf wax *n*-alkane distributions in and across modern plants: Implications for paleoecology and chemotaxonomy. Geochim. Cosmochim. Ac., 117, 161–179, https://doi.org/10.1016/j.gca.2013.04.016, 2013.

Cranwell, P. A.: Chain-length distribution of *n*-alkanes from lake sediments in relation to post-glacial environmental change, Freshwater Biol., 3, 259–165, https://doi.org/10.1111/j.1365-2427.1973.tb00921.x, 1973.

Dansgaard, W.: Stable isotopes in precipitation, Tellus A, 16, 436–468, 1964.

de Bary, A.: Über die Wachsüberzüge der Epidermis, Botanische Zeitung, 29, 9–11, 1871.

Diefendorf, A. F., Freeman, K. H., Wing, S. L., and Graham, H. V.: Production of *n*-alkyl lipids in living plants and implications for the geologic past, Geochim. Cosmochim. Ac., 75, 7472–7485, https://doi.org/10.1016/j.gca.2011.09.028, 2011.

Drescher-Schneider, R., Jacquat C., and Schoch, C.: Palaeobotanical investigations at the mammoth site of Niederweningen (Kanton Zürich), Switzerland, Quatern. Int., 164–165, 113–129, https://doi.org/10.1016/j.quaint.2006.11.016, 2007.

Eglinton, G. and Hamilton, R. J.: The Distribution of Alkanes, in: Chemical Plant Taxonomy, edited by: Swain, T., Academic Press, London, UK, New York, USA, 187–217, 1963.

Eglinton, G. and Hamilton, R. J.: Leaf Epicuticular Waxes, Science, 156, 1322–1335, https://doi.org/10.1126/science.156.3780.1322, 1967.

Eglinton, T. I. and Eglinton, G.: Molecular proxies for paleoclimatology, Earth Planet. Sc. Lett., 275, 1–16, https://doi.org/10.1016/j.epsl.2008.07.012, 2008.

Farquhar, G. D., Cernusak, L. A., and Barnes, B.: Heavy Water Fractionation during Transpiration, Plant Physiol., 143, 11–18, https://doi.org/10.1104/pp.106.093278, 2007.

Frigola, J., Moreno, A., Cacho, I., Canals, M., Sierro, F. J., Flores, J. A., and Grimalt, J. O.: Evidence of abrupt changes in Western Mediterranean Deep Water circulation during the last 50 kyr: A high-resolution marine record from the Balearic Sea, Quatern. Int., 181, 88–104, 2008.

Gaar, D. and Preusser, F.: Age of the Most Extensive Glaciation of the Northern Switzerland: Evidence from scientific drilling at Möhliner Feld, E&G Quaternary Sci. J., 66, 1–5, https://doi.org/10.3285/eg.66.1.er1, 2017.

Gao, L., Burnier, A., and Huang, Y.: Quantifying instantaneous regeneration rates of plant leaf waxes using stable hydrogen isotope labeling, Rapid Commun. Mass Sp., 26, 115–122, https://doi.org/10.1002/rcm.5313, 2012.

Gao, L., Edwards, E. J., Zeng, Y., and Huang, Y.: Major Evolutionary Trends in Hydrogen Isotope Fractionation of Vascular Plant Leaf Waxes, PloS one, 9, e112610, https://doi.org/10.1371/journal.pone.0112610, 2014.

Gocke, M., Peth, S., and Wiesenberg, G. L.: Lateral and depth variation of loess organic matter overprint related to rhizoliths – Revealed by lipid molecular proxies and X-ray tomography. Landscapes and Soils through Time, Catena, 112, 72–85, https://doi.org/10.1016/j.catena.2012.11.011, 2014.

Gouda, G.: Untersuchungen an Lössen der Nordschweiz, Geogr. Helv., 17, 137–221, https://doi.org/10.5194/gh-17-137-1962, 1962.

Graf, H. R.: Stratigraphie von Mittel- und Spätpleistozän in der Nordschweiz. Beiträge zur Geologischen Karte der Schweiz 168, Bundesamt für Landestopografie swisstopo, Wabern, Switzerland, 2009.

Gutzwiler, A.: Die Diluvialbildung in der Umgebung von Basel. Mitteilungen der naturforschenden Gesellschaft Basel, 10, 512–690, Basel, Switzerland, 1894.

Haas, M., Bliedtner, M., Borodynkin, I., Salazar, G., Szidat, S., Eglinton, T. I., and Zech, R.: Radiocarbon dating of leaf waxes 1 in the loess-paleosol sequence Kurtak, Central Siberia, Radiocarbon, 59, 165–176, https://doi.org/10.1017/RDC.2017.1, 2017.

Haase, D., Fink, J., Haase, G., Ruske, R., Pécsi, M., Richter, H., Altermann, M., and Jäger, K.-D.: Loess in Europe – its spatial distribution based on a European Loess Map, scale 1 : 2 500 000, Quaternary Sci. Rev., 26, 1301–1312, https://doi.org/10.1016/j.quascirev.2007.02.003, 2007.

Häggi, C., Zech, R., McIntyre, C., Zech, M., and Eglinton, T. I.: On the stratigraphic integrity of leaf-wax biomarkers in loess paleosols, Biogeosciences, 11, 2455–2463, https://doi.org/10.5194/bg-11-2455-2014, 2014.

Hepp, J., Tuthorn, M., Zech, R., Mügler, I., Schlütz, F., Zech, W., and Zech, M.: Reconstructing lake evaporation history and the isotopic composition of precipitation by a coupled $\delta^{18}O$–δ^2H biomarker approach. Advances in Paleohydrology Research and Applications, J. Hydrol., 529, 622–631, https://doi.org/10.1016/j.jhydrol.2014.10.012, 2015.

Hoefs, M. J., Rijpstra, W. C., and Sinninghe Damsté, J. S.: The influence of oxic degradation on the sedimentary biomarker record I: evidence from Madeira Abyssal Plain turbidites, Geochim. Cosmochim. Ac., 66, 2719–2735, https://doi.org/10.1016/S0016-7037(02)00864-5, 2002.

Kahmen, A., Schefuß, E., and Sachse, D.: Leaf water deuterium enrichment shapes leaf wax n-alkane δD values of angiosperm plants I: Experimental evidence and mechanistic insights. Hydrogen Isotopes, Geochim. Cosmochim. Ac., 111, 39–49, https://doi.org/10.1016/j.gca.2012.09.003, 2013.

Keller, O. and Krayss, E.: Mittel- und spätpleistozäne Stratigraphie und Morphogenese in Schlüsselregionen der Nordschweiz, E&G Quaternary Sci. J., 59, 88–119, https://doi.org/10.3285/eg.59.1-2.08, 2011.

Kunst, L.: Biosynthesis and secretion of plant cuticular wax, Prog. Lipid Res., 42, 51–80, https://doi.org/10.1016/S0163-7827(02)00045-0, 2003.

Liu, W. and Huang, Y.: Compound specific D/H ratios and molecular distributions of higher plant leaf waxes as novel paleoenvironmental indicators in the Chinese Loess Plateau, Org. Geochem., 36, 851–860, https://doi.org/10.1016/j.orggeochem.2005.01.006, 2005.

Luetscher, M., Boch, R., Sodemann, H., Spötl, C., Cheng, H., Edwards, R. L., Frisia, S., Hof, F., and Müller, W.: North Atlantic storm track changes during the Last Glacial Maximum recorded by Alpine speleothems, Nat. Commun., 6, 6344, https://doi.org/10.1038/ncomms7344, 2015.

Marseille, F., Disnar, J. R., Guillet, B., and Noack, Y.: n-Alkanes and free fatty acids in humus and A1 horizons of soils under beech, spruce and grass in the Massif-Central (Mont-Lozère), France, Eur. J. Soil Sci., 50, 433–441, https://doi.org/10.1046/j.1365-2389.1999.00243.x, 1999.

Müller, M. D.: Simulation of thermally induced and synoptically driven wind fields in complex terrain – An evaluation of the mesoscale model MetPhoMod, Master thesis, University of Basel, Basel, Switzerland, 2001.

Penck, A. and Brückner, E.: Die Alpen im Eiszeitalter, 3 Vol., C. H. Tauchnitz, Leipzig, Germany, 1909.

Poynter, J. G., Farrimond, P., Robinson, N., and Eglinton, G.: Aeolian-Derived Higher Plant Lipids in the Marine Sedimentary Record: Links with Palaeoclimate, Springer Netherlands, Dordrecht, the Netherlands, 1989.

Preusser, F., Geyh, M. A., and Schlüchter, C.: Timing of Late Pleistocene climate change in lowland Switzerland, Quaternary Sci. Rev., 22, 1435–1445, https://doi.org/10.1016/S0277-3791(03)00127-6, 2003.

Preusser, F., Graf, H. R., Keller, O., Krayss, E., and Schlüchter, C.: Quaternary glaciation history of northern Switzerland, E&G Quaternary Sci. J., 60, 282–305, 2011.

Ramsey, C. B.: Bayesian Analysis of Radiocarbon Dates, Radiocarbon, 51, 337–360, https://doi.org/10.1017/S0033822200033865, 2009.

Reimer, P. J., Bard, E., Bayliss, A., Beck, J. W., Blackwell, P. G., Ramsey, C. B., Buck, C. E., Cheng, H., Edwards, R. L., Friedrich, M., Grootes, P. M., Guilderson, T. P., Haflidason, H., Hajdas, I., Hatté, C., Heaton, T. J., Hoffmann, D. L., Hogg, A. G., Hughen, K. A., Kaiser, K. F., Kromer, B., Manning, S. W., Niu, M., Reimer, R. W., Richards, D. A., Scott, E. M., Southon, J. R., Staff, R. A., Turney, C. S. M., and van der Plicht, J.: IntCal13 and Marine13 Radiocarbon Age Calibration Curves 0–50 000 Years cal BP, Radiocarbon, 55, 1869–1887, https://doi.org/10.2458/azu_js_rc.55.16947, 2013.

Ruff, M., Fahrni, S., Gaggeler, H. W., Hajdas, I., Suter, M., Synal, H.-A., Szidat, S., and Wacker, L.: On-line Radiocarbon Measurements of Small Samples Using Elemental Analyzer and MICADAS Gas Ion Source, Radiocarbon, 52, 1645–1656, https://doi.org/10.1017/S003382220005637X, 2010.

Sachse, D., Radke, J., and Gleixner, G.: δD values of individual n-alkanes from terrestrial plants along a climatic gradient – Implications for the sedimentary biomarker record, Org. Geochem., 37, 469–483, https://doi.org/10.1016/j.orggeochem.2005.12.003, 2006.

Sachse, D., Billault, I., Bowen, G. J., Chikaraishi, Y., Dawson, T. E., Feakins, S. J., Freeman, K. H., Magill, C. R., McInerney, F. A., van der Meer, Marcel T.J., Polissar, P., Robins, R. J., Sachs, J. P., Schmidt, H.-L., Sessions, A. L., White, J. W., West, J. B., and Kahmen, A.: Molecular Paleohydrology. Interpreting the Hydrogen-Isotopic Composition of Lipid Biomarkers from Photosynthesizing Organisms, Annu. Rev. Earth Pl. Sc., 40, 221–249, https://doi.org/10.1146/annurev-earth-042711-105535, 2012.

Salazar, G., Zhang, Y. L., Agrios, K., and Szidat, S.: Development of a method for fast and automatic radiocarbon measurement of aerosol samples by online coupling of an elemental analyzer with a MICADAS AMS, Nucl. Instrum. Meth. B, 365, 163–167, https://doi.org/10.1016/j.nimb.2015.03.051, 2015.

Samuels, L., Kunst, L., and Jetter, R.: Sealing plant surfaces: cuticular wax formation by epidermal cells, Annu. Rev. Plant Biol., 59, 683–707, https://doi.org/10.1146/annurev.arplant.59.103006.093219, 2008.

Schäfer, I. K., Lanny, V., Franke, J., Eglinton, T. I., Zech, M., Vysloužilová, B., and Zech, R.: Leaf waxes in litter and topsoils along a European transect, SOIL, 2, 551–564, https://doi.org/10.5194/soil-2-551-2016, 2016a.

Schäfer, I. K., Bliedtner, M., Wolf, D., Faust, D., and Zech, R.: Evidence for humid conditions during the last glacial from leaf wax patterns in the loess paleosol sequence El Paraiso, Central Spain, Quatern. Int., 407, 64–73, https://doi.org/10.1016/j.quaint.2016.01.061, 2016b.

Schimmelmann, A., Sessions, A. L., and Mastalerz, M.: Hydrogen isotopic (D/H) composition of organic matter during diagenesis and thermal maturation, Annu. Rev. Earth Pl. Sc., 34, 501–533, https://doi.org/10.1146/annurev.earth.34.031405.125011, 2006.

Schlüchter, C., Maisch, M., Suter, J., Fitze, P., Keller, W. A., Burga, C. A., and Wynistorf, E.: Das Schieferkohlenprofil von Gossau (Kt. Zürich) und seine stratigraphische Stellung innerhalb der letzten Eiszeit, Vierteljahrsschrift der Naturforschenden Gesellschaft in Zürich, 132, 135–174, 1987.

Schüepp, W.: Untersuchungen über die Windverhältnisse in der Nordwestschweiz, Geogr. Helv., 37, 208–214, https://doi.org/10.5194/gh-37-208-1982, 1982.

Schwark, L., Zink, K., and Lechterbeck, J.: Reconstruction of postglacial to early Holocene vegetation history in terrestrial Central Europe via cuticular lipid biomarkers and pollen records from lake sediments, Geology, 30, 463–466, https://doi.org/10.1130/0091-7613(2002)030<0463:ROPTEH>2.0.CO;2, 2002.

Sessions, A. L., Burgoyne, T. W., Schimmelmann, A., and Hayes, J. M.: Fractionation of hydrogen isotopes in lipid biosynthesis, Org. Geochem., 30, 1193–1200, https://doi.org/10.1016/S0146-6380(99)00094-7, 1999.

Shepherd, T. and Wynne Griffiths, D.: The effects of stress on plant cuticular waxes, New Phytol., 171, 469–499, https://doi.org/10.1111/j.1469-8137.2006.01826.x, 2006.

Szidat, S., Salazar, G. A., Vogel, E., Battaglia, M., Wacker, L., Synal, H.-A., and Türler, A.: Analysis and Sample Preparation at the New Bern Laboratory for the Analysis of Radiocarbon with AMS (LARA), Radiocarbon, 56, 561–566, https://doi.org/10.1017/S0033822200049602, 2014.

Tarasov, P. E., Müller, S., Zech, M., Andreeva, D., Diekmann, B., and Leipe, C.: Last glacial vegetation reconstructions in the extreme-continental eastern Asia: Potentials of pollen and n-alkane biomarker analyses, Quatern. Int., 290–291, 253–263, https://doi.org/10.1016/j.quaint.2012.04.007, 2013.

Tipple, B. J., Berke, M. A., Doman, C. E., Khachaturyan, S., and Ehleringer, J. R.: Leaf-wax n-alkanes record the plant–water environment at leaf flush, P. Natl. Acad. Sci. USA, 110, 2659–2664, https://doi.org/10.1073/pnas.1213875110, 2013.

Tuthorn, M., Zech, R., Ruppenthal, M., Oelmann, Y., Kahmen, A., del Valle, H. F., Eglinton, T., Rozanski, K., and Zech, M.: Coupling δ^2H and δ^{18}O biomarker results yields information on relative humidity and isotopic composition of precipitation – a climate transect validation study, Biogeosciences, 12, 3913–3924, https://doi.org/10.5194/bg-12-3913-2015, 2015.

Wang, M., Zhang, W., and Hou, J.: Is average chain length of plant lipids a potential proxy for vegetation, environment and climate changes?, Biogeosciences Discuss., https://doi.org/10.5194/bgd-12-5477-2015, 2015.

Wirsig, C., Zasadni, J., Christl, M., Akçar, N., and Ivy-Ochs, S.: Dating the onset of LGM ice surface lowering in the High Alps, Quaternary Sci. Rev., 143, 37–50, https://doi.org/10.1016/j.quascirev.2016.05.001, 2016.

Wüthrich, L., Garcia Morabito, E., Zech, J., Gnägi, C., Trauerstein, M., Veit, H., Merchel, S., Scharf, A., Rugel, G., Christl, M., and Zech, R.: ^{10}Be surface exposure dating of the last deglaciation in the Aare Valley, Switzerland, Swiss J. Geosci., accepted, 2017a.

Wüthrich, L., Bliedtner, M., Schäfer, I. K., Zech, J., Shajari, F., Gaar, D., Preusser, F., Salazar, G., Szidat, S., and Zech, R.: n-Alkane composition from the Loess Paleosol Sequence Möhlin, Switzerland, PANGAEA, https://doi.org/10.1594/PANGAEA.884114, 2017b.

Zech, M., Buggle, B., Kleiber, K., Marković, S., Glaser, B., Hambach, U., Huwe, B., Stevens, T., Sümegi, P., Wiesenberg, G., and Zöller, L.: Reconstructing Quaternary vegetation history in the Carpathian Basin, SE-Europe, using n-alkane biomarkers as molecular fossils, E&G Quaternary Sci. J., 58, 148–155, https://doi.org/10.3285/eg.58.2.03, 2010.

Zech, M., Pedentchouk, N., Buggle, B., Leiber, K., Kalbitz, K., Marković, S. B., and Glaser, B.: Effect of leaf litter degradation and seasonality on D / H isotope ratios of n-alkane biomarkers, Geochim. Cosmochim. Ac., 75, 4917–4928, https://doi.org/10.1016/j.gca.2011.06.006, 2011.

Zech, M., Tuthorn, M., Detsch, F., Rozanski, K., Zech, R., Zöller, L., Zech, W., and Glaser, B.: A 220 ka terrestrial δ^{18}O and deuterium excess biomarker record from an eolian permafrost paleosol sequence, NE-Siberia, Chem. Geol., 360–361, 220–230, https://doi.org/10.1016/j.chemgeo.2013.10.023, 2013.

Zech, M., Zech, R., Rozanski, K., Gleixner, G., and Zech, W.: Do n-alkane biomarkers in soils/sediments reflect the δ^2H isotopic composition of precipitation? A case study from Mt. Kilimanjaro and implications for paleoaltimetry and paleoclimate research, Isot. Environ. Healt. S., 51, 1–17, https://doi.org/10.1080/10256016.2015.1058790, 2015.

Zech, M., Kreutzer, S., Zech, R., Goslar, T., Meszner, S., McIntyre, C., Häggi, C., Eglinton, T. I., Faust, D., and Fuchs, M.: Comparative ^{14}C and OSL dating of loess-paleosol sequences to evaluate post-depositional contamination of n-alkane biomarkers, Quaternary Res., 87, 180–189, https://doi.org/10.1017/qua.2016.7, 2017.

Zech, R., Zech, M., Marković, S., Hambach, U., and Huang, Y.: Humid glacials, arid interglacials? Critical thoughts on pedogenesis and paleoclimate based on multiproxy analyses of the loess–paleosol sequence Crvenka, Northern Serbia, Palaeogeogr. Palaeocl., 387, 165–175, https://doi.org/10.1016/j.palaeo.2013.07.023, 2013.

Zech, R., Mayr, C., and Doppler, G.: Löss und Paläoböden in Bobingen. Eine geochemische Reise in die letzte Eiszeit, in: DBG Mitteilungen, edited by: Auerswald, K. und Ahl, C., Bd. 117: Deutsche bodenkundliche Gesellschaft, München, Germany, 139–148, 2015.

E&G **Quaternary Science Journal**

Open Access

Thesis abstract

Weichselian phases and ice dynamics of the Scandinavian Ice Sheet in northeast Germany: a reassessment based on geochronological and geomorphological investigations in Brandenburg

Jacob Hardt

Fachbereich Geowissenschaften, Physische Geographie, Freie Universität Berlin, Berlin, Germany

Correspondence:	Jacob Hardt (jacob.hardt@fu-berlin.de)

Supervisors: Margot Böse, Markus Fuchs, Christopher Lüthgens
Dissertation online:
http://www.diss.fu-berlin.de/diss/receive/FUDISS_thesis_000000104286

This thesis presents new geochronological and geomorphological data concerning Weichselian ice dynamics of the Scandinavian Ice Sheet for the northeast German lowland area. The largest Weichselian ice extent in Brandenburg (Brandenburg phase) occurred in the late marine isotope stage 3. The global Last Glacial Maximum is represented by the Pomeranian ice marginal position in Brandenburg ($\sim$20 ka). Therefore, a 2-fold Last Glacial Maximum in Brandenburg, as previously proposed by Lüthgens and Böse (2011), is confirmed.

For the first time, we determined optically stimulated luminescence (OSL) ages of glaciofluvial deposits associated with the Weichselian Frankfurt phase at a site in Ladeburg (central Brandenburg; Fig. 1). Furthermore, we report new OSL ages of glaciofluvial deposits from the lignite mine Jänschwalde (southern Brandenburg), a key site regarding the Weichselian maximum extent during the Brandenburg phase. In combination with cosmogenic nuclide surface exposure ages of glacigenic boulders, which were collected from liter-

ature and recalibrated with an updated ^{10}Be production rate, a consistent process-based model of the Weichselian ice dynamics in Brandenburg was developed (Fig. 1).

The ice advance of the Brandenburg phase was dated to 34.1 ± 4.6 ka. For the formation of the Brandenburg ice marginal position, a mean age of 30 ± 4 ka was determined at Jänschwalde. The succeeding meltdown during the so-called Frankfurt phase was dated to 26.3 ± 3.7 ka at Ladeburg. The subsequent landscape stabilization phase started at around 24 ± 2 ka in central Brandenburg, which was deduced by recalibrated exposure ages of glacigenic boulders (Hardt et al., 2016). These ages are corroborated by other published OSL ages from the region (Fig. 1).

The recalibration of previously published cosmogenic exposure ages from glacigenic boulders with an up-to-date ^{10}Be production rate (Heyman, 2014) resulted in a considerable increase of the ages (9–15 %; Hardt and Böse, 2017). In combination, the OSL ages and the cosmogenic nuclide exposure ages now provide a consistent geochronology of the Weichselian ice dynamics in Brandenburg. The largest Weichselian ice extent during the late marine isotope stage 3 (Brandenburg phase) corresponds with the so-called Klintholm advance in Denmark (Houmark-Nielsen, 2010) and a possible ice advance in central Poland (Marks, 2012).
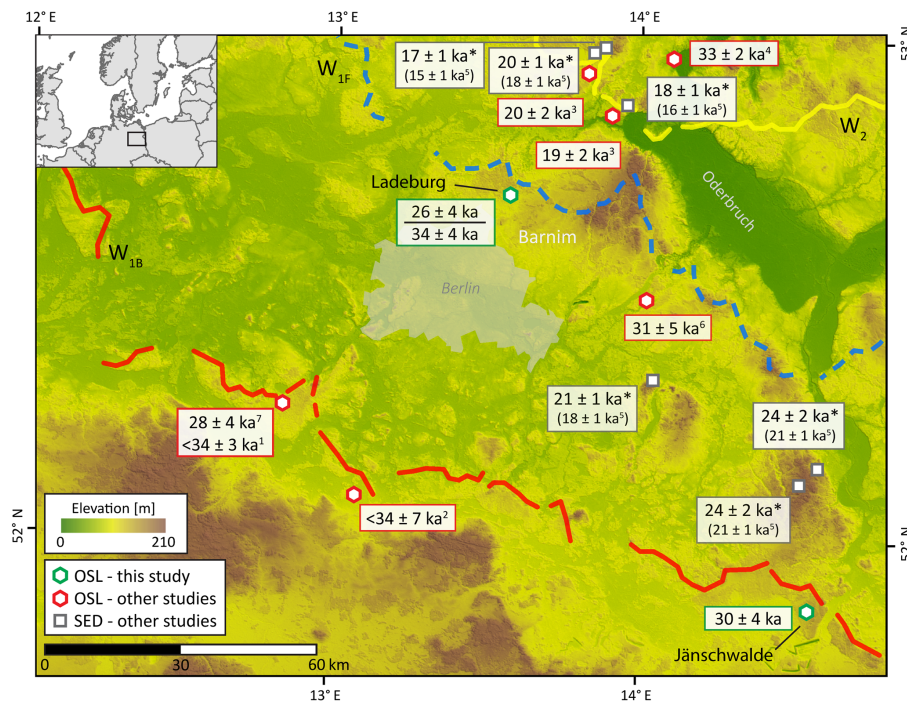
Figure 1. Overview map showing compiled ages from the thesis (green) and other authors (red/grey). OSL is optically stimulated lumines-cence dating. SED is cosmogenic nuclide surface exposure dating. Figure modified from Hardt et al. (2016) and references therein. See the respective paper and the thesis for a detailed list of the cited ages.

In the area of the supposed Frankfurt ice marginal position on the Barnim plateau (a till plain to the north of Berlin), we detected a series of ice marginal fans by analysis of a high-resolution lidar (light detection and ranging) digital elevation model. These arcuate, parallel landforms rise up to 10 m from the surroundings and extend up to 15 km in length and up to 1.5 km in width. Outcrop studies, geophysical investigations (electrical resistivity tomography) and map interpretation revealed that the ice marginal fans consist of diamictic material (Hardt et al., 2015). OSL dating of glaciofluvial deposits beneath and above one of the structures revealed that their formation took place in the Frankfurt phase (26 ± 4 ka; Hardt et al., 2016), during the successional downwasting of the ice after the Brandenburg phase.

Data availability. The data are publicly available via the thesis and the references therein.

Competing interests. The author declares that he has no conflict of interest.

References

Hardt, J. and Böse, M.: The timing of the Weichselian Pomeranian ice marginal position south of the Baltic Sea: A critical review of morphological and geochronological results, Quatern. Int., in press, 2017.

Hardt, J., Hebenstreit, R., Lüthgens, C., and Böse, M.: High-resolution mapping of ice-marginal landforms in the Barnim region, northeast Germany, Geomorphology, 250, 41–52, 2015.

Hardt, J., Lüthgens, C., Hebenstreit, R., and Böse, M.: Geochrono-logical (OSL) and geomorphological investigations at the pre-sumed Frankfurt ice marginal position in northeast Germany, Quaternary Sci. Rev., 154, 85–99, 2016.

Heyman, J.: Paleoglaciation of the Tibetan Plateau and surround-ing mountains based on exposure ages and ELA depression esti-mates, Quaternary Sci. Rev., 91, 30–41, 2014.

Houmark-Nielsen, M.: Extent, age and dynamics of Marine Isotope Stage 3 glaciations in the southwestern Baltic Basin, Boreas, 39, 343–359, 2010.

Lüthgens, C. and Böse, M.: Chronology of Weichselian main ice marginal positions in north-eastern Germany, E&G Quaternary Sci. J., 60, 236–247, 2011.

Marks, L.: Timing of the Late Vistulian (Weichselian) glacial phases in Poland, Quaternary Sci. Rev., 44, 81–88, 2012.

Open Access

E&G Quaternary Science Journal

Express report

Lipid biomarkers in aeolian sediments under desert pavements – potential and first results from the Black Rock Desert, Utah, USA, and Fuerteventura, Canary Islands, Spain

Marcel Lerch[1], **Marcel Bliedtner**[2], **Christopher-Bastian Roettig**[1], **Jan-Uwe Schmidt**[1], **Sönke Szidat**[3], **Gary Salazar**[3], **Roland Zech**[2,4], **Bruno Glaser**[5], **Arno Kleber**[1], and **Michael Zech**[1,5]

[1]Department of Geosciences, Institute of Geography, University of Technology Dresden,
Helmholtzstraße 10, 01069 Dresden, Germany
[2]Institute of Geography and Oeschger Centre for Climate Change Research, Biogeochemistry and
Palaeoclimatology Group, University of Bern, Hallerstrasse 12, 3012 Bern, Switzerland
[3]Department for Chemistry and Biochemistry and Oeschger Centre for Climate Change Research,
University of Bern, Freiestrasse 3, 3012 Bern, Switzerland
[4]Institute of Geography, Chair of Physical Geography, Friedrich Schiller University Jena,
Löbdergraben 32, 07743 Jena, Germany
[5]Institute of Agronomy and Nutritional Sciences, Soil Biogeochemistry, Martin Luther University
Halle-Wittenberg, Von-Seckendorff-Platz 3, 06120 Halle (Saale), Germany

Correspondence: Marcel Lerch (marcel.lerch@mailbox.tu-dresden.de)

Relevant dates: Published: 3 January 2018

How to cite: Lerch, M., Bliedtner, M., Roettig, C.-B., Schmidt, J.-U., Szidat, S., Salazar, G., Zech, R., Glaser, B., Kleber, A., and Zech, M.: Lipid biomarkers in aeolian sediments under desert pavements – potential and first results from the Black Rock Desert, Utah, USA, and Fuerteventura, Canary Islands, Spain, E&G Quaternary Sci. J., 66, 103–108, https://doi.org/10.5194/egqsj-66-103-2017, 2017.

1   Introduction

The analysis of lipid biomarkers, particularly n-alkanes, has become a popular and widely applied tool in paleoenvironmental and climate research during the last decades (Zech et al., 2011). Whereas long-chain n-alkane homologues ($> n\mathrm{C}_{27}$) with a strong odd-over-even predominance (OEP) are characteristic for higher plant leaf waxes, short-chain and mid-chain homologues ($n\mathrm{C}_{16}$-$n\mathrm{C}_{26}$) indicate aquatic or microbial sources of n-alkanes. Furthermore, $n\mathrm{C}_{31}$ and $n\mathrm{C}_{33}$ were found to dominate in most grasses and herbs, whereas $n\mathrm{C}_{27}$ and $n\mathrm{C}_{29}$ were reported to dominate in most trees and shrubs (Zech et al., 2009). Therefore, sedimentary long-chain n-alkanes have been used for reconstructing vegetation changes, among others, from loess–paleosol sequences (Zech et al., 2012, 2013).

In contrast, aeolian sediments under desert pavements, potentially very useful terrestrial archives in arid regions (Dietze et al., 2016; Schmidt, 2008; Faust et al., 2015), have not been investigated for lipid biomarkers so far. Here, apart from long-chain n-alkanes as proxies for vegetation reconstructions, short- and mid-chain n-alkanes may also help to shed light on the role of soil microorganisms and biological soil crusts for the formation of desert soils.

Therefore, the aim of this study was to test the applicability of n-alkane analyses in such settings. We chose two pilot study areas, namely the Black Rock Desert, which is located in western Utah (USA), and the island of Fuerteventura, which belongs to the Canary Islands (Spain). Specifically, we addressed the following objectives and research questions:

1. Quantification of *n*-alkane biomarkers in the investigated aeolian sediments under desert pavements.

2. Do the leaf-wax-derived long-chain *n*-alkanes of aeolian sediments under desert pavements allow us to distinguish between different vegetation types?

3. Are the *n*-alkane concentrations in aeolian sediments under desert pavements high enough to carry out radiocarbon dating?

4. Do short- and mid-chain *n*-alkanes as well as the ^{14}C ages of the *n*-alkanes provide information about the genesis of desert soils under desert pavements?

2 Material and methods

2.1 Study areas

One study area is located in the Black Rock Desert (Utah, USA). This semiarid region belongs to the southern part of the Sevier Desert and covers an area of 7000 km^2. The geographic coordinates are northernmost point 39°16′ N, southernmost point 38°37′ N, easternmost point 112°15′ W and westernmost point 113°02′ W. To the west and the east, the Black Rock Desert is bounded by mountain ranges. Following the effective climate classification by Köppen, the climate for this study area corresponds to a cold arid steppe climate (BSk) (Schmidt, 2008). The natural vegetation mainly consists of *Artemisia tridentata* and a high variation of different shrubs. It was influenced by anthropogenic effects (Schmidt, 2008).

The second study area is located in the northern part of the Canary Island Fuerteventura. Two soil profiles were chosen for sampling. The coordinates of soil profile 1 (SP1) are 28°65′60″ N and 13°87′07″ W. Soil profile 2 (SP2) is classified with the coordinates 28°65′15″ N and 13°85′14″ W. Volcanic landforms and Quaternary sand dunes are typical for the study area on Fuerteventura (Criado et al., 2004). The northern part of the island has an arid to semiarid climate. According to the climate classification by Köppen, there is a hot arid desert climate (BWh). Because of the arid climate conditions, no abundant vegetation exists, comprising few shrubs, disperse grassland and various kinds of lichens.

2.2 Sampling

For this biomarker pilot study we chose 26 samples in total (Table 1). The 22 samples from the Black Rock Desert are from 6 soil profiles and were previously investigated for certain parameters, such as grain size distribution, total organic carbon (TOC) and carbonate content (CaCO$_3$) (Schmidt, 2008). The soil profiles are Ice Springs 1 (IS1), Lava Ridge 3 (LR3), Pavant Butte 4 (PB4), Pot Mountain 1 (PM1), Pot Mountain 2 (PM2) and Tabernacle Hill 1 (TH1).

Samples were taken for each horizon and therefore from various depths. According to the grain size distribution, the aeolian sediments of the soil profiles IS1, LR3, PM1 and TH1 can be qualified as desert loess because of their high amount of fine sand and coarse silt. The profiles PB4 and PM2 have lower silt contents, but they can also be qualified as aeolian sediments. The TOC values range from 0.3 to 1.6 %.

The four samples from Fuerteventura originate from two soil profiles (samples F/335 and F/336 from soil profile SP1 and samples F/337 and F/338 from soil profile SP2), which are located in the northern part of the island and are approximately 1.5 km apart. Although TOC analyses have not been carried out for these samples, a comparison with the study of Faust et al. (2015) suggests TOC values smaller than 0.25 %. Both soil profiles SP1 and SP2 have desert pavements on the soil surface. Desert pavements mainly consist of basaltic rocks for both study areas.

2.3 *n*-Alkane biomarker quantification and radiocarbon dating

Total lipid extracts (TLEs) were obtained using Soxhlet apparatuses and DCM : MeOH (2 : 1) as solvent for 24 h. After drying the TLEs under nitrogen, a lipid fractionation was realized via aminopropyl columns. The aliphatic fraction, containing the *n*-alkanes, was eluted with 3 mL *n*-hexane. Quantification of the *n*-alkanes was performed on a gas chromatograph coupled to a flame ionization detector (GC-FID) and an external alkane standard mixture (*n*C$_8$–*n*C$_{40}$).

Given that the *n*-alkane chromatograms from the Black Rock Desert and Fuerteventura yielded large UCM humps (unresolved complex mixture) as they are often observed also for loess–paleosol samples (Zech et al., 2013), a second purification step was necessary before radiocarbon dating could be performed according to the procedure described by Zech et al. (2017). In brief, the *n*-alkanes were purified over silver nitrate (AgNO$_3$-coated silica gel) and zeolite (Zeolite A) columns. The zeolite, containing the purified *n*-alkanes, was dissolved using hydrofluoric acid. After liquid–liquid extraction with *n*-hexane, the purified *n*-alkanes were measured and quantified again on the GC-FID.

Based on the *n*-alkane amounts per sample, the location and the stratigraphical position, 10 samples were selected for radiocarbon dating (^{14}C): IS1_1, IS1_3, PM1_3, TH1_1, TH1_3, LR3_1, LR3_4, F/335/3, F/336/3 and F/338/3 (Table 1 and Fig. 2). The amounts of *n*-alkanes ranged between 15 and 80 µg per vial for the samples from Fuerteventura. For the samples from the Black Rock Desert, the *n*-alkane amounts ranged between 30 and 53 µg per vial. Radiocarbon dating was carried out using accelerated mass spectrometry (AMS) at the University of Bern (Szidat et al., 2014). Results of radiocarbon dating were corrected for constant and cross contamination (Haas et al., 2017). All ^{14}C ages were calibrated using the Intcal 13 calibration curve (Table 1).

Table 1. Soil profiles, sample list and n-alkane biomarker results from the Black Rock Desert, Utah, USA, and Fuerteventura, Canary Islands, Spain. TOC content is the total organic carbon content, TAC is the total n-alkane concentration, OEP is the odd-over-even predominance, LSR is the ratio of long-chain to short- and mid-chain n-alkanes, $n\text{C}_{max}$ is the dominant n-alkane homologue and n.a. indicates no value available.

Sample number	Sample name		Sample label	Average value (depth)	TOC content	TAC	OEP	LSR[b]	$n\text{C}_{max}$	[14]C ages		Desert pavements
No.	Soil profile	No.	Name	cm	%	$\mu\text{g g}^{-1}$		%		uncal years BP	cal years BP	
1	IS1	1	IS1_1	2.5	1.6	1.11	6.84	86	$n\text{C}_{29}$	778 ± 89	733 ± 84	initial
2	IS1	2	IS1_2	7.5	0.9	0.51	9.25	83	$n\text{C}_{29}$			
3	IS1	3	IS1_3	15.0	0.8	1.35	6.74	81	$n\text{C}_{29}$	3181 ± 113	3395 ± 141	
4	IS1	4	IS1_4	25.0	n. a.	0.17	n.a.[c]	34	$n\text{C}_{29}$			
5	LR3	1	LR3_1	1.5	1.0	1.21	9.29	84	$n\text{C}_{29}$	1285 ± 67	1200 ± 71	initial
6	LR3	2	LR3_2	6.5	0.7	0.57	8.98	87	$n\text{C}_{29}$			
7	LR3	3	LR3_3	15.0	n. a.	0.35	6.70	76	$n\text{C}_{29}$			
8	LR3	4	LR3_4	25.0	n. a.	0.83	3.48	70	$n\text{C}_{29}$	4340 ± 77	4960 ± 128	
9	LR3	5	LR3_5	45.0	n. a.	0.34	2.79	64	$n\text{C}_{27}$			
10	PB4	1	PB4_1	5.0	0.3	0.14	6.48	86	$n\text{C}_{29}$			yes
11	PB4	2	PB4_2	13.0	0.4	0.10	n.a.[c]	83	$n\text{C}_{29}$			
12	PB4	3	PB4_3	20.0	n. a.	0.13	8.66	62	$n\text{C}_{29}$			
13	PB4	4	PB4_4	29.5	n. a.	0.00	n.a.[c]	n.a.	n.a.			
14	PB4	5	PB4_5	47.5	n.a.	0.00	n.a.[c]	n.a.	n.a.			
15	PM1	1	PM1_1	2.5	0.5	0.42	10.15	75	$n\text{C}_{29}$			yes
16	PM1	2	PM1_2	8.5	0.5	0.59	10.78	76	$n\text{C}_{29}$			
17	PM1	3	PM1_3	17.0	n. a.	0.91	9.78	67	$n\text{C}_{29}$	7830 ± 123	8689 ± 16	
18	PM2	1	PM2_1	4.0	0.4	0.28	13.94	76	$n\text{C}_{31}$			yes
19	PM2	2	PM2_2	19.0	1.1	0.36	6.73	24	$n\text{C}_{29}$			
20	TH1	1	TH1_1	2.5	1.0	0.88	7.07	83	$n\text{C}_{29}$	1587 ± 90	1490 ± 96	initial
21	TH1	2	TH1_2	7.5	0.5	0.79	7.25	86	$n\text{C}_{29}$			
22	TH1	3	TH1_3	15.0	n. a.	0.69	6.58	80	$n\text{C}_{29}$	3767 ± 75	4149 ± 120	
23	F/335/SP1	3	F/335/3	30.0	$<0.25^a$	0.62	11.23	90	$n\text{C}_{33}$	3732 ± 75	4095 ± 116	yes
24	F/336/SP1	3	F/336/3	60.0	$<0.25^a$	0.28	6.55	85	$n\text{C}_{31}, n\text{C}_{33}$	5456 ± 82	6236 ± 101	
25	F/337/SP2	3	F/337/3	22.5	$<0.25^a$	0.15	n.a.[c]	71	$n\text{C}_{29}, n\text{C}_{31}$			yes
26	F/338/SP2	3	F/338/3	40.0	$<0.25^a$	1.87	1.12	77	$n\text{C}_{29}, n\text{C}_{31}$	$19\,734 \pm 227$	$23\,760 \pm 276$	

[a] No own values for TOC available. TOC values refer to results of Faust et al. (2015). Study area: Lajares III, Fuerteventura, Spain.
[b] Modified after Zech et al. (2012) with long-chain n-alkanes $\geq n\text{C}_{27}$ and short- and mid-chain n-alkanes $< n\text{C}_{27}$.
[c] No even n-alkanes detectable.

3 Results

The total n-alkane concentrations (TAC = sum of $n\text{C}_{16}$ to $n\text{C}_{33}$) for all 26 samples range from 0 to 1.87 $\mu\text{g g}^{-1}$ sediment (Table 1). For comparison, n-alkane concentrations of up to 5.1 and 12.6 $\mu\text{g g}^{-1}$ sediment have been reported for the long-chain n-alkanes from loess–paleosol sequences alone (Zech et al., 2012, 2013). This reflects the very low sedimentary organic carbon contents of the aeolian sediments under desert pavements.

The long-chain n-alkanes clearly dominate over short- and mid-chain n-alkanes (ratio of long-chain to short- and mid-chain n-alkanes – LSR), as it is typically observed for plant leaf waxes. The percentages of long-chain to total n-alkanes are greater than or equal to 71 % in the topsoils and generally become smaller with increasing soil depth (LSR, Table 1). This likely indicates that the soil organic matter is becoming stronger degraded in the subsoils compared to the topsoils. Whereas the n-alkane homologue $n\text{C}_{29}$ is predominant in most samples from the Black Rock Desert, $n\text{C}_{29}$, $n\text{C}_{31}$

and/or $n\text{C}_{33}$ predominate in the samples from Fuerteventura ($n\text{C}_{max}$, Table 1).

The OEP, which is typically high in fresh plant material and decreases with degradation, ranges from 1 to 14 for all investigated samples (Table 1 and Fig. 1) and, similar to the LSRs, generally decreases with increasing soil depth.

It is generally considered that a carbon amount of $>20\,\mu\text{g C sample}^{-1}$ is needed for radiocarbon dating. This prerequisite was fulfilled for 14 of the total 26 prepared n-alkane samples and for 9 of the samples chosen for radiocarbon dating (except sample F/336/3 with 15 μg C). The n-alkane ^{14}C ages range from 733 ± 84 to $23\,760 \pm 276$ cal years BP and are stratigraphically consistent for all soil profiles with two ^{14}C results (Table 1 and Fig. 2). This also holds true for sample F/336/3, which furthermore does also not strike by its measurement uncertainty and is therefore considered to be robust.
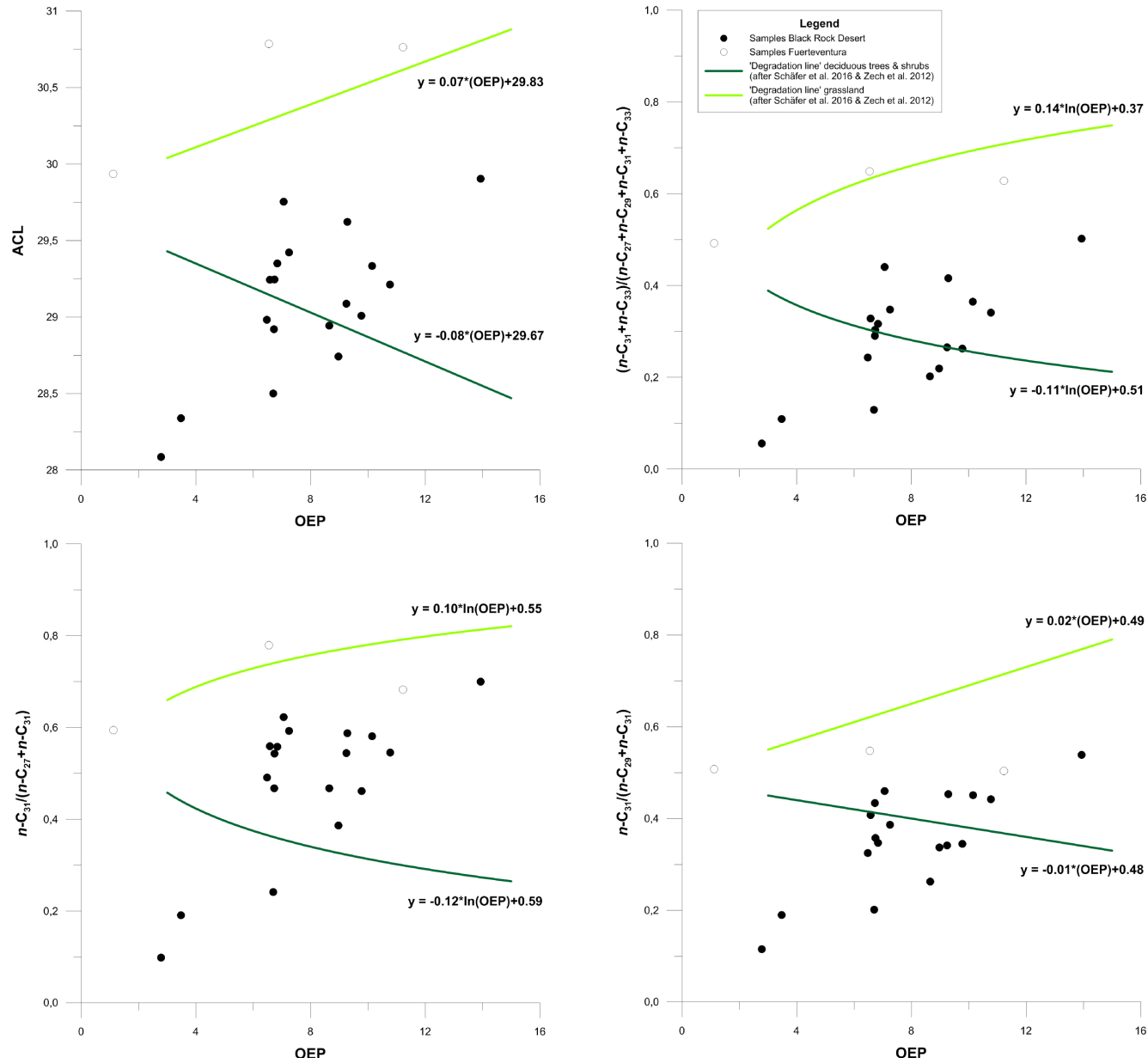
Figure 1. Endmember plots for samples of the study areas Black Rock Desert, Utah, USA, and Fuerteventura, Canary Islands, Spain. Degradation lines for grassland and deciduous trees and shrubs, respectively, are derived from datasets of Schäfer et al. (2016) and Zech et al. (2012). ACL is the average chain length and OEP is the odd-over-even predominance.

4 Discussion

4.1 Vegetation reconstruction

The predominant n-alkane homologue (nC$_{max}$) of most samples from the Black Rock Desert is nC$_{29}$, whereas nC$_{29}$, nC$_{31}$ and/or nC$_{33}$ predominate in the samples from Fuerteventura (nC$_{max}$, Table 1). This may serve as a first indication that the n-alkanes in the Black Rock Desert are mainly shrub derived, whereas the n-alkanes on Fuerteventura are mainly grass derived. Indeed, this interpretation is in agree-

ment with the modern vegetation, which is shrub dominated in the Black Rock Desert and grass dominated on Fuerteventura. The very low n-alkane concentrations in the subsoils of the soil profiles allow no reliable statements on the past vegetation cover for both study areas.

As mentioned above, organic matter degradation may affect the n-alkane patterns (LSR, OEP and nC$_{max}$). Therefore, we plotted various n-alkane ratios (ACL,   (nC$_{31}$ + nC$_{33}$) / (nC$_{27}$ + nC$_{29}$ + nC$_{31}$ + nC$_{33}$), nC$_{31}$ / (nC$_{27}$ + nC$_{31}$) and nC$_{31}$ / (nC$_{29}$ + nC$_{31}$)) against the
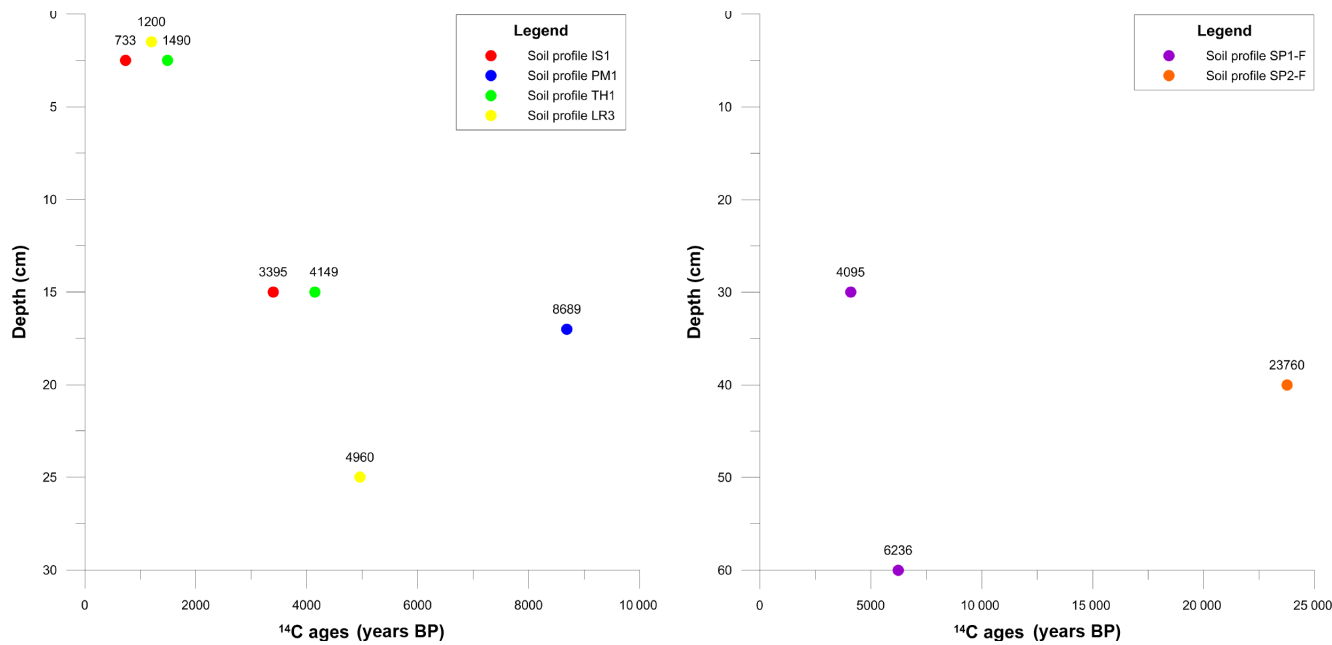
Figure 2. n-Alkane ^{14}C ages for soil profiles from the Black Rock Desert, Utah, USA (left), and Fuerteventura, Canary Islands, Spain (right). All ^{14}C ages are plotted as calibrated ages. IS1 is Ice Springs 1, PM1 is Pot Mountain 1, TH1 is Tabernacle Hill 1, LR3 is Lava Ridge 3, SP1-F is stone pavement sample location 1 – Fuerteventura and SP2-F is stone pavement sample location 2 – Fuerteventura.

degradation proxy OEP (Fig. 1). This approach was originally introduced by Zech et al. (2009), further developed by Zech et al. (2012, 2013) and Schäfer et al. (2016), and allows us to illustrate and account for degradation effects. The "degradation lines" for grassland vs. deciduous trees and shrubs are based on modern plant and soil reference dataset. Samples from Fuerteventura plot close to the degradation line of grassland, whereas the samples from the Black Rock Desert plot – albeit with a large scattering – around or closer to the degradation line of deciduous trees and shrubs (Fig. 1).

This illustrates the potential of n-alkane analyses in aeolian sediments under desert pavements for environmental and vegetation reconstruction. For this study, we refrain from calculating the percent of grass–herb versus shrub–tree contributions using endmember modeling given the lack of continuous archives. Nevertheless, we would like to point to the updated functions in Fig. 1 describing the degradation lines, which will make endmember-model calculations possible in future studies.

4.2 Potential for studying desert soils and contribution of soil microorganisms

The high LSR and OEP values in our samples indicate that the n-alkanes in aeolian sediments under desert pavements are primarily plant derived. Lower LSR and OEP values with increasing depth probably reflect enhanced degradation, but there is no evidence at least from the n-alkane biomarkers for the abundant occurrence of soil microorganisms forming biological soil crusts.

While the n-alkane ^{14}C ages are stratigraphically consistent, it is noteworthy that the n-alkanes within the topmost 2.5 cm yielded ages > 733 cal years BP. n-Alkanes at or below 15 cm soil depth yielded ages > 3395 cal years BP. This suggests first that the input of modern n-alkanes to the topsoils is very low – likely reflecting the low biomass production in the arid study areas – and that there is no substantial incorporation of modern n-alkanes by roots or rhizomicrobial processes to the subsoils (Zech et al., 2017). Moreover, this suggests that the accumulation and sedimentation rates are very low or erosive processes by heavy rainfall events or deflation – possibly induced by grazing – cannot be excluded.

5 Conclusions and outlook

Although n-alkane concentrations are very low in the studied aeolian sediments under desert pavements, it was possible in this pilot study (i) to distinguish between samples from the Black Rock Desert (mainly shrub-derived n-alkanes) and from Fuerteventura (mainly grass-derived n-alkanes) and (ii) to perform radiocarbon dating on bulk n-alkanes. Ongoing studies now aim at building up modern plant and soil reference datasets from the study areas rather than relying on published reference datasets established for central Europe (Schäfer et al., 2016).

The n-alkane patterns provide no evidence for major input from soil microorganisms. Further studies investigating the potential role of biological soil crusts for the development of desert pavements focusing on other biomarkers than

n-alkanes are encouraged. The *n*-alkane ^{14}C ages from the Black Rock Desert and from Fuerteventura suggest low organic matter input, low sedimentation rates and low incorporation of root-derived *n*-alkanes. Comparative optically stimulated luminescence dating for the soil profiles under study is in progress.

The Supplement related to this article is available online at https://doi.org/10.5194/egqsj-66-103-2018-supplement.

References

Criado, C., Guillou, H., Hansen, A., Hansen, C., Lillo, P., Torres, J. M., and Naranjo, A.: Geomorphological Evolution of Parque Natural de Las Dunas de Corralejo (Fuerteventura, Canary Islands), Reunion Nacional de Geomorfologia, 8, 291–297, 2004.

Dietze, M., Dietze, E., Lomax, J., Fuchs, M., Kleber, A., and Wells, S. G.: Environmental history recorded in aeolian deposits under stone pavements, Mojave Desert, USA, Quaternary Res., 85, 4–16, 2016.

Faust, D., Yanes, Y., Willkommen, T., Roettig, C., Richter, D., Richter, D., Suchodoletz, H. V., and Zöller, L.: A contribution to the understanding of late Pleistocene dune sand-paleosol-sequences in Fuerteventura (Canary Islands), Geomorphology, 246, 290–304, 2015.

Haas, M., Bliedtner, M., Borodynkin, I., Salazar, G., Szidat, S., Eglinton, T. I., and Zech, R.: Radiocarbon Dating of Leaf Waxes in the Loess-Paleosol Sequence Kurtak, Central Siberia, Radiocarbon, 59, 1–12, 2017.

Schäfer, I. K., Lanny, V., Franke, J., Eglinton, T. I., Zech, M., Vysloužilová, B., and Zech, R.: Leaf waxes in litter and topsoils along a European transect, SOIL, 2, 551–564, https://doi.org/10.5194/soil-2-551-2016, 2016.

Schmidt, J.-U.: Bodenevolution während der letzten 30 000 Jahre in der Black Rock Desert, W Utah, SW USA, Diploma thesis, Institute of Geography, University of Technology Dresden, Dresden, Germany, 183 pp., 2008.

Szidat, S., Salazar, G. A., Vogel, E., Battaglia, M., Wacker, L., Synal, H. A., and Türler, A.: [14]C analysis and sample preparation at the new Bern Laboratory for the Analysis of Radiocarbon with AMS (LARA), Radiocarbon, 56, 561–566, 2014.

Zech, M., Buggle, B., Leiber, K., Markovic, S., Glaser, B., Hambach, U., Huwe, B., Stevens, T., Sümegi, P., Wiesenberg, G., and Zöller, L.: Reconstructing Quaternary vegetation history in the Carpathian Basin, SE Europe, using *n*-alkane biomarkers as molecular fossils, E&G Quaternary Sci. J., 58, 148–155, 2009.

Zech, M., Zech, R., Buggle, B., and Zöller, L.: Novel methodological approaches in loess research – interrogating biomarkers and compound specific stable isotopes, E&G Quaternary Sci. J., 60, 170–187, 2011.

Zech, M., Rass, S., Buggle, B., Löscher, M., and Zöller, L.: Reconstruction of the late Quaternary paleoenvironments of the Nussloch loess-paleosol sequence, Germany, using *n*-alkane biomarkers, Quaternary Res., 78, 226–235, 2012.

Zech, M., Krause, T., Meszner, S., and Faust, D.: Incorrect when uncorrected: Reconstructing vegetation history using *n*-alkane biomarkers in loess-paleosol sequences – A case study from the Saxonian loess region, Germany, Quatern. Int., 296, 108–116, 2013.

Zech, M., Kreutzer, S., Zech, R., Goslar, T., Meszner, S., McIntyre, C., Häggi, C., Eglinton, T., Faust, D., and Fuchs, M.: Comparative ^{14}C and OSL dating of loess-paleosol sequences to evaluate post-depositional contamination of *n*-alkane biomarkers, Quaternary Res., 87, 180–189, 2017.

Open Access

E&G Quaternary Science Journal

Express report

Leaf waxes from aeolianite–paleosol sequences on Fuerteventura and their potential for paleoenvironmental and climate reconstructions in the arid subtropics

Julian Struck[1,a], **Christopher B. Roettig**[2], **Dominik Faust**[3], and **Roland Zech**[1,a]

[1]Institute of Geography and Oeschger Centre for Climate Change Research,
University of Bern, Bern, Switzerland
[2]Landscape Ecology, Dresden University of Technology, Dresden, Germany
[3]Physical Geography, Dresden University of Technology, Dresden, Germany
[a]now at: Physical Geography, Friedrich-Schiller University, Jena, Germany

1 Introduction

One of the biggest challenges for our civilization is climate change. Especially regions that are characterized by harsh conditions today will be affected by major changes in the future. It is therefore essential to investigate and understand anthropogenic effects and natural climate variability in the past, and attention should be paid particularly to arid and semiarid regions, which may suffer from further aridization.

Fuerteventura is such a region, yet little is known about past climate and environmental conditions. Paleoenvironmental reconstructions on Fuerteventura are mainly based on morphodynamic and stratigraphical investigations of aeolianite–paleosol sequences (Faust et al., 2015; Roettig et al., 2017, and references therein).

Lipid biomarkers, especially *n*-alkanes, may serve as a powerful, novel tool for paleoenvironmental reconstruction. Long-chain *n*-alkanes are epicuticular leaf waxes, which protect the plant from various environmental influences (Castañeda et al., 2016). They can provide numerous environmental information. The chain length patterns, for example, can reflect the dominant vegetation type (Zech et al., 2009, 2013; Schäfer et al., 2016b). Moreover, the hydrogen isotopic com-

position of *n*-alkanes may serve as proxy for paleohydrological conditions, recording changes in precipitation, evapotranspiration and temperature (Sachse et al., 2012; Zech et al., 2013). Furthermore, recent technological developments allow compound-specific ^{14}C dating by accelerated mass spectroscopy to establish more robust chronologies (Häggi et al., 2014; Haas et al., 2017).

For this study *n*-alkane analyses were applied for two aeolianite–paleosol sequences on Fuerteventura to test their potential for paleoenvironmental reconstructions under arid conditions in general and the *n*-alkanes preservation in a sparsely vegetated landscape in particular.

2 Geographical setting

The northern tip of Fuerteventura is mainly characterized by Tertiary and Pleistocene volcanism. Within the volcanic fields, composed of lava and pyroclastics, several fields of dunes and sand sheets developed during the Pleistocene and Holocene (Fig. 1) (Roettig et al., 2017). In the interior of the islands up to 13 m thick successions of alternating sand layers and paleosols are perfect archives to reflect past climate
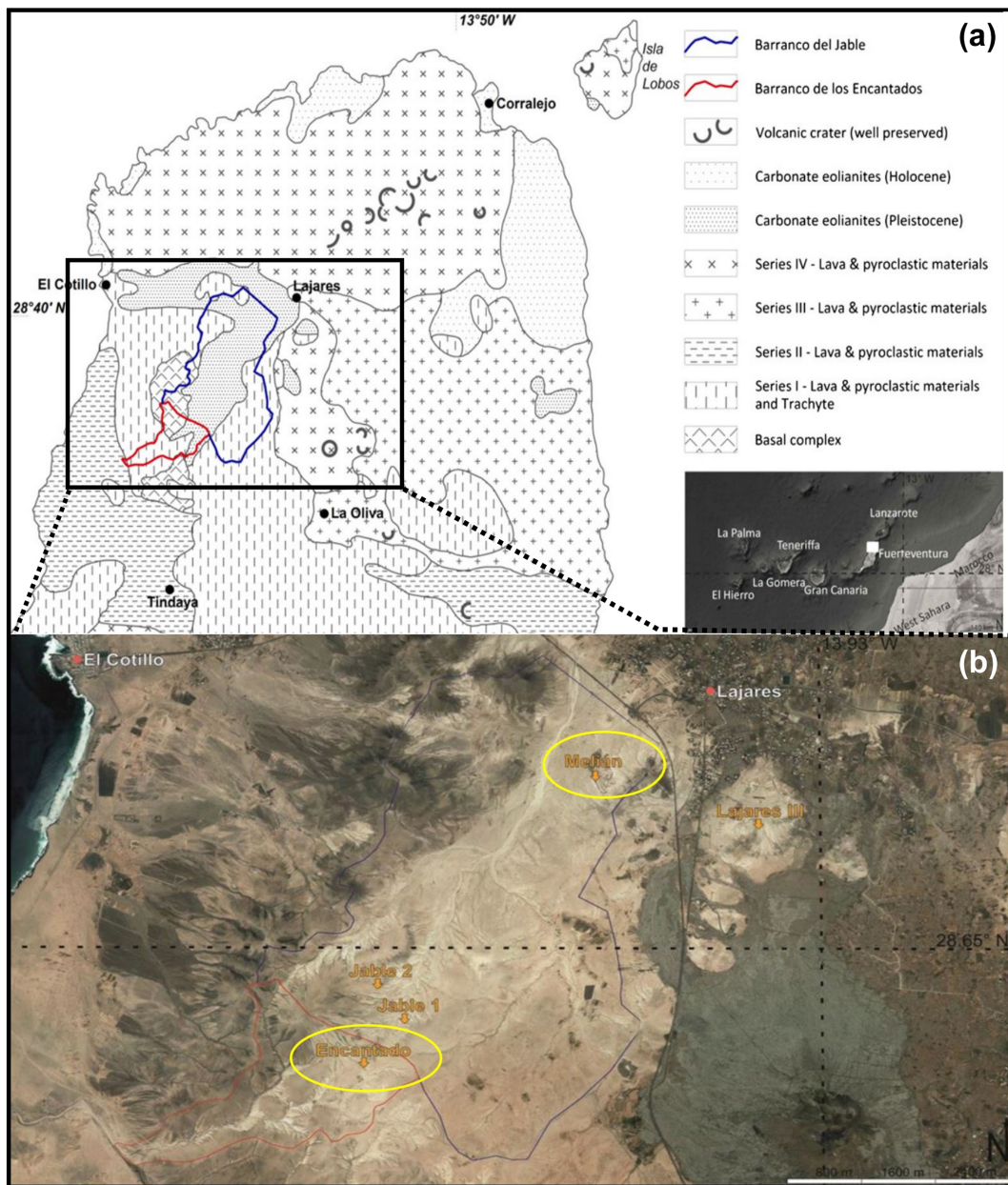
Figure 1. Location map and the northern tip of Fuerteventura showing major geological units and both catchments of the study area **(a)**. Google Earth image of the catchments Barranco del Jable (blue) and Barranco de los Encantados (red). Aeolianite–paleosol sequences are marked in yellow **(b)** (modified after Roettig et al., 2017).

changes as well as geological and morphological processes shaping this landscape. The sediments are mainly composed of biogenetic coarse sands of shelf origin (dune sands), partly mixed with volcanic material and dust from the Sahara.

Nowadays, deeply incised gully systems allow the recognition of different paleosurfaces which document periods of soil-forming processes and prevailing dust imprint. The study area can be separated into two catchments: the Barranco de los Encantados and the Barranco del Jable (Fig. 1). Both are characterized by arid conditions (like the whole is-

land), sparse vegetation cover and active morphodynamics in the form of huge gully systems (Faust et al., 2015; Roettig et al., 2017).

Five aeolianite–paleosol sequences have previously been investigated for sediment composition, sedimentation, soil formation and geochemical features (Faust et al., 2015; Roettig et al., 2017). Based on these investigations and 16 infrared stimulated luminescence ages, Roettig et al. (2017) correlated all five sequences and established a preliminary chronology.

From two of these aeolianite–paleosol sequences, we selected a total of 15 samples (Encantado: 7; Melián: 8) for leaf wax *n*-alkane analyses. Samples from Encantado cover the time back to 280 ka, while samples from Melián go back to 140 ka.

3 Methods

Dry, homogenized bulk sediments (~ 35 g, < 2 mm) were extracted using an accelerating solvent extractor (6.9 MPa, 100 °C; Dionex 200) with a dichloromethane / methanol ratio of 9 : 1. The total lipid extracts were separated into aliphatic, polar and acidic fractions over aminopropyl silica gel (45 mm; Supelco) pipette columns. The aliphatics (including *n*-alkanes) were eluted with hexane and spiked with 5a-androstanone as an internal standard. The *n*-alkane concentrations were quantified by a gas chromatography–flame ionization detector (GC-FID) relative to the internal standard and two external standards (*n*-C_{20} to *n*-C_{40} alkane mixture; Supelco: 40, 4 ng). After quantification, all samples were additionally cleaned over coupled zeolite–silver nitrate pipette columns, and the measuring procedure on the GC-FID was repeated.

Total *n*-alkane concentration was calculated as the sum of *n*-C_{25} to *n*-C_{35}. The average chain length (ACL) was determined by the following equation:

$$ACL = \frac{(27 \times n\text{-}C_{27} + 29 \times n\text{-}C_{29} + 31 \times n\text{-}C_{31} + 33 \times n\text{-}C_{33})}{(n\text{-}C_{27} + n\text{-}C_{29} + n\text{-}C_{31} + n\text{-}C_{33})}. \quad (1)$$

The ACL indicates chain length variations of *n*-alkanes and can be used as proxy for vegetation changes. Longer chain lengths, typically *n*-C_{31} and *n*-C_{33}, indicate a dominance of grasses and herbs, whereas shorter chain lengths (*n*-C_{27} and *n*-C_{29}) mainly derive from shrubs and deciduous trees (Zech et al., 2009, 2013; Schäfer et al., 2016b). The odd-over-even predominance (OEP) of the *n*-alkanes is a proxy for degradation of the *n*-alkanes:

$$OEP = \frac{(n\text{-}C_{27} + n\text{-}C_{29} + n\text{-}C_{31} + n\text{-}C_{33})}{(n\text{-}C_{26} + n\text{-}C_{28} + n\text{-}C_{30} + n\text{-}C_{32})}. \quad (2)$$

High OEP values are typical for fresh plant material, whereas lower OEPs (< 5) indicate enhanced degradation (Zech et al., 2009; Schäfer et al., 2016b).

4 Results

Total *n*-alkane concentrations for the aeolianite–paleosol sequence Encantado are low, ranging from 0.22 to 0.52 µg g^{-1} (Fig. 2). The OEPs are also very low, with values not even exceeding 2.1. The ACL ranges from 29.9 to 30.4.

Five samples from Melián also have low *n*-alkane concentrations between 0.38 and 0.58 µg g^{-1} (Fig. 2). The other three samples have higher concentrations up to 2.16 µg g^{-1}. The OEP follows the same down profile trend. Samples with

a low concentration show also low OEPs, whereas the higher concentrated samples have OEPs above 5, indicating good preservation. The ACL ranges from 29.8 to 31.6 and has the same pattern as the concentration and OEP.

5 Discussion

As might be expected, *n*-alkane concentrations for the aeolianite–paleosol sequences on Fuerteventura remain on a relatively low level. In this respect, our study area in the arid subtropics, such as the loess–paleosol sequence (LPS) El Paraiso in central Spain, which ranges from 0.04 to ~ 0.5 µg g^{-1} for the last glacial period (Schäfer et al., 2016a). Much higher concentrations are found in more humid areas such as the LPS Crvenka (Carpathian Basin) with concentrations of up to 4.5 µg g^{-1} (Zech et al., 2013). Most probably, the combination of little wax production (sparse vegetation) and poor preservation, as indicated by the low OEPs, is responsible for the low concentrations in the sandy sequences on Fuerteventura. OEPs in the LPS El Paraiso and LPS Crvenka, for example, are mostly > 5, indicating much better preservation (Schäfer et al., 2016a; Zech et al., 2013).

Given the poor preservation of the *n*-alkanes at Encantado and Melián, it cannot be ruled out that chain length variations, as indicated by the ACL, are effected by degradation. Indeed, the ACL closely follows the down-profile patterns of the OEP, and the chain length variations may be more artifacts related to degradation rather than a record of paleovegetation. This would mean that paleoenvironmental reconstructions in terms of paleovegetation is hardly possible. In order to further investigate this issue, we plotted all samples in an endmember model (Fig. 3). Endmember models combine the OEP (i.e., degradation) versus *n*-alkane ratios (i.e., chain length as proxy for the vegetation type). Plants and topsoil samples typically plot along so-called degradation lines, and several calibration studies in Europe have confirmed the notion that longer chains (*n*-C_{31} and *n*-C_{33}) indicate input from grasses and herbs, whereas shorter chains (*n*-C_{27} and *n*-C_{29}) indicate input from deciduous trees and shrubs (Zech et al., 2013; Schäfer et al., 2016b). Additionally, however, the endmember plots and the degradation lines illustrate the challenge to interpret samples with low OEP values. With decreasing OEP, both degradation lines converge, and an interpretation in terms of vegetation type is no longer possible. In the case of Encantado and Melián, all samples from Encantado and most samples from Melián plot very far left; i.e., they are strongly degraded and an attribution of these samples to a vegetation type is no longer reliable (Fig. 3).

Only three samples from Melián are sufficiently well preserved. These three samples are the ones characterized by higher *n*-alkane concentrations (> 1.5 µg g^{-1}) and ACLs above 30.8. Their chain length patterns can be interpreted to indicate a dominant leaf wax input from grasses and herbs,
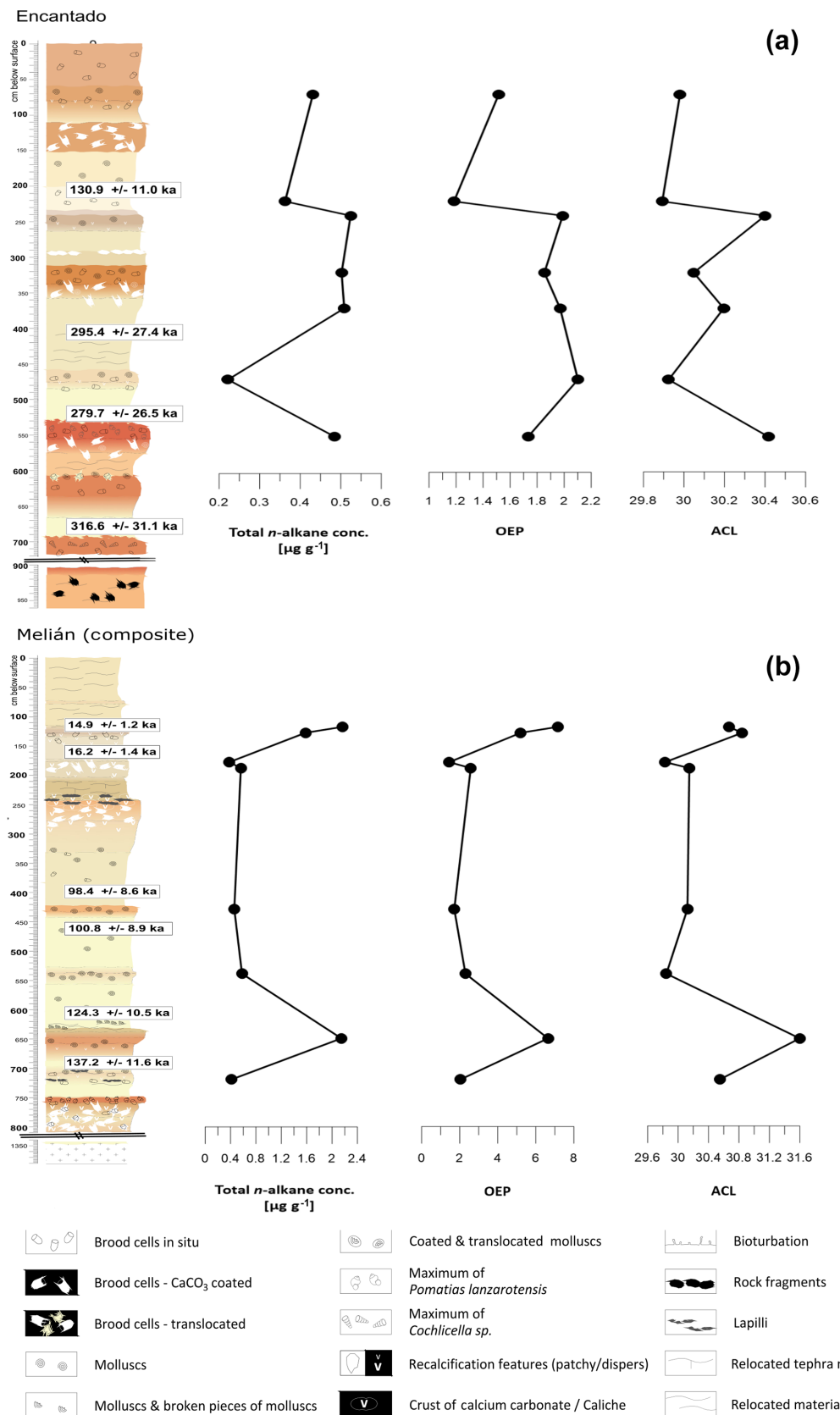
**Figure 2.** *n*-Alkane results for the aeolianite–paleosol sequence Encantado **(a)** and Melián **(b)**. Detailed stratigraphic interpretation can be found in Roettig et al. (2017). Profile sketches are modified after Roettig et al. (2017).
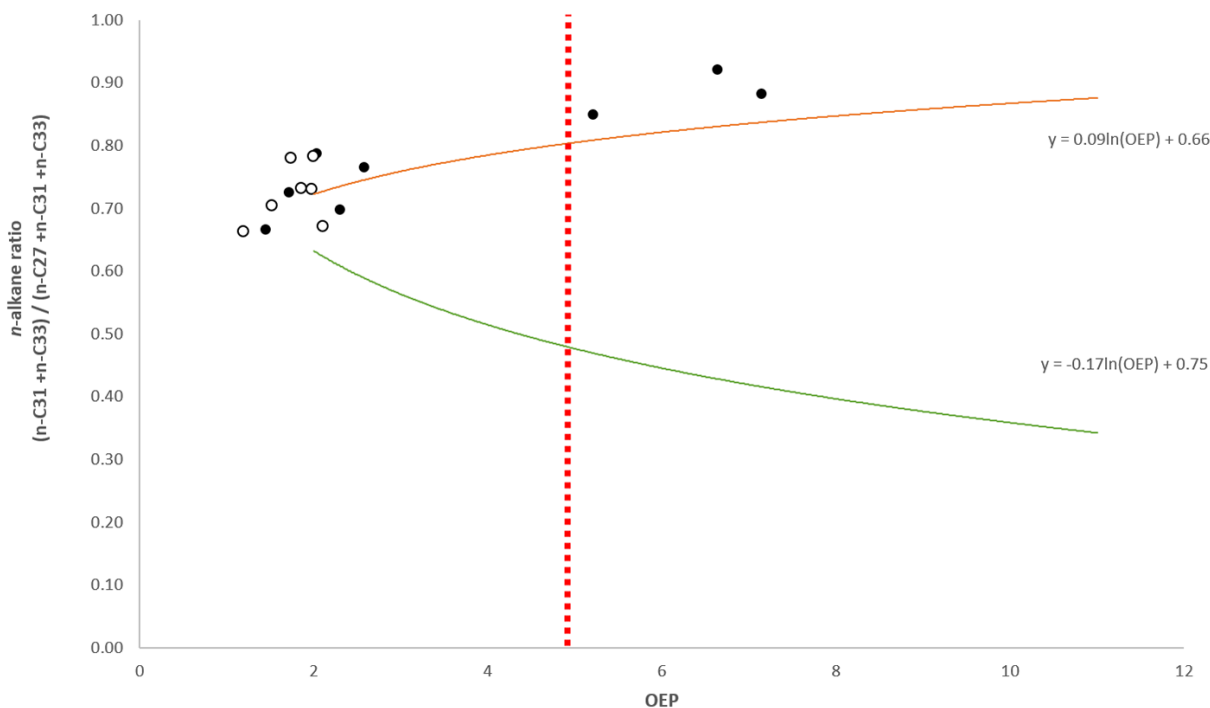
Figure 3. Endmember model for the samples from Encantado (white) and Melián (black). The dotted red line separates samples with good preservation (OEP > 5) and strongly degraded samples (OEP < 5). The orange line represents the degradation line for grasses and herbs, the green line the degradation line for deciduous trees and shrubs (after Schäfer et al., 2016b).

which were thus likely the dominant type of vegetation ~ 15 and ~ 130 ka (Fig. 2).

6 Conclusions

n-Alkane concentrations are relatively low in the two investigated aeolianite–paleosol sequences Encantado and Melián, most likely due to low leaf wax production (sparse vegetation) and poor preservation. Apart from three samples, OEP values are below 5, indicating strong degradation. This prevents a robust interpretation of the chain length patterns, and only the three sufficiently preserved samples can be interpreted in terms of paleovegetation, documenting dominant input from grasses and herbs at ~ 15 and 130 ka. It must be considered that an interpretation in terms of long-chain vs. short-chain n-alkanes is based on previous studies (e.g., Zech et al., 2013, and Schäfer et al., 2016a, b). For Fuerteventura, recent plant material has not been measured yet and would be necessary for further interpretations.

Even though concentrations are low and preservation is poor, there is potential for compound-specific deuterium isotope measurements and paleohydrological reconstruction because the lipid extracts from most samples contained sufficient amounts of possible target compounds ($\sim 1 \mu$g for n-C$_{31}$). Concentrations are also high enough in most samples for compound-specific ^{14}C measurements ($\sim 20 \mu$g total n-

alkane concentration), which could help to establish robust chronologies for the sequences back to ~ 30 ka.

References

Castañeda, I. S., Thibaut, C., Dupont, L., Jung-Hyun, K., Malaizé, B., and Schouten, S.: Middle to Late Pleis-

tocene vegetation and climate change in subtropical southern East Africa, Earth Planet. Sc. Lett., 450, 306–316, https://doi.org/10.1016/j.epsl.2016.06.049, 2016.

Faust, D., Yanes, Y., Willkommen, T., Roettig, C., Richter, D., Richter, D., v. Suchodoletz, H., and Zöller, L.: A contribution to the understanding of late Pleistocene dune sand-paleosol-sequences in Fuerteventura (Canary Islands), Geomorphology, 246, 290–304, https://doi.org/10.1016/j.geomorph.2015.06.023, 2015.

Haas, M., Bliedtner, M., Borodynkin, I., Salazar, G., Szidat, S., Eglinton, T. I., and Zech, R.: Radiocarbon Dating of Leaf Waxes in the Loess-Paleosol Sequence Kurtak, Central Siberia, Radiocarbon, 59, 165–176, https://doi.org/10.1017/RDC.2017.1, 2017.

Häggi, C., Zech, R., McIntyre, C., Zech, M., and Eglinton, T. I.: On the stratigraphic integrity of leaf-wax biomarkers in loess paleosols, Biogeosciences, 11, 2455–2463, https://doi.org/10.5194/bg-11-2455-2014, 2014.

Roettig, C.-B., Kolb, T., Wolf, D., Baumgart, P., Richter, C., Schleicher, A., Zöller, L., and Faust, D.: Complexity of Quaternary aeolian dynamics (Canary Islands), Palaeogeogr. Palaeocl., 472, 146–162, https://doi.org/10.1016/j.palaeo.2017.01.039, 2017.

Sachse, D., Billault, I., Bowen, G. J., Chikaraishi, Y., Dawson, T. E., Feakins, S. J., Freeman, K. H., Magill, C. R., McInerney, F. A., van der Meer, M. T. J., Polissar, P., Robins, R. J., Sachs, J. P., Schmidt, H.-L., Sessions, A. L., White, J. W. C., West, J. B., and Kahmen, A.: Molecular Paleohydrology: Interpreting the Hydrogen-Isotopic Composition of Lipid Biomarkers from Photosynthesizing Organisms, Annu. Rev. Earth Pl. Sc., 40, 221–249, https://doi.org/10.1146/annurev-earth-042711-105535, 2012.

Schäfer, I. K., Bliedtner, M., Wolf, D., Faust, D., and Zech, R.: Evidence for humid conditions during the last glacial from leaf wax patterns in the loess-paleosol sequence El Paraíso, Central Spain, Quatern. Int., 407, 64–73, https://doi.org/10.1016/j.quaint.2016.01.061, 2016a.

Schäfer, I. K., Lanny, V., Franke, J., Eglinton, T. I., Zech, M., Vysloužilová, B., and Zech, R.: Leaf waxes in litter and topsoils along a European transect, SOIL, 2, 551–564, https://doi.org/10.5194/soil-2-551-2016, 2016b.

Zech, M., Buggle, B., Leiber, K., Marković, S., Glaser, B., Hambach, U., Huwe, B., Stevens, T., Sümegi, P., Wiesenberg, G., and Zöller, L.: Reconstructing Quaternary vegetation history in the Carpathian Basin, SE Europe, using n-alkane biomarkers as molecular fossils. Problems and possible solutions, potential and limitations, E&G Quaternary Sci. J., 58, 148–155, https://doi.org/10.3285/eg.58.2.03, 2009.

Zech, R., Zech, M., Marković, S., Hambach, U., and Huang, Y.: Humid glacials, arid interglacials? Critical thoughts on pedogenesis and paleoclimate based on multi-proxy analyses of the loess–paleosol sequence Crvenka, Northern Serbia, Palaeogeogr. Palaeocl., 387, 165–175, https://doi.org/10.1016/j.palaeo.2013.07.023, 2013.

Open Access

E&G Quaternary Science Journal

Research article

Albrecht Penck: Vorbereiter und Wegbereiter der NS-Lebensraumpolitik?

Hans Dietrich Schultz

Geographisches Institut, Humboldt-Universität zu Berlin, Unter den Linden 6, 10099 Berlin, Germany

Kurzfassung: Albrecht Penck gehört zu den bedeutendsten Quartärforschern der ersten Hälfte des 20. Jahrhunderts, doch daneben gab es auch einen politisch-geographischen Penck, der nach 1945 lange Zeit von Fachvertretern ausgeblendet oder verharmlost wurde. Heute wird er mit seinem Konstrukt des Volks- und Kulturbodens der 1920er Jahren als derjenige betrachtet, der die völkische Wende der deutschen Geographie eingeleitet hat. Damit, so der Vorwurf, habe er der nationalsozialistischen Lebensraumpolitik im Osten Europas den Weg geebnet und sei zum Mittäter ihrer mörderischen Politik geworden. Der vorliegende Beitrag untersucht Pencks politisch-geographisches Weltbild und kommt bezüglich der Vorwürfe zu einem ambivalenten Urteil.

Abstract: Albrecht Penck was one of the eminent representatives of Quaternary research in the first half of the twentieth century. But apart from this, there was a political-geographical side to Penck, which, since 1945, has long been ignored or downplayed by geographers. Today, given his concept of *Volks- und Kulturboden*, he is considered as having ushered in German geography the *völkisch* (ethnonationalistic) turn. Thus, critics say, he paved the way for Nazi *Lebensraum* policies and became an accomplice in the resulting crimes. The present contribution examines Penck's political-geographical worldview and reaches an ambivalent conclusion regarding the accusations.

1   Der Tatvorwurf

Der 52. Deutsche Geographentag 1999 in Hamburg begann mit einem Paukenschlag. Einen Tag vor seiner Eröffnung sorgte Michael Fahlbusch in der Rolle des Staatsanwaltes mit einem ganzseitigen Artikel in der *Frankfurter Rundschau* für Aufregung. Unter der provokanten Überschrift: „Die verlorene Ehre der deutschen Geographie" klagte er im Untertitel an: „Bis heute wird die Mittäterschaft der akademischen Väter am Völkermord der Nationalsozialisten verdrängt" (Fahlbusch, 1999a: S. 6). Penck war durch seine „berüchtigte Karte des deutschen Volks- und Kulturbodens von 1925" be-

sonders prominent in dem Artikel vertreten. Diese wie unzählige andere Karten dieses Genres hätten nach dem verlorenen Weltkrieg der amtlichen deutschen Kulturpropaganda dazu gedient, die Forderung nach einer Revision der Grenzen „„wissenschaftlich'" zu untermauern. Mit dem Machtantritt der Nationalsozialisten 1933 hätten sich dann „Penck, Metz, Hassinger und Meynen am Ziel ihres politischen Strebens" gesehen: „Sie kooperierten hinfort mit der SS, der NSDAP und den ‚gleichgeschalteten' Reichsministerien. Sie bereiteten die Grundlagen für die deutsche Volksgruppenpolitik vor. Ihrer völkischen Logik zufolge sollten nur jene Völker den Status der Schutzwürdigkeit zugewiesen bekommen, die ‚bo-

denständig' waren, Juden und Zigeuner erhielten diesen Status nicht. Sie wurden gemäß der Nürnberger Rassengesetze für vogelfrei erklärt" (S. 6).

Was immer und begründet an diesem provokanten Artikel und an den Ergebnissen der Forschungen Fahlbuschs (1999b) zu kritisieren war: Er hat eine überfällige Diskussion vorangebracht und weiterführende Arbeiten angestoßen, die gezeigt haben, dass die Volks- und Kulturbodenforschung nicht nur anschlussfähig an die Lebensraumideologie der Nationalsozialisten war, sondern viele ihrer Vertreter auch durch ihre Praktiken einer verbrecherischen Politik dienten.

Auf Penck bezogen hat von geographischer Seite Herb festgestellt, dass „die Übereinstimmung" der von ihm „postulierten Gebiete deutschen Kultureinflusses mit den Lebensraumvorstellungen der Nationalsozialisten bzw. den deutschen Eroberungen im Zweiten Weltkrieg (...) nicht zu übersehen" (Herb, 2005: S. 190) sei. Etwas umständlicher, aber ähnlich konstatierte Jureit aus historischer Sicht, Pencks „als Fortschrittsnarrativ arrangierte Kulturbodentheorie" habe es ermöglicht, territoriale Ansprüche jenseits der aktuellen Besiedlungsverhältnisse und damit unabhängig von den Identitätsentwürfen der derzeitigen Bewohner zu rechtfertigen" (Jureit, 2012: S. 243). Mommsens Urteil, die Volks- und Kulturbodentheorie, die mit den Geographen und Penck als „Schlüsselfigur" begonnen habe, habe „ursprünglich mit dem Nationalsozialismus überhaupt nichts zu tun" (Mommsen, 1999: S. 2) gehabt, scheint sich damit erledigt zu haben, erst recht aber, in Penck einen der Großen zu sehen, von dem in der „Geschichte unseres Faches auch noch in einer fernen Zukunft mit ähnlicher Verehrung" (Sölch, 1946: S. 88) gesprochen werde wie von Alexander v. Humboldt, Carl Ritter und Ferdinand von Richthofen.

So scheint also kein Weg daran vorbeizuführen, auch Penck und seine Schule auf die Politik des NS-Regimes beziehen zu müssen und in seinen politisch-geographischen Arbeiten ein weiteres Beispiel für die „fließende Grenze zwischen Propaganda und Wissenschaftlichkeit" (Kost, 1988: S. 346) zu erkennen. Doch ist der staatsanwaltliche Zugriff, den auch viele Historiker für die Geschichtsschreibung des Nationalsozialismus präferieren, der einzig sinnvolle? Reicht es, auf der Basis „akribischer Quellenarbeit" herausfinden zu wollen, „was ein Individuum von den Verbrechen des Nationalsozialismus wusste, inwieweit der Einzelne sie vorbereitete und inwieweit man ihm Verantwortung oder Schuld zuschreiben kann", um ihn „als ‚Vordenker der Vernichtung' (...) oder zumindest als Vordenker des Faschismus" zu entlarven (Etzemüller, 2004: S. 27)?

„Zweifellos", so Etzemüller, selbst Historiker, sei ein solcher Ansatz „notwendig" – „Ohne Individuen, deren Intentionen man kausal auf die Verbrechen des NS bezöge, könnte man eine Geschichte des Nationalsozialismus gar nicht schreiben" –, doch ergäben sich zwei Probleme: Erstens werde bei posthumen Schulduntersuchungen leicht „die Unschuldsvermutung von vornherein" ausgeblendet, um „methodische Ansätze mit moralischen Argumenten" (Etzemül-

ler, 2004: S. 27) zu bekämpfen, zweitens verdecke die nachträgliche Einstufung von Individuen als Schuldige oder (lediglich) Verführte mehr, als dass sie dazu beitrage, die eigentlich wichtige Frage beantworten zu helfen, „wie der Nationalsozialismus sich entfalten konnte" (S. 28). Besser sei es darum, folgende drei Analyseebenen zu unterscheiden: (1) die Ebene des „*Wollens*", der man Schuld zuordnen könne, (2) die Ebene des „*Nichtsehen-Wollens*", die die Folge von Verdrängung sei, und (3) die Ebene des „*Nichtsehen-Könnens*", die Praktiken beinhalte, die im Sinne des Regimes und seiner Verbrechen Effekte gezeigt hätten, die die Beteiligten „tatsächlich nicht sehen konnten" (S. 31, Herv. HDS)[1]. Gerade den letzten Punkt hält er für besonders wichtig, denn mit ihm lasse sich beobachten, „wie von Betroffenen Handlungen in ein kognitives System eingefügt wurden, so daß diese Handlungen legitim erschienen, während die Effekte" (S. 31) den Nationalsozialisten zugerechnet werden konnten.

Im Folgenden werde ich auf der Basis von Pencks Publikationen seine politisch-geographischen Vorstellungen in ihren Hauptzügen skizzieren und dazu einen kolonialpolitischen, einen politisch-geographischen und einen ethnopolitischen Penck unterscheiden. Im abschließenden Urteil orientiere ich mich an Etzemüller, speziell an seinem letzten Punkt.

2   Der kolonialpolitische Penck

Den kolonialpolitischen Penck halte ich kurz. Penck trat entschieden für deutsche Kolonien ein und brachte stets folgende drei Argumente vor: Erstens bedeuteten Kolonien schon durch den Flächenzuwachs mehr Macht für das Mutterland, zweitens könnten sie überschüssige Bevölkerung aufnehmen, die so dem eigenen Volke nicht verloren gehe, und drittens böten die fruchtbaren Tropen die Lösung der Ernährungsfrage der Menschheit.

Die Kolonien gingen im Ersten Weltkrieg rasch verloren, doch tröstete sich Penck damit, dass die Gewinne in Belgien und Nordfrankreich bei weitem die kolonialen Verluste überwögen. Der bisherige Kriegsverlauf, Stand 1917, habe Deutschlands „kontinentale Stellung in Europa" gestärkt und werde es „ermöglichen, sie zurückzuverlangen mit einer ansehnlichen Zugabe bisherigen französischen und belgischen Kolonialbesitzes" (Penck, 1915a: S. 19f.). In seiner Antrittsrede als Rektor der Berliner Universität forderte Penck „einen Kolonialbesitz (...), groß und reich genug, um uns mit den unentbehrlich gewordenen Rohstoffen der Tropen zu versehen" (Penck, 1917: S. 31).

Auch nach dem Verlust der Kolonien propagierte Penck unermüdlich die Tropen als „Länder der Zukunft". Allerdings nicht für massenhafte Siedlung! Doch böten sie den Weißen genügend Gelegenheit, sich „als Pflanzer, Ingenieure, Kaufleute oder Beamte" zu betätigen, „nicht als Herren über Sklaven, sondern als Vormünder über Unmündi-

---

[1]Alle folgenden Kursivstellen innerhalb von Zitaten sind Hervorhebungen im Original.

ge" (Penck, 1936: S. 263). Deutschland als Kolonialmacht auszuschließen, sei ein Riesenfehler; denn man brauche den Einstrom weißen Blutes, ohne den die Macht der Weißen über die Farbigen nicht aufrechterhalten werden könne. Außerdem waren in Pencks Augen Kolonien ein hervorragendes Erziehungsprogramm. Befreit von der Enge des eigenen Raumes, würden hier deutsche Menschen „zu Führern" erzogen werden können, „prächtige Menschen" (Penck, 1936: S. 263), wie man gesehen habe.

Auffällig ist, dass Penck bei der Forderung nach Rückgabe der Kolonien immer wieder die Trommel der Menschheit rührte, doch das war bei den Kolonialbefürwortern üblich, denen es im Kern darum ging, die Herrschaft der Weißen als Dienst am Fortschritt der Menschheit zu rechtfertigen und aufrechtzuerhalten.

3　Der politisch-geographische (geo-politische) Penck

Um den politisch-geographischen Penck zu verstehen, muss man wissen, dass die Geographie sich seinerzeit als *Länderkunde* verstand, die angesichts politisch unruhiger Zeiten um 1800 als Alternative zur Staatenkunde aufgekommen war und sich nach längerem Hin und Her um 1900 soweit durchgesetzt hatte, dass sie als die *Kernaufgabe* der Geographie galt. Parallel dazu hatte sich ebenfalls durchgesetzt, dass die Geographie zwar eine Brücke zu den sogenannten Geisteswissenschaften bilde, indem sie Natur und Kultur miteinander verschmelze, aber dies von einer naturwissenschaftlichen Grundposition heraus. Geographisch zu denken, bedeutete, *den Menschen* (das Gesellschaftliche, das Wirtschaftliche und das Politische) primär in seiner Abhängigkeit von der Natur der Länder zu betrachten, wofür (Wahrscheinlichkeits-) Gesetze gefunden werden sollten. Länder waren *die* Teile der Erdoberfläche, die sich durch ihre *Eigenart* als Natur- und Kulturräume charakteristisch voneinander unterschieden.

Der Dauerstreit, der sich mit der Umstellung von Staaten auf Länder für die Geographie ergab, war das Verhältnis dieser beiden Raumbegriffe zueinander, wobei die Spannweite der Positionen von der Annahme einer Deckungstendenz bis zur Behauptung einer völligen Unabhängigkeit der beiden Kategorien reichte. Dazu kamen noch die Siedlungsräume der Völker, deren Beziehung zu den beiden anderen den Geographen ebenfalls interessierte. Zwar erkannte man schon in der ersten Hälfte des 19. Jahrhunderts, dass Länder meist allmählich ineinander übergingen, und sprach von Grenzräumen und -säumen, dennoch blieb der Begriff der „natürlichen Grenzen" im Sinne mehr oder weniger linearer Marken, einmal in die Welt gesetzt, ein Dauerbrenner geographischer Diskussionen.

Penck beschäftigte sich in seinen Publikationen mit solchen Fragen intensiv erst seit dem Ersten Weltkrieg. Zunächst, 1915, versuchte er zu klären, welche meridionale

Gliederung Europa jenseits der Ebene der Länder aufwies, da er davon ausging, „*daß die geographische Lage der Länder die gemeinsamen Interessen der Völker in weitem Umfange*" bestimme. Er nannte die drei Streifen Vorder-, Zwischen- und Hintereuropa und prognostizierte für *Zwischeneuropa*, dass es als „*ein eng zusammengeschlossenes*" Gebiet, „*das vom Weißen Meer bis zum Bosporus*" reiche, „*das feste Rückgrat für Europa abgeben*" (Penck, 1915b: S. 40) werde. Anhand von Diagonalen, die die Ecken Europas miteinander verbanden und deren Mitten sich nahe der Quelle der Memel trafen, veranschaulichte Penck, dass derzeit allerdings noch Russland weit nach Mitteleuropa hineinreiche. Es hatte damit aus Pencks Sicht jene Grenzen missachtet, welche die Natur ihm angewiesen hatte, und sollte daher auf sein natürliches Gebiet, Hintereuropa, zurückgedrängt werden. Ein eindringlicher Blick auf das Land zeigte Penck die natürlichen „Nähte", „an welchen das Zarenreich nur oberflächlich zusammengeschweißt" sei und „längs derer es leicht wieder auseinanderfallen" (Penck, 1918a: S. 40) könne.

Zugearbeitet hatte ihm diesbezüglich sein Schüler Rudnyćkyj, der nachweisen zu können glaubte, dass Osteuropa keineswegs, wie allgemein angenommen, ein gliederungsfreier, homogener Naturraum sei, sondern morphologische, hydrographische, klimatische, pedologische und pflanzengeographische Unterschiede (Rudnyćkyj, 1916: S. 5) aufweise, die sich in natürlichen Einheiten niederschlügen, die ihrerseits eine große Einheitlichkeit zeigten, darunter Baltland, Weißrußland und die Ukraina. Penck ließ es sich nicht nehmen, in einem langen Artikel die Existenz eines selbständigen ukrainischen Staates geographisch zu begründen und Mitteleuropa anzuschließen: „natürliche Grenzen würden einen solchen Staat von Rußland scheiden" (Penck, 1916a: S. 477).

Auch Polen, das Penck nur als ein loses Anhängsel an das Zarenreich betrachtete, galt ihm als echtes Stück des „germanischen Mitteleuropas", da es gleich diesem einen Dreiklang der morphologischen Großformen aufweise, nämlich „Karpathen, vorgelagerte Landschwelle und Tiefland" (Penck, 1918b: S. 127). Den Begriff des „Dreiklangs" übernahm er von Partsch, der ihn 1904, was damals noch als ungewöhnlich galt, als Charakteristikum für „das weite Ländergebiet zwischen Ostende und Genf, Memel und Burgas" bestimmt hatte, das „den zentralen Kern der europäischen Staatenfamilie" (Partsch, 1904: S. 5) darstelle. Bis auf wenige Stellen würden die politischen Grenzen dieser Staatengruppe von den natürlichen „selten weit entfernt" bleiben, nur mit Deutsch-Lothringen, Teilen Bulgariens und Galiziens „über die natürlichen Schranken" (S. 5) hinausgreifen, mit der jütischen Halbinsel und Polen hingegen dahinter zurückbleiben. Über Partsch hinausgehend, setzte Penck weiter östlich noch ein „sarmatisches Mitteleuropa" (Penck, 1918b: S. 129) an. Außerdem schaltete er zwischen Hintereuropa und Zwischeneuropa einen breiten Grenzsaum ein, den er nach dem Zug der schwedischen Waräger als „warägischen Grenzsaum" bezeichnete. Dieser ziehe vom Finnischen Golf

an den Pripjetsümpfen vorbei bis zum Asowschen Meer und trenne „das plumpe kontinentale von dem mehr gegliederten Europa" (S. 127).

Eine besondere Herausforderung war für Penck Österreich-Ungarn. Im Gegensatz zu zahlreichen reichsdeutschen Kollegen, die diesen Staat als besonders ungeographisches Gebilde einstuften, das vor dem Zusammenbruch stehe, verteidigte Penck, der zwei Jahrzehnte in Wien gelehrt hatte, ihn entschieden als naturgewollt. So wehrte er Italiens Ansprüche auf Süd-Tirol, die es mit der Wasserscheidengrenze begründete, mit Verweis darauf ab, dass das „Paßland" Tirol „ein Ganzes, eine geographische Einheit" (Penck, 1916b: S. 47) sei, die über die Wasserscheide hinweggehe und noch nicht einmal völlig politisch ausgefüllt werde. Die „einende Kraft" der geographischen Züge des Landes sei „eine so starke, daß, wie in anderen Paßländern, Menschen verschiedener Zunge in *einem* Lande zusammengefaßt worden" (S. 44) seien. Den Gesamtstaat Österreich-Ungarn verteidigte Penck mit dem Argument, er sei „*unter dem Zwange geographischer Verhältnisse*" (Penck, 1915b: S. 18) zusammengewachsen. Dieser Staat sei „kein Eroberstaat, zusammengeschweißt durch den eisernen Willen eines Herrschers", aber auch „kein Nationalstaat, sondern ein Agglomerat von Völkern", das auf der besonderen Natur des Landes beruhe: „Ein solcher, durch die Natur zusammengehaltener Staat braucht Naturgrenzen" (Penck, 1916b: S. 75). Das Wiener Becken wirke dabei als geographischer Anziehungspunkt für die umliegenden Landschaften; und sogar hinter dem Zweibund steckte laut Penck „das Nachwirken starker natürlicher Ursachen" (Penck, 1915b: S. 20). Er war für ihn keine zufällige Erscheinung.

Ausführlicher theoretisch äußerte sich Penck (mit erkennbarer Anlehnung an Ratzels *Politische Geographie*) zur Frage der „natürlichen Grenzen", die „eine der schwiersten der politischen Geographie" (Penck, 1916b: S. 8) sei, in seiner Antrittsrede als Rektor der Berliner Universität im Herbst 1917. Solche Grenzen, meinte er, seien nicht schon per se gute Grenzen, sie böten „lediglich die Idee, den Leitsatz, zur Ziehung einer solchen Grenze", seien „aber vielfach nur ein leeres Schlagwort zur Rechtfertigung von Gebietsansprüchen"; kein zivilisierter Staat begnüge „sich heute mit bloßen natürlichen Grenzen", erst ihre „Vermarkung" verleihe ihnen „Eindeutigkeit" (Penck, 1917: S. 8). Wähle ein Staat eine natürliche Grenze zur Vermarkung aus, dann sei sie nur dann auch eine gute, eine „*organische*" Grenze, wenn sie zur „Natur" dieses Staates passe, d.h., „aus dem Staate heraus verstanden" werde; doch selbst im Falle von natürlichen Grenzen mit einer „solch starken Wirkung" wie im Falle der Schweiz würde ein „noch so starker Bürgersinn" (S. 14f.) gegenüber einem stärkeren Nachbarn nichts ausrichten können. Allerdings könne „die Kraft geographischer Verhältnisse" (S. 15) bei der Staatenbildung sich nur dann begünstigend auswirken, wenn deren Größe zeitgemäss sei. Wüchsen die Staaten flächenmäßig, so verlören einst zu ihnen passende Räume und organische natürliche Grenzen ihre Funktion.

Penck beruhigte aber seine „Volksgenossen" in Österreich und der Schweiz, sie nicht als „unerlöste Brüder'" (S. 17) zu betrachten und in Grenzvorsprüngen eher „Gebiete der Berührung als solche der Reibung" zu sehen.

Den Inhalt des Staates sah Penck „in einer unlösbaren Verknüpfung von Land und Volk": „Aus dem Volke fließen die immer sich erneuernden staatsbildenden Kräfte, im Lande wurzeln die staatserhaltenden Faktoren. Das Land ist der Boden, auf dem der Staat wurzelt und gedeiht" (Penck, 1917: S. 18). Pencks politisches Ideal war erfüllt, wenn ein „weitblickender Herrscher" die Entwicklung eines Staates „behutsam auf einen bestimmten *Lebensraum*" (S. 18) lenkte. Dieser sollte so groß sein, dass er „die wirtschaftlichen Grundlagen für das staatliche Leben" bot und den Zusammenhalt des Staates sowie seine Sicherheit begünstigte. Reine Eroberstaaten würden dagegen rasch wieder zerfallen. Neben einem Herrscherwillen könne aber auch der „Volkswille", wie das Beispiel Italiens zeige, „auf nationaler Grundlage einen scharf ausgesprochenen Lebensraum gewinnen", doch wolle die italienische Nationalbewegung sich Länder aneignen, „die außerhalb seiner durch das Meer und die Alpen gezogenen organischen Grenze" (S. 18f.) lägen.

In einem anderen Teil Europas, dem Gebiet „zwischen der östlichen Ostsee und dem östlichen Mittelmeere", lasse der Boden zwar auch „einzelne Lebensräume" erkennen, doch zeige „die Völkerkarte ein buntscheckiges Bild", weil die „Völker und Nationen" sich hier nicht „im geringsten" um diese Lebensräume kümmern würden. Hier seien Nationalstaaten, „die sich mit bestimmten Lebensräumen decken, unmöglich" (Penck, 1917: S. 19).

Flüsse galten Penck auf keinen Fall als „naturgemäße" politische Grenzen, mochten sie auch aus militärischer Sicht guten Schutz bieten und sich „bei der Aufteilung eines Landes in Grundeigentum" eignen: „Große Ströme bilden mehr das Gerüst von Staaten" (Penck, 1917: S. 24). Den „beste[n] Rahmen für einen Lebensraum" sah er von Meeresküsten, hohen Gebirgen, Wüsten und Sümpfen gezogen. Solche wenngleich breiten Übergangsräume gäben „den Staaten naturgemäße, organische Grenzen" (S. 23). Daneben gebe es Lebensräume, deren Grenzen „unbestimmt" seien oder „gänzlich" fehlten, so daß die Staaten, die in sie hineingewachsen seien, nicht durch „*naturgemäße organische* Grenzen" geschieden werden könnten. Hier sorge das Macht- und Kräfteverhältnis im Hin und Her um eine immer deutlicher erkennbare Mittellinie herum allmählich für einen Ausgleich, der den Lebensbedürfnissen der Staaten gerecht werde. Für Penck entsprach dies Vorgängen, wie sie auch im Pflanzen- und Tierreich abliefen, hatte also für ihn „naturwissenschaftliche Bedeutung" (S. 24).

Hatte Penck 1917 noch auf eine Präzisierung seines Lebensraum-Begriffs verzichtet, so holte er dies 1926 nach. Der Begriff umfasse eine natürliche „Formengesellschaft" von „Landschaften", die sich mit ihrer räumlichen „Gestalt" deutlich von einer anders gearteten Umgebung abhöben. Man dürfe sie allerdings nicht so missverstehen, als seien sie

jeweils für die Aufnahme eines *bestimmten* Volkes vorgesehen. Die staatenbildenden Kräfte des Landes stellten einzig mit den „natürlichen Gegebenheiten" das Potenzial für eine Staatenbildung dar. Das Angebot der Natur konnten somit verschiedene Völker nutzen und zu ihrem Lebensraum umgestalten. Vorgefundene Bevölkerungen würden dabei, oft gewaltsam, assimiliert. Teleologische Spekulationen lehnte Penck entschieden ab. „Das Zusammenfallen von geographischen Gestalten mit Volks- und Staatenräumen" spiegele keine „natürliche Zweckbestimmung der Länder" (Penck, 1926: S. 81). Nicht die Erdoberfläche schaffe sich den Staat, sondern der Wille eines Einzelnen oder ganzer Völker, wie Penck ähnlich schon 1916b für die österreichische Alpengrenze und 1917 in seiner Rektoratsrede betont hatte.

Doch obwohl Penck auf den ersten Blick die Staatenbildung allein vom Willen der Menschen abhängig zu machen scheint, nahm er zugleich an, dass dieser Wille „bei der großen Masse" des Volkes „unter stiller Beeinflussung von Seiten ihrer Umgebung" stehe. „Harmonische Landschaften" würden „das Gefühl der Zusammengehörigkeit und den Wunsch des Zusammenschlusses" zeitigen. Das war für Penck die geistige Macht des Bodens, die schließlich „zu einer dauernd wirkenden, Staaten bildenden Kraft" führe, die „dem Willen der Einzelnen wie der zündenden Macht einer Idee" (Penck, 1926: S. 81) trotze. Niemand konnte sich demzufolge über die Gegebenheiten der Natur überheben!

Zu Ende gedacht, müsste das dazu führen, dass ein willkürlich an einen Staat angeschlossenes Stück Natur, das nicht zum Lebensraum dieses Staates passte, disharmonische Spannungen unter seinen Bewohnern aufkommen lassen würde. Ein solcher natürlicher Unruheherd durfte nicht bestehen bleiben; und tatsächlich befand Penck (wie unter Länderkundlern gang und gäbe): „Auf die Dauer ist die Natur stärker als der Mensch" (Penck, 1926: S. 81). So bleibt als Credo des Geographen: Der Mensch beherrscht die Natur nur scheinbar, tatsächlich beherrscht sie ihn! Denn was immer er tat, Bestand hatte auf lange Sicht nur, was sich ihren Bedingungen fügte. Also doch politisch-geographische Teleologie?

4 Der Sonderfall Deutschland

Bleibt zum politisch-geographischen Penck noch seine Sicht auf Deutschland übrig, das unter Geographen als Sonderfall Europas galt. Schon in seiner Rektoratsrede beklagte er, „daß jahrhundertelang keine zielbewußte Hand" sein „Hineinwachsen in einen bestimmen Lebensraum" gelenkt habe, wie deutlich daran sichtbar werde, „daß ihm Quellgebiet und Mündungsgebiet des Rheines fehlen" (Penck, 1917: S. 24).

Erstmals war Penck in den 1880er Jahren mit der Frage nach Deutschland als einem geographischen Land durch seine Mitarbeit an der von Alfred Kirchhoff herausgegebenen *Länderkunde von Europa* konfrontiert worden. Penck hatte den Band zum Deutschen Reich übernommen, den eine

von Kirchhoff verfasste länderkundlichen Skizze zu Europa einleitete, die davon ausging, dass sich „in den Staatengrenzen Europas (...) vorwiegend die Umriß- und Bodenbaugliederung" (Kirchhoff, 1887: S. 87) des Erdteils abspiegele. Pencks Teil begann jedoch nicht sofort mit dem Deutschen Reich, sondern einer physikalischen Skizze von „Mitteleuropa", mit der ausgedrückt werden sollte, dass das Reich „innerhalb natürlicher Grenzen, innerhalb ein und desselben von der Natur einheitlich charakterisierten Gebietes" lag, dieses jedoch nicht vollständig ausfüllte, da ihm „äußerst wichtige Glieder Mitteleuropas, wie das böhmische Becken und vor allem die Rheinmündungen" (Penck, 1887: S. 133f.) fehlten. Dennoch hielt es Penck für unbestreitbar, dass es „nicht bloß ein nationaler, sondern auch ein geographischer Begriff" (S. 134) sei.

Diese Konzession musste er machen, weil Kirchhoff entgegen aller bisherigen Fachtradition und auch seiner eigenen früheren Auffassung inzwischen die kleindeutsche Reichsgründung als geographisch begründet und somit politisch berechtigt vertrat, was bei seinen großdeutsch denkenden Kollegen auf heftigen Widerstand stieß. Für sich selbst löste Kirchhoff den Widerspruch zu seiner früheren Position, indem er auch ein größeres Deutschland für geographisch möglich erklärte, doch habe die historische Entwicklung dazu geführt, dass sich an der Peripherie dieses Gebietes auf der Basis spezieller natürlicher Verhältnisse politische Sonderinteressen entwickelt hätten, die eine eigene Staatenbildung zur Folge gehabt hätten. „Mitteleuropa" war bei Kirchhoff somit Ersatzbezeichnung für das ältere natürliche Deutschland der Geographen, das auch die Niederlande, Belgien, Luxemburg, die Schweiz und Österreich einschloss und manchmal noch Dänemark. Kirchhoffs Deutschlandversion kam Penck allerdings insofern entgegen, als ihm, dem in Österreich Lehrenden, andernfalls eine geographische Rechtfertigung Österreich-Ungarns verbaut gewesen wäre. Freilich fällt auf, dass er den eigenständigen Landcharakter des Deutschen Reiches einfach hinnahm, ohne ihn eingehender zu begründen.

Nach dem Ersten Weltkrieg ergab sich für Penck eine neue Situation, nachdem Österreich-Ungarn, dem er im Krieg eine natürliche Legitimation beschafft hatte, von der Landkarte verschwunden war. Sein oben schon im Zusammenhang mit dem Lebensraum-Begriff zitierter Aufsatz *Deutschland als geographische Gestalt* von 1926 beginnt mit dem Postulat: „Deutschland ist für uns eine natürliche Einheit und nicht bloß ein politischer Begriff. Ein solcher ist das Deutsche Reich" (Penck, 1926: S. 72). Deutschland sei aber auch nicht „das Land, in dem nur deutsch gesprochen" werde, denn es greife „von altersher über den deutschen Sprachboden hinweg" und decke sich „nicht mit diesem"; vielmehr sei Deutschland, was seit Jahren gelte, „ein bestimmter Teil der Erdoberfläche mit charakteristischen Eigenheiten, von eigener Gestalt" (S. 73), so wie dies auch für andere Länder gelte. Wie ein Teppich verschiedene Muster biete, so höben sich in Europa bestimmte Ländergestalten voneinander ab. Um sie

zu erkennen, dürfe man sich jedoch nicht an äußere natürliche Marken, z.B. Wasserscheiden, halten, vielmehr komme es auf „ihren geographischen Inhalt" (S. 74) an. Der Geograph, der sie „sehen" wolle, müsse sich an „die neuere physiologische Psychologie" halten, um sie methodisch als „ganze Formengesellschaften" wahrnehmen zu können, die „morphologisch als *Landschaften* bezeichnet worden" (S. 74) seien. Penck verwies dabei auf sich selbst und seine *Morphologie der Erdoberfläche* von 1894 (Penck, 1894).

Die Grenzfrage war für Penck damit aber keineswegs bedeutungslos geworden, auch Gestalten brauchten Grenzen, nur seien sie im Falle Deutschlands trotz klarer Eigenart seiner Gestalt „wenig deutlich" (Penck, 1926: S. 79). Was Penck bot, war jedoch seit der ersten Hälfte des 19. Jahrhunderts altbekannt. Nachdem Österreich-Ungarn nicht mehr existierte, umgrenzte er sein natürliches Deutschland jetzt unbeschwert in deutlicher Anlehnung an die Territorialverhältnisse des mittelalterlichen Alten Reiches und begann mit der Straße von Calais. Den weiteren Verlauf markieren, wie schon im frühen 19. Jahrhundert gängig, Ardennen, Vogesen und der Schweizer Jura. Im Südwesten wird die Grenze zunächst vom Alpenkamm getragen, dann aber greift sie darüber hinweg, um „die beiden Längstalzüge innerhalb des Gebirges" (S. 79) ganz zu umfassen. Ein Großteil der Alpen ist nun geographisches Deutschland. Zwischen Donau und Oder lieferten Penck „die Höhen einzelner Karpathenstücke (...) eine gute Grenze gegen das pannonische Becken" (S. 79), doch im Osten suchte er, wie andere vor ihm, vergeblich nach natürlichen Anhaltspunkten für eine Begrenzung. Während frühere Versuche sich darauf konzentrierten, zwischen Oder und Weichsel doch noch schwache Andeutungen zu entdecken, die als natürliche Grenzen taugten, fand Penck erst in den Pripjetsümpfen eine eindeutige Grenzmarke, die ihm jedoch zu weit weg lag, um ernsthaft als natürliche Begrenzung Deutschlands in Betracht zu kommen, ja, Penck spielte nicht einmal mit dem Gedanken, sie anzupeilen. Vielmehr schob er, nachdem im Ersten Weltkrieg klar wurde, dass Polen eine staatliche Wiedergeburt erleben würde, dieses als eine weitere geographische Landgestalt zwischen Deutschland und Russland ein.

Anfangs, 1918, hatte Penck (s.o.) Polen noch mit Partsch in den mitteleuropäischen Dreiklang einbezogen, jetzt, nachdem sich die politische Landkarte Europas auf dem Boden der Mittelmächte dramatisch geändert hatte, erkannte er für Polen nur noch einen *Zweiklang*, der sich vom „eigenartigen und sehr charakteristischen" (Penck, 1926: S. 79) deutschen *Dreiklang* deutlich abhebe. Hatte Partsch einst unter Einschluss der mittleren Weichsel formuliert: „Der Dreiklang Alpen, Mittelgebirge, Tiefland beherrscht die Symphonie des mitteleuropäischen Länderbildes. Wo einer seiner Töne ausklingt, ist Mitteleuropa zu Ende" (Partsch, 1904: S. 4), so dekretierte Penck jetzt: „Diese Sinfonie ist nur für ihn [den deutschen Boden] charakteristisch" (Penck, 1926: S. 77). Polen falle aus dem Dreiklang heraus, weil es über kein zusammenhängendes Hochgebirge verfüge und auch sein Mittelge-

birge sich in deutlich anderer Gestalt zeige als das deutsche. Letzteres bestehe aus einem Gebirgsgürtel mit zwei Beckenlandschaften, während dem polnischen beides fehle (zur polnischen Sicht vgl. Briesewitz, 2014).

Eines der beiden großen süddeutschen Becken und damit zugleich des geographischen Deutschlands war für Penck das Böhmische Becken, das er früher, solange Österreich-Ungarn noch existierte, durch die geographischen Verhältnisse auf den Mittelpunkt Wien hingezwungen sah. Während er 1887 befand: „Im Böhmischen Becken verschmelzen Umwallung und Einsenkung zu einem Massive und verhalten sich völlig einheitlich" (Penck, 1887: S. 206), argumentierte er nach dem Krieg, dass die gebirgige Umwallung Böhmens und sein meist durch Hochland ausgefülltes Becken zwei geographisch verschiedene Räume seien. Deutlich hebe sich „Deutsch-Böhmen auch geographisch gegenüber Tschechisch-Böhmen hervor" (Penck, 1918/19: S. 177). Es sei nicht wahr, „daß der tschechische Staat die historische Grenze Böhmens als natürlich Grenze brauchte" (S. 178).

Besonders heftig kritisierte Penck seinen Mitstreiter in Deutschtumsfragen, Wilhelm Volz, der sich besonders im Kampf um Oberschlesien hervorgetan hatte. Er warf ihm „politische Kurzsichtigkeit" und ein „Verkennen von Tatsächlichem" (Penck, 1930/31: S. 514) vor, womit Volz' Begriff des „natürlichen Deutschlands" gemeint war. Volz ging nämlich davon aus, dass die Alpen als eine eigenständige natürliche Landschaft „neben" dem geographischen resp. natürlichem Deutschland zu gelten hätten, das nur bis zum Alpenrand reiche, wenngleich auch die Alpen überwiegend „deutsches Siedlungsland und deutscher Volksboden" seien; das deutsche Volk bewohne eben „*zwei* natürliche Landschaften, seiner Menschenzahl entsprechend" (Volz, 1927: S. 12). Penck rügte dies. Würde der Alpenraum nicht zum natürlichen Deutschland gehören, würde den dort lebenden Deutschen „die geographische Grundlage ihres Daseins entzogen" (Penck, 1930/31: S. 514).

Wie die angeführten Beispiele zeigen, flüchtete Penck keineswegs aus der Länderkunde; ein Paradigmen-*Bruch*, d.h. ein Wechsel von einem *geozentrischen* zu einem *ethnozentrischen* Territorialkonzept, wie Herb (2005: S. 188) meint, findet mit ihm nicht statt. Wenn Penck bedauert, dass das Deutsche Reich „seine Ländergestalt" „am wenigsten" erfülle, während Frankreich dabei sei, die Deutschen „außerhalb seiner Ländergestalt" (Penck, 1926: S. 81) zu französisieren, so unterstreicht dies nur, dass auch er daran festhielt, dass sich Länder („Lebensräume") und Staaten möglichst decken sollten. Allerdings seien die Einwirkungen des Menschen auf den Boden „viel stärker" als umgekehrt, da der Einfluß des Landes auf seine Bewohner „nur sehr langsam zur Geltung" komme und „nicht einmal in langer Zeit [die] Stammesunterschiede verwischt" (Penck, 1930/31: S. 514) habe. Aber wirkungslos war er auch aus Pencks Sicht nicht.

5 Der ethnopolitische Penck

Der ethnopolitische Penck ist an den Doppelbegriff des „deutschen Volks- und Kulturbodens" geknüpft. Der Historiker Hermann Aubin stellte 1937 fest: „Albrecht Penck prägte mit dem Wort vom deutschen Volksboden den anschaulichen und inhaltsreichen Begriff der Fläche, welche die Deutschen in Europa innehaben. (...) Penck lehrte weiter, über den deutschen Volksboden hinaus den deutschen Kulturboden zu erkennen" (Aubin, 1937: S. 45).

Einzeln kommen beide Bestandteile des Doppelbegriffs beiläufig schon in der ersten Hälfte des 19. Jahrhunderts vor, auch in der Geographie (Schultz, 2011: S. 119ff.). Bei Mendelssohn heißt es 1836 bei einem Vergleich von Russland mit Nord-Amerika: „Das eine Volk aus der Barbarei so eben auftauchend; das andre durch Verpflanzung aus altem Kulturboden in eine neue Erde verjüngt" (Mendelssohn, 1836: S. 474). In Roons „Physischer Geographie" werden „die zusammenhängenden Flächen des Kulturbodens" im nordöstlichen Europa erwähnt, „namentlich die Gebiete um die Kama und mittlere Wolga (...), die Landschaft um den mittleren Dnjepr, um die mittlere Weichsel etc.", die „vermöge ihrer Fruchtbarkeit, auf weiten Räumen die mannigfaltige Abwechselung" zeigten, „welche allen Kulturlandschaften eigen" (von Roon, 1838: S. 315) sei. „Kulturboden" wird hier offenkundig weitgehend synonym mit „Kulturlandschaft" gebraucht, ebenso die im Umfeld des Zitates auftauchenden Begriffe „Kulturfläche" (S. 313) und „Kulturland" (S. 314) sowie an anderer Stelle der Begriff des „Fruchtbodens" (S. 257).

In all diesen Begriffsvarianten steckt die anbauende landwirtschaftliche, die materielle Tätigkeit des Menschen, doch ist damals auch schon von „deutschem Boden" die Rede, so beim schon zitierten Mendelssohn, doch ist mit der Kontrastierung, dass er „einen entschieden abweichenden Charakter von der des westlichen Nachbarlandes" (Mendelssohn, 1836: S. 115) trage, noch keine ethnische Wertung verbunden. Es geht Mendelssohn allein um die „auffallende Eigenthümlichkeit" des Reliefs „andern Ländern, z.B. Frankreich oder England gegenüber" (S. 120). Die Kulturzustände zwischen einzelnen Völkern, die Mendelssohn (s.o.) anspricht und nach hoch/höher und tief/tiefer bewertet (z.B. S. 263 u. S. 413), macht er aber nicht an unveränderlichen Wesensmerkmalen der Völker fest, sondern, wie zwischen Russen und Nord-Amerikanern (s.o.), an gesellschaftlichen Zuständen (S. 474).

Allerdings wurde schon in der Startphase der modernen Geographie ein enger Zusammenhang zwischen der „Cultur der Einwohner" eines Landes und der „Cultur des Bodens" sowie der „Gesammtcultur des Landes" dergestalt hergestellt, dass eine Veränderung des Kulturzustandes der Bewohner sich auch auf das Land „veredeln[d]" oder „verschlimmern[d]" auswirken müsse: „Sinkt die Cultur der Einwohner, werden die Menschen in einem Lande, weichlich, schlaff, träge, dumm etc. so verwildern die angebauten Fel-

der wieder, Straßen und Canäle verfallen, Gebäude stürzen ein, ganze Städte sinken in Ruinen u.s.w." (Henning, 1812: S. 303f.). Der Schluss, dass sich die Kulturhöhe der Völker auch im Landschaftsbild spiegelt, gehört zur Grundeinsicht der länderkundlichen Geographie, er war ihr paradigmatischer Kern. Wie das Land, so das Volk, wie das Volk, so das Land, lautete die Devise ihrer Vertreter seit Beginn des 19. Jahrhunderts (vgl. Schultz, 2015, S. 176ff.).

Um 1900 sind beide Begriffe, „Volksboden" wie „Kulturboden", im Zusammenhang mit den österreichischen Nationalitätenkämpfen und der Agitation der alldeutschen Publizistik als „politisch aufgeladene Schlagwörter" fest in den völkisch-nationalen Diskursen verankert, wurden allerdings „noch in keinem gemeinsamen Konzept konkret aufeinander bezogen" (Henniges, 2015: S. 1314).

Unter dem Titel „Die Besiedlung des deutschen Volksbodens", verfasst vom Vorsitzenden des *Alldeutschen Verbandes*, Ernst Hasse, erschien 1905 ein Heft zur „Heimatpolitik", das diese Politisierung als expansionistische Programmatik offen zum Ausdruck brachte. Hasse, der von sich selbst sagt, er sei „weder Geschichtsschreiber, noch Geograph, noch Ethnograph", sah es als seine Aufgabe an, die Bedeutung des Volksbodens als „die Grundlage unseres staatlichen Daseins" in der „Gesamtheit" aller Einzeltatsachen zu würdigen, was dem deutschen „Volksbewußtsein" bislang noch fehle. Historiker, Geographen und Ethnographen, darunter Friedrich Ratzel (ebenfalls Mitglied des *Alldeutschen Verbandes*) werden von Hasse aufgerufen, an einem Überblick der „riesenhaften Literatur" zum Thema mitzuwirken, um „etwas [zu] schaffen, was auf der Höhe der deutschen Wissenschaft stände" (Hasse, 1905: S. 1f.). Im Schlusskapitel forderte Hasse, dass „die *Eindeutschung der undeutschen Grenzmarken*" erst dann „*zum Stillstand gelangen*" dürfe, wenn es gelungen sei, „den deutschen Volksboden mit den Grenzen des deutschen Reichs in Uebereinstimmung zu bringen, *alle noch fremdvölkisch besiedelten Reste des Deutschen Reiches einzudeutschen* und dem ausdehnungsbedürftigen deutschen Volke nach dem Maße seiner Ausdehnungskraft und Ausdehnungslust *neuen Volksboden* zur Verfügung zu stellen" (S. 125). Das war ein uferloses Programm! Kannte es Penck?

Einen ersten Anstoß zur Deutschtumsarbeit, berichtet Penck, habe er schon als Student bei einem Pragaufenthalt erhalten. Dabei habe er die Erfahrung gemacht, dass Klagen über die Unterdrückung des Deutschtums nur noch mündlich weitergeben wurden statt per Post, was ihm „ein Wink fürs Leben" gewesen sei. Wer, wie er, in Österreich länger gelebt habe, der wisse, „wie systematisch dort alle deutschen Regungen unterdrückt" (Penck, 1930/31: S. 512) worden seien. Später, in seiner Zeit als Hochschullehrer in Wien, haben ihn auch die Forschungen seiner Schüler, darunter vor allem Hanslik mit seinen Arbeiten, mit ethnopolitischen Diskursen vertraut gemacht (Henniges, 2015: S. 1317ff.).

Schriftlich äußerte sich Penck erstmals ausführlicher zu Deutschtumsfragen 1907 in einem Aufsatz mit dem Titel

Deutsches Volk und deutsche Erde. Seine Ausführungen sind ein einziges Klagelied über den weltweiten Rückzug des Deutschtums. Besonders störte ihn, dass die Deutschen im Reich, „gleichgültig" zusähen, „wie bei den peripherisch wohnenden Deutschen Sprachinsel auf Sprachinsel verloren" gehe, „wie Schritt für Schritt die Sprachgrenze zu unseren Ungunsten verschoben" (Penck, 1907: S. 180) werde. Speziell die tschechisierten, polonisierten, slawonisierten oder magyarisierten Deutschen würden für das deutsche „Weltbürgertum" verloren sein, also nicht mehr deutsche Interessen in der Welt vertreten. Daher sei es „nicht bloß eine nationale Pflicht, sondern auch ein Gebot des Humanismus, das Auslanddeutschtum zu schützen" (S. 181f.). Für die in den Städten lebenden Deutschen sei dies nur schwer möglich, darum konzentrierte sich Penck auf den „deutschen Bauern", der an alter Art und Sitte und an seiner deutschen Sprache festhielt: „Faßt das Deutschtum Wurzeln, gesellt sich zum deutschen Volkstum seine Erde, so ist es lebenskräftig für lange Zeiten" (S. 182). Hier hätte nun das Begriffspaar „Volks- und Kulturboden" einspringen können, doch taucht im Text nur der Begriff des „Sprachbodens" auf, ohne besonders herausgestellt zu werden.

Im Krieg stürzte sich Penck dann verstärkt in die bisher von ihm vernachlässigte Politische Geographie, doch trotz mancher Anklänge an Ratzel, etwa durch Übernahme des Lebensraum-Begriffs oder die Auffassung, dass die natürlichen Räume dem Wachstum der Staaten angepasst werden müssten (s. o.), entwickelte Penck seine Vorstellungen nicht am Schreibtisch, sondern nach Art des im Gelände arbeitenden Geomorphologen beobachtend im Feld. Nicht Bücher, sondern das Auge lieferte ihm die Belege für seine Theorien. So auch als Mitbegründer auf einer Reise der *Landeskundlichen Kommission beim Generalgouvernement Warschau* im Mai 1916 in die okkupierten Gebiete in Russisch-Polen. Nur wenige Tage reichten ihm, um durch Augenscheinnahme sein ethnopolitisch-geographisches Weltbild nach einem stereotypen, dichotomischen Beschreibungsschema zu formatieren (Henniges, 2015: S. 1315f. u. 1326f.).

Zwei Welten, auch dieses Motiv übrigens schon bei Ratzel (1898: S. 304) angelegt, stießen Penck zufolge im Osten schroff aufeinander, eine Welt der *Ordnung* und eine Welt der *Unordnung*. Auf der Ordnungsseite fand er saubere, freundliche und ansehnliche Siedlungen mit einem reichbebauten Boden, auf der Seite der Unordnung erbärmliche, schmutzige, unscheinbare Häuser und ein verwahrlostes Land. Auch die Menschen wurden diesem Wertungsschema unterworfen. Nur wo Ordnung herrschte, da zeigten sie sich Penck geistig beweglich, arbeitsam und tüchtig, vor allem aber als gelehrige Schüler der Deutschen. Selten nur attestierte Penck nicht-deutschen Völkern, aus eigenem Antrieb etwas Ordentliches geleistet zu haben, einigen bescheinigte er, über einen guten Kern zu verfügen, der entwicklungsfähig sei, immer aber galt als Maßstab der Beurteilung der Entwicklungsstand bei „uns". Das war gegen Ende des Weltkriegs Pencks Weltbild, auf das er später immer wieder zurückgriff. Aus sei-

nen subjektiven (Vor-)Urteilen wurden objektive Merkmale, doch fehlte vom Doppelbegriff des „Volks- und Kulturbodens", der solche Unterscheidungen stützte, weiterhin jede Spur. Nur beiläufig tauchte der „deutsche Volksboden" (Penck, 1918b: S. 127) auf.

Der Endstand der terminologischen Entwicklung ging aus Aktivitäten von Wissenschaftlern, Deutschtumsfunktionären und Politikern seit Beginn der 1920er hervor, die sich neben der Suche nach institutionellen Möglichkeiten, Forschungen zum Grenz- und Auslandsdeutschtum anzustoßen und zu koordinieren, auch um eine begriffliche Klärung des neuen Forschungsfeldes bemühten. 1923 kam es zur Gründung der Leipziger *Mittelstelle für zwischeneuropäische Fragen*, die wenig später auf Initiative von Volz und Penck in *Mittelstelle für Volks- und Kulturbodenforschung* umbenannt wurde (Haar, 2000: S. 30). 1925 erschien dann in dem Sammelband *Volk unter Völkern* Pencks Aufsatz *Der deutsche Volks- und Kulturboden*. Beigefügt war ihm die eingangs dieses Beitrags schon erwähnte, von Penck konzipierte Schwarz-Weiß-Karte, die der nationalen Propaganda dienen sollte (Haar, 2000: S. 377). Außerdem gab es noch zwei von Penck entworfene farbige Versionen: eine Wandkarte (1925) und eine Handkarte (1926).

Pencks Karten regten zu unzähligen Variationen und Modifikationen an, sein Aufsatz wurde zu einem Referenztext für die Begründung der neuen interdisziplinären Forschungsrichtung (vgl. Herb, 1997: S. 55ff.). Durch diesen überwältigenden Erfolg ging unter, dass Penck stets an der *politisch-geographischen* Seite seines Land-Volk-Denkens festhielt und sich explizit in der länderkundlichen Traditionslinie der Geographie verankerte. Auch die heutige Wissenschaftsgeschichte, scheint mir, kann mit dieser Seite Pencks wenig anfangen.

Penck bot allerdings für die Volkstumsforschung kein ausgearbeitetes Forschungsprogramm, sondern im Grunde nur weltanschaulichen Trost, der über die deutsche Kränkung durch Versailles hinweghelfen sollte. „Wo deutsches Volk siedelt, ist deutscher Volksboden, da hört man deutsche Sprache und sieht man deutsche Arbeit" (Penck, 1925: S. 62). Durch die „Tüchtigkeit" seiner Menschen habe er „allenthalben ein bestimmtes, deutlich erkennbares Gepräge erhalten" (S. 64). Die politische Brisanz scheint auf, wenn Penck die staatliche Zersplitterung der Deutschen anspricht: „Fünf Staaten erstrecken sich heute im Bereiche des deutschen Volksbodens: das Deutsche Reich, das nur Dreiviertel desselben umfaßt, Österreich, Danzig, Luxemburg und Liechtenstein. Zehn Staaten greifen in das [sic] Bereich des deutschen Volksbodens über: Dänemark, Litauen, Polen, Tschechoslowakei, Ungarn, Jugoslawien, Italien, Schweiz, Frankreich und Belgien" (S. 63).

Der deutsche Volksboden war für Penck zugleich deutscher Kulturboden, der sich markant von „benachbarten Kulturgebieten" abhob. Charakteristisch, erläuterte er, sei für ihn eine „äußerst sorgfältige Bebauung" (Penck, 1925: S. 64), die zeige, dass der Deutsche selbst dort nicht kapituliere,

wo es schwierig werde. Nichts bleibe, wo Deutsche siedelten, ungenützt liegen, Nachlässigkeit werde nicht geduldet, und der Boden danke es mit ertragreichen Ernten. Selbst die Blumen auf den deutschen Gräbern mussten dafür herhalten, die romanischen Friedhöfe mit ihren Steinplatten zu disqualifizieren. Die kompensatorische Funktion für die Niederlage scheint auf, wenn Penck rühmend betont: „Der deutsche Kulturboden ist die größte Leistung des deutschen Volkes" (S. 69).

Als Besonderheit des deutschen Kulturbodens hob Penck sein globales Vorkommen hervor. Ob in Brasiliens Urwäldern, an der regenreichen Westküste Chiles, im halbariden Kontinentalgebiet an der Wolga oder am Saume der Wüsten Südwest-Afrikas: „Wo immer auch Deutsche gesellig wohnen und die Erdoberfläche nutzen, tritt er [der deutsche Kulturboden] in Erscheinung" (Penck, 1925: S. 69). Damit stellte Penck klar, dass der deutsche Kulturboden (resp. die deutsche Kulturlandschaft) nicht auf physische Faktoren und deren Zusammenwirken zurückging, sondern allein „das Werk bestimmt veranlagter Menschen" war, „die die Natur nach ihrem Willen" (S. 70) geformt hatten. So spiegelte der deutsche Kulturboden als „das Werk deutscher Intelligenz, deutschen Fleißes und deutscher Arbeit" den Grundzug des deutschen „Wesens und Könnens" (S. 72) wider, der unter jeglichen geographischen Verhältnissen auf der Erdoberfläche entstehen konnte. Jedermann konnte das Deutschtum am deutschen Kulturboden unmittelbar sehen, so wie einst die deutschen Soldaten im Weltkrieg. Die alt-geographische Doppelformel: Wie das Land, so das Volk, wie das Volk so das Land, war hier einseitig auf die Richtung vom Volk zum Land beschränkt. Als „Deutschland" wollte er diese Gebiete in anderen Kontinenten jedoch nicht angesprochen wissen, auch nicht den Kulturboden des Inseldeutschtums in Europa, wie z.B. in Siebenbürgen (Penck, 1933: S. 322).

Als weitere Besonderheit des deutschen Kulturbodens befand Penck, dass auch Nicht-Deutsche ihn schaffen konnten. „Schon eine kleine Zahl von Deutschen" habe oftmals genügt „um ein großes Land in deutschen Kulturboden zu verwandeln" (Penck, 1925: S. 69f.), ohne auch zum deutschen Volksboden geworden zu sein, wie die ehemaligen russischen Ostseeprovinzen, aber auch slawisch besiedelte Gebiete, speziell in Böhmen und Mähren und bis zur Weichsel, zeigten. „Eine eigene tschechische Kulturlandschaft" gebe es nicht; hier habe eine tausendjährige Zugehörigkeit zum Deutschen Reich dazu geführt, dass sich die tschechische von der deutschen Kulturlandschaft „lediglich durch den geringeren Grad von Sauberkeit" (S. 68) unterscheide. Im Gebiet bis zur Weichsel wiederum hätten vor der Völkerwanderung germanische Stämme gesessen und dort einen „altgermanischen Kulturboden", den „lugischen", geschaffen, der jedoch seine „voller Wertung" erst durch die späteren deutschen Siedler erfahren habe. Diese Siedler hätten dann den in der Völkerwanderungszeit nachgerückten Slawen beigebracht, „gleiches zu tun" (S. 69), doch sei es zu einer völligen Einbeziehung des altgermanischen Kulturbodens in den deutschen nicht gekommen.

Schließlich stellte Penck dem geschlossenen deutschen Volks- und Kulturboden noch die ihm vorgelagerten kleineren und größeren Volksboden-„Inseln" zur Seite, „umgeben von Kränzen deutschen Kulturbodens" (Penck, 1925: S. 66), die vor allem im Osten eine aufgelöste Grenzsituation geschaffen hätten. Hier, „auf der Ostseite des deutschen Volksbodens", liege schon aufgrund des Ineinandergekeiltseins von Deutschen und Slawen „die große Schwierigkeit der Begrenzung eines rein nationalen Deutschland" (S. 62).

Nach 1933 diente Penck seine Volks- und Kulturboden-Ideologie dem neuen Regime als „nationale Erdkunde" an. Sie sollte der Jugend die deutsche Geschichte als Geschichte eines arbeitsamen, schaffensfreudigen Heldenvolkes präsentieren nach dem Motto: „Gott schuf den Raum und wir machten Deutschland daraus" (Penck, 1934a: S. 260). Zwar fülle das deutsche Volk „den deutschen geographischen Raum" (Penck, 1933: S. 323) nicht völlig aus, habe aber als „arbeitendes, schaffensfreudige Volk" seine natürlichen Gegebenheiten zu einem „einzigartigen deutschen Kulturboden" (S. 335) gemacht, der sich klar von Kulturlandschaften im Süden und Westen abhebe, die eine „gealterte Kulturlandschaft" zeigten, „die nicht so leistungsfähig" sei „wie die deutsche, ausgereifte" (S. 327). Immerhin gestand Penck für das deutsche Volk den früheren Kulturtransfer aus dem Süden und Westen ein, doch befand er anmaßend und überheblich, dem Osten habe es immer nur gegeben, so wie es der ganzen Welt wie kein anderes Volk Dichter und Denker, Entdecker und Erfinder gegeben habe. Ein solches „Weltbürgertum" sei als Erziehungsziel nur noch zu akzeptieren, wenn es „fest im eigenen Volke" (S. 332) wurzele.

Aber nicht erst ab 1933, von Anfang an verstand Penck die Kulturgeographie als ein *volkspädagogisches* Projekt, das durch entsprechende Erziehung der Jugend das Wiedererstarken Deutschlands einleiten sollte! Schon 1921, bevor er den Volks- und den Kulturbodenbegriff zum Doppelbegriff zusammenzog, riet er dem preußischen Kultusministerium, im Geographieunterricht die Erdoberfläche nicht als Schauplatz geschichtlicher Vorgänge, sondern „der menschlichen Arbeit" behandeln zu lassen, damit der Schüler sehe, wie weit der „grösste Kampf" die Menschheit, ihr Kampf mit der Natur, „an einer bestimmten Stelle gediehen" sei, um „einen besseren *Massstab für die Arbeit der einzelnen Völker* auf der Erde" zu erhalten, was „durch blosse Würdigung ihrer politischen oder ihrer in Ein- und Ausfuhrzahlen sich spiegelnde wirtschaftliche Stärke" nicht erreicht werden könne. „Gerade in der gegenwärtigen Zeit" bedürfe das deutsche Volk „etwas, an dem es sich erheben (...) und aufrichten" (Penck, 1921: Blatt 229) könne. In seinem späteren Volks- und Kulturbodenaufsatz bekräftigte er, dass ein Nationalgefühl nur durch das Beispiel einer „uneingeschränkt großen Leistung" anerzogen werden könne, einer Leistung, wie sie „in der Schaffung eines deutschen Kulturbodens" (Penck, 1925: S. 72) vorliege.

In den Erdkundeschulbüchern der Weimarer Republik fand Pencks Gedankenwelt – inklusive der einschlägigen Karten – breiten Eingang (vgl. Schultz, 2011: S. 130ff.). Es ist schwer vorstellbar, dass bei entsprechender Agitation durch die Lehrer bei den Schülern nicht, wie diffus auch immer, der Eindruck entstehen musste, im Osten seien die Grenzen im „Kampf der Völker" um Lebensraum politisch noch nicht ausgekämpft. Warum sollte der im Kartenbild weit sich öffnende Wirkungs- und Einflussraum der Deutschen im Osten, der vom Finnischen Meerbusen bis zum Schwarze Meer ging und darüber hinaus deutsche Volkstumsinseln bis zur Krim, zur unteren Wolga und zum Kaukasus zeigte, nicht eines Tages für das Deutsche Reich, in welcher Form auch immer, politisch wiederbelebt werden können? Jedenfalls legten ihnen Schulbücher, Wandkarten und geopolitische Kartenskizzen in suggestiver Form nahe, dass speziell im Osten die deutschen Grenzen lediglich das Momentbild einer langen, noch unabgeschlossenen Entwicklung waren (Henniges und Meyer, 2016).

6   Land im Osten für ein Volk ohne Raum?

War aber den Beteiligten auch klar, dass sie damit einem Anwendungszusammenhang in die Hände arbeiteten, der brutale Konsequenzen bis hin zum Völkermord einschloss? Und wenn nicht, trugen sie dann gleichwohl eine Mitverantwortung für die spätere Umsiedlungs-, Deportations- und Mordpolitik der Nazis, weil sie mit der teils klaren, teils diffusen Volks- und Kulturbodentheorie die Wertungen geliefert und die Stimmung erzeugt hatten, die die Grundlage für die Akzeptanz einer solchen Politik abgaben?

Penck dachte sowohl in Bezug auf das Deutsche Reich als auch das deutsche Volk *machtpolitisch*. Seinen schon zitierten Aufsatz von 1907 leitete er mit der stolzen Feststellung ein: „Mächtig wie niemals zuvor ist das Deutsche Reich, kräftiger denn je das deutsche Volk", und das sei nicht durch „Waffengewalt" erreicht worden, „sondern durch friedliche Arbeit". „Uneingeschränkt" sei „die Anerkennung, die ihm für wissenschaftliche und technische Leistungen, für die Beteiligung am Weltverkehr gezollt" (Penck, 1907: S. 179) werde. *Ethnopolitisch* habe das Reich jedoch zur Aufrechterhaltung seiner „achtunggebietenden Stellung" (S. 179) auf allen Seiten zu kämpfen, denn seitdem „der einzelne Deutsche" im Gegensatz zum früheren zersplitterten Deutschland „Glied eines mächtigen Volkes" sei, werde er von anderen gefürchtet mit der Folge, dass Deutsche um der „wirtschaftlichen Vorteile" (S. 180) wegen nur noch willkommen seien, wenn sie ihr Deutschtum aufgäben. Damit schwächten sie natürlich auch Deutschlands Machtstellung. Denn die Macht eines Staates, so dachten mit Penck damals viele, hänge von der Menge seiner Bevölkerung ab und somit zugleich von der ihm zur Verfügung stehenden Menge an Land (vgl. Ratzel, 1903: S. 423ff.). Wollte ein Machtstaat sich als Machtstaat unter Machtstaaten behaupten oder seine Position in der

Rangfolge dieser Staaten verbessern, so musste er dafür sorgen, dass seine Menschen möglichst nicht ins Ausland abwanderten, um dort als der sprichwörtliche „Kulturdünger" zu dienen.

Mit dem Weltkrieg waren diese Probleme für Penck zu einer Existenzfrage des Deutschtums eskaliert, denn es bestand für ihn „kein Zweifel mehr: *der große Krieg ist ein Krieg gegen das Deutschtum überhaupt*" (Penck, 1915b: S. 9). „Eng und klein" sei „die Fläche, welche uns Deutschen auf der Erde zur Verfügung" (S. 9) stehe, doch: „*Ein wachsendes Volk braucht Raum*" (S. 10). Zwei Fragen beschäftigten Penck daher im zweiten Kriegsjahr brennend. Erstens: „Soll Deutschland in Zukunft das verderbliche Zwei-Kindersystem aufgreifen und wie Frankreich auf den natürlichen Zuwachs seiner Bevölkerung verzichten?" (S. 10). Und zweitens: „Soll es fortfahren, den Überschuss seiner Bevölkerung abzugeben an das Ausland, das ihn aufschluckt und seinem Volkstum gewaltsam entfremdet, wie es die Gegenwart lehrt?" (S. 10). Auf diese beiden „großen Fragen für die Zukunft des deutschen Volkstums" gab es für Penck „aus nationalen Gründen" nur ein „entschiedenes Nein"; die „richtige Lösung des Bevölkerungsproblems" liege vielmehr „auf politisch-geographischem Gebiete" (S. 10).

So war die Bevölkerungsfrage zur Raumfrage und die Raumfrage zur Frage nach den deutschen *Kriegszielen* geworden, denn innerhalb der eigenen Grenzen sah Penck kaum noch Platz, und auch rings um die deutschen Grenzen herum sei der Raum „weggegeben, stellenweise dicht besiedelt" (Penck, 1915b: S. 10). Wo also war „leerer" Raum zu haben? „Der Krieg", freute sich Penck, habe ihn „geschaffen" (S. 10). Mit der russischen Armee hätten sich auch Litauer und Letten zurückziehen müssen, um dem vorrückenden deutschen Heer „ein menschenleeres, daher unwirtliches Land zu überlassen" (S. 10); Russland denke aber nicht daran, sie zurückkehren zu lassen, ihr Wohngebiet werde künftig Sibirien sein. Sollten aber Litauen und Kurland bei Russland bleiben, so würden dort Russen einziehen. Dann würde das Deutsche Reich nicht nur auf Russland, sondern auf „echtes Russentum" stoßen, was „unter allen Umständen vermieden werden" (S. 11) müsse. Somit stand für Penck fest, wie er seinem Freund Partsch am Neujahrstag 1916 brieflich erläuterte, dass er „die natürliche Westgrenze Russland", die er vom Peipussee zum Dnjepr gezogen habe (s.o.), nicht zugleich als die Grenze des Deutschen Reiches betrachte. Vielmehr wünsche er sich „die deutschen Grenzen so wenig als möglich" hinausgeschoben, „am ehesten gegen Kurland", während Satellitenstaaten „mit eigener innerer Verwaltung und starker deutscher Beeinflussung" (Albrecht Penck, pers. Mitteilung, 1916, zit. n. Brogiato und Schellhaas, 2014: S. 364) das Deutsche Reich und Russland auseinander halten sollten.

Mit der Niederlage waren solche Träume vorerst ausgeträumt, doch statt die Friedensregelung z.B. an jenen Regelungen zu messen, die man selbst in Brest-Litowsk gegenüber Russland durchgesetzt hatte, pochte man auf Wilsons *Selbstbestimmungsrecht* der Völker, das mit dem Siegerrecht

kollidierte, das man selbst praktiziert hatte. Vor allem an der Ostgrenze war dies ein großes Problem. Mit dem Mythos der so genannten Ostkolonisation, der im 18. Jahrhundert im Gefolge der Aufteilung Polens erfunden worden war, tröstete man sich über die traurige Gegenwart hinweg und träumte für die Zukunft von einem neuerlichen deutschen Macht- und Einflussraum im Osten. Das Deutsche Reich, so redete man sich stark, werde nach einer vorübergehenden Schwächephase in einem zweiten Anlauf erst als Großmacht auf die europäische, dann als Weltmacht auf die Weltbühne zurückkehren.

Pencks Volks- und Kulturboden-Theorie eröffnete solchen neuen Träumen die Wege. Was als Paradigmenbruch erscheint, war keiner, denn die Fugen des Mensch-Natur-Verhältnisses, die rhetorisch aufgerissen wurden, konnten leicht wieder geschlossen werden. Je nachdem, welche Seite des Mensch-Natur-Verhältnisses gerade in den öffentlichen Diskursen angesagt war, konnte der Geograph sich darauf einstellen: sich entweder mehr auf die Seite der Natur oder mehr auf die Seite des Menschen schlagen oder sich irgendwo dazwischen positionieren. Penck hat mit dieser Möglichkeit virtuos ein *raumbegriffliches Doppelspiel* inszeniert. Durch den kategorial weiträumig ausgreifenden politisch-geographischen Unterbau seines ethnopolitischen Denkens verlieh er den revisionistischen Wunschträumen in Richtung Osten Adlerflügel. Wie weit reichten seine konkreten territorialen Vorstellungen?

Was Polen anging, glaubte Penck noch kurz vor dem Kriegsende daran, dass es diesem gelingen werde, sich „ohne das Bleigewicht Litauens und Weißrußlands an seinen Füßen (...) so gedeihlich zu entwickeln", dass es nicht nur durch „Natur und Bodenbeschaffenheit auf das innigste mit dem germanischen Mitteleuropa" verknüpft sei, sondern auch kulturell „ein Stück echten mitteleuropäischen Bodens" werde, während es aktuell nur als „Zwischenland" erscheine, weil der „hohe kulturgeographische Gegensatz" (Penck, 1918b: S. 131) seine Zugehörigkeit zu Mitteleuropa noch verschleiere. Hoffnung machte ihm, dass nach Ansicht seines Schülers Hanslik die Kulturgrenze des altpolnischen Reiches innerhalb des Deutschen Reiches im Schwinden begriffen sei, so dass Gleiches auch „an der Grenze von Kongreßpolen" (S. 131) erwartet werden könne.

Nachdem sich das neue Polen nicht bescheiden an den von der Natur vorgeschriebenen geographischen Verhältnissen orientierte, die ihm von Penck zugestanden wurden, kam er nicht mehr auf die Entwicklungsfähigkeit des polnischen Volkes zurück und schloss sich wieder der Geringschätzung der slawischen Völker an, die seit Mitte des 19. Jahrhunderts in zahlreichen deutschen Schriften grassierte. Für ihre Verfasser war der slawische Osten Europas ein heruntergekommener, verwahrloster Raum, der durch seine mehr schlecht als recht vor sich hinlebende Bevölkerung niemals in eine blühende Landschaft verwandelt werden würde. Gehörten solche passiven, unschöpferischen Völker (vgl. Schultz, 2015, S. 180ff.) überhaupt hierher, wo ihnen doch ganz of-

fensichtlich jene kulturlandschaftsbildende Kraft der Deutschen fehlte, die gebraucht würde, um aus dem östlichen Mitteleuropa ein echtes Mitteleuropa zu machen, ja, die zum Teil noch sich selbst der Natur und die Natur sich selbst überließen?

Ein solches antislawisches Weltbild im „Daseinskampf der Völker" vertraten freilich auch andere Geographen, nicht nur Penck. In Termini der Küstenmorphologie beklagte Joseph Partsch 1906 zeitgleich mit Pencks Klage über den Rückgang des Deutschtums auf der Welt (s.o.) den „Ansturm der slawischen Völkerwogen gegen den Besitzstand deutschen Volkstums" und forderte dazu auf, „mit scharfer Aufmerksamkeit den Ufersaum im Auge zu behalten, um nicht durch Landverluste überrascht zu werden" (Partsch, 1906: S. 4). Schon sei die „schöpferische Lebenskraft" der slawisch umfassten deutschen Städte Oberschlesiens bedrängt und bedroht, und auch „der deutsche Besitz an schlesischem Boden" erleide „neuerdings einen Abbruch" (S. 4). In seiner Ansprache zur Eröffnung des 21. Deutschen Geographentages 1925 in Breslau rüttelte Philippson in fast apokalyptischen Tönen seine Zuhörer wach: „Und dieses alte *Zentrum* deutscher Kultur und Geschichte [Breslau] steht auf vorgeschobenem Posten der Ostmark, als ein Fanal deutscher Bildung und Kraft, umbrandet von den *gierigen Wellen des Slaventums*!" (Philippson, 1926: S. 26).

Immerhin räumte auch Philippson, wie einst Penck (s.o.), Polen eine, wenngleich nur schwache, geographische Existenzberechtigung ein, auf keinen Fall aber in seinem gegenwärtigen Grenzumriss. Als natürliche Einheit umfasse Polen nur „die Stromgebiete der Weichsel oberhalb des Knies bei Thorn (Russisch-Polen und Westgalizien) und das der Warthe etwa bis zur Vereinigung mit der Netze (preußische Provinz Posen)." Das sei „das Land, welches allein wir geographisch und national als Polen anerkennen können" (Philippson, 1928: S. 78). Dieses Polen, das seine neue politische Existenz den deutschen Siegen im Osten verdanke (ohne den Deutschen dankbar zu sein), gehöre zu Mitteleuropa und habe seine Kultur „von Westen, von den Deutschen" (S. 79) erhalten.

7 Abschließende Reflexionen zur Anklage Pencks

Nach dieser Sichtung einschlägiger Arbeiten Pencks will ich abschließend eine Antwort auf die Frage versuchen, inwieweit die Anklage, Penck gehöre zu den Mittätern am Völkermord der Nationalsozialisten, berechtigt ist. Hat er, wie auch der Historiker Ingo Haar im *Handbuch der völkischen Wissenschaften* meint, jenen völkischen Wissenschaftlern zugearbeitet, deren „bevölkerungspolitisches Szenario (...) die expansionistische und rassistische Grundlage der Groß- und Lebensraumpolitik des ‚Dritten Reiches'" (Haar, 2008: S. 380) antizipiert habe? Oder trifft eher Burkerts vorsichtigeres Urteil zu, dass Pencks Vorstellungen über den offiziellen Revisionismus der Weimarer Republik hinausgin-

gen, aber hinter den Vorstellungen der Nationalsozialisten zurückblieben (Burkert, 2000: S. 590)?

Tatsächlich hielt sich Penck bezüglich der *staatsrechtlichen* Konsequenzen seines fragwürdigen Volks- und Kulturbodenkonzepts zurück, (fast) alles ließ er in der Schwebe, eine Aufforderung zur politischen Aktion mit konkreten territorial- und bevölkerungspolitischen Empfehlungen vermied er in seinen Schriften. Stattdessen erklärte er: „Von vornherein ist der Begriff Deutschland ein unpolitischer", der dem „Volksbewußtsein" (Penck, 1933: S. 323f.) entspringe. War Pencks Deutschlandbegriff damit wirklich politisch harmlos? Keinesfalls, denn „unpolitisch" bedeutete für ihn lediglich, dass der *ethnographische* wie der *geographische* Deutschlandbegriff Gebiete umfasste, die nicht mit dem aktuellen *staatsrechtlichen* Begriff des Deutschen Reiches zusammenfielen. In jedem Bedauern, dass dies nicht der Fall sei, lag als emotionaler Unterstrom der Wunsch nach mehr Deckung der drei Kategorien. Was nicht war, konnte ja noch werden, was nicht mehr war, wieder werden. Schrie nicht „der deutsche Kulturboden in Pomerellen", der laut Penck (1933: S. 327) nach dem Exodus von Deutschen „schon verwahrlost[e]", geradezu nach Revision? Wie provozierend musste es erscheinen, wenn man den Völkern der Nachbarstaaten zumutete, sie siedelten und lebten, obgleich staatlich anders verfasst, in Deutschland, Deutschland im Sinne der Kulturbodenkategorie?

Immerhin: Die Schweiz, die ja auch zu einem erheblichen Teil deutscher Volks- und Kulturboden war, stand für Penck nicht zur Disposition, die Niederlande sowie der flämische Teil Belgiens wurden von ihm in der Schwarz-Weiß Karte überhaupt nicht in eine Beziehung zum Volks- und Kulturboden-Deutschland gebracht und in den beiden farbigen Karten, der Wand- und Handkarte, lediglich als Gebiete der niederdeutschen Sprache ausgewiesen. Auch schwebte ihm keine „geopolitische Restitution" (Haar, 2008: S. 380) Österreich-Ungarns vor, von der einige völkische Wissenschaftler wohl noch träumten.

Völlig abwegig wäre es gar, wollte man Penck unterstellen, im Osten auch Gebiete bis zur Wolga, Kaukasien, die Krim, Bessarabien und Wolhynien als Teile eines künftigen deutschen Staates anzusehen, weil hier, kartographisch dokumentiert, ein Streuinseldeutschtum existierte. Sein politisches Wunsch-Deutschland umfasste im Wesentlichen den „geschlossenen Volks- und Kulturboden" in Mitteleuropa. Ob und welche Gebiete des deutschen Kulturbodens auch ohne oder nur mit einer sehr geringen Anzahl deutscher Bewohner dazugehören sollten, ließ sich Penck nicht entlocken.

Das Volks- und Kulturbodenkonzept entstand als nichtrassistisches Konzept im biologischen Sinne. Zwar griff Penck nach 1933 auch den Rassenbegriff auf. So verwies er warnend darauf, dass „germanisches oder deutsches Blut, sobald es sich mit fremdem mischte oder nur fremde Sprache annahm, uns feindlich wurde" (Penck, 1933: S. 328). Auch sah er die Umgestaltung der Natur- in eine Kulturlandschaft abhängig vom „Können" und von der „Rasse" des Menschen

(Penck, 1934a: S. 262). Doch blieb es bei solchen eher beiläufigen Anbiederungen an das NS-Regime. Privat äußerte er hingegen im September 1933, dass es „nicht so sehr auf die Rasse" ankomme, wie vielfach jetzt gelehrt" werde, „sondern auf den Geist, der im Körper" wohne. „Tüchtige Menschen" dürfe man „nicht gering achten, weil sie von Juden abstammen oder Juden sind". Hier liege „ein grundsätzlicher Fehler in der neuen Bewegung", an der ihn ansonsten vieles freue, was sie anstrebe (zit. n. Henniges, 2015: S. 1342).

Eine andere Sache ist es, dass Penck mit seinem Volks- und Kulturbodenkonzept einen *nationalen Kulturdünkel* bediente. Im Bild der Kulturlandschaft erkannte der auf Beobachtung trainierte Geograph die Möglichkeiten und Grenzen der Völker bei der Gestaltung ihres Lebensraumes. Deswegen war ihm „die Kulturlandschaft ein Kennzeichen der Kulturhöhe" (Penck, 1933: S. 331). Kombinierte man diese Wertung mit der weit verbreiteten Auffassung, dass nur dasjenige Volk sein Land zu Recht besaß, das es auch ordentlich bebaute, so mussten die Weiten des Ostens als quasi herrenloses Land der Zukunft erscheinen, über dessen endgültiges Schicksal das letzte Wort noch nicht gesprochen war.

Zusätzliche Schubkraft gewann das Bild vom lockenden Lebensraum im Osten, der nur darauf zu warten schien, unter den deutschen Pflug genommen zu werden, durch Verknüpfung mit dem *Volk-ohne-Raum-Motiv*, das Penck bereits im Ersten Weltkrieg zur Rechtfertigung von Annexionen diente, wenngleich bei weitem nicht in alldeutschen Dimensionen. Denn wenn die slawische Bevölkerung allein schon aufgrund ihrer geringen Zahl diesen Raum nicht zu füllen und zu kultivieren vermochte, so drängte sich unweigerlich der Schluss auf, dass ein so genanntes Leistungsvolk, wie das deutsche, dem es angeblich an Raum zu seiner Entwicklung fehlte, einen *natürlichen* Anspruch darauf hatte, sich diesen Raum zu Lasten der dort lebenden Bevölkerung kolonisierend anzueignen. Die bösen Folgen dieser Logik sind bekannt.

Allerdings hat Penck in seinen Schriften solche Konsequenzen weder offen noch andeutungsweise einkalkuliert. Auch nahm er in keiner der Schriften zu den ausgreifenden Raumphantasien anderer völkischer Wissenschaftler und Publizisten Stellung. Wohl aber haben seine *politisch-geographischen* und *ethnopolitischen* Raumbilder dazu beigetragen, den Osten und Südosten Europas wie selbstverständlich als Experimentierfeld der deutschen Revisionspolitik und über diese hinaus wahrzunehmen und die ideologischen Nachfahren der früheren „Ostreiter" in der Auffassung zu stärken, der vermeintlichen slawischen Unkultur die Segnungen deutscher Kultur und Ordnung bringen zu müssen.

Auszugehen ist davon, dass Penck auch nach dem verlorenen Weltkrieg seine Kriegszielvorstellungen aus der Kriegszeit weiter fest im Blick behielt: die Wiedergewinnung der Kolonien und die Zurückdrängung Russlands hinter eine Linie vom Weißen Meer und Finnischen Meerbusen bis zur Krim, die teilweise mit der Unabhängigkeit Finnlands und der Gründung der baltischen Staaten und Polens nach dem Weltkrieg realisiert worden war, nur eben nicht so, wie sich

Penck dies vorgestellt hatte: mit dem Deutschen Reich als unangefochtener Ordnungs- und Hegemonialmacht in der Mitte Europas. Die Aussiedlung von „Fremdvölkern" war für ihn jedenfalls (s.o.) kein grundsätzliches Hindernis für seine territorialpolitischen Vorstellungen. Dass am Ende einer radikalen geo- *und* ethnopolitisch motivierten Politik im Tarnmantel vermeintlich *strenger* Wissenschaft die Massenvernichtung von Menschen, der Völkermord, stehen würde, wollte er, scheint es, nicht sehen.

Dieses Nichtsehen-Wollen oder Wegblenden lässt sich allerdings vom Nichtsehen-Können, einer professionellen Blindheit, nicht scharf trennen. Um Letzteres auszuloten, muss auf Pencks *naturwissenschaftlichen* Habitus zurückgegangen werden, der ihn auch Politik, Wirtschaft und Gesellschaft, soweit der Geograph mit ihnen zu tun hatte, als gesteuert von Naturgesetzen verstehen ließ: „Die Freiheit des menschlichen Willens gleicht der Freiheit der einzelnen unter dem Gesetze. Auch sie steht unter den Gesetzen der mechanischen Kausalität, welche uneingeschränkt über die Massen herrschen, aber nicht in dem Einzelfalle klar zu erkennen sind" (Penck, 1928: S. 38). Die Massen, d.h. die Völker, sind *gesetzlich* dazu verdammt, einen nie aufhörenden „Kampf um Lebensraum" zu führen, auch wenn ihnen dies selbst nicht ständig bewusst ist. Aufgabe des Geographen ist es, über den Stand dieses Kampfes aufzuklären, wie er sich ihm im Bilde der Kulturlandschaft offenbart, und die Gesetze auszusprechen, die ihn steuern. Die Erkenntnis, dass das Mensch-Natur-Verhältnis ein *innergesellschaftliches* ist, war ihm wie allen Geographen, die am klassischen Paradigma hingen, verbaut.

Bemerkenswert ist in diesem Zusammenhang überdies, dass sich Penck von der Geopolitik deutlich absetzte, weil sie ihm die naturwissenschaftlichen Grundlagen der Geographie zu sehr zu vernachlässigen schien. Die Erdoberfläche, mit welcher der Geograph es zu tun hatte, blieb für ihn das Dauernde im geschichtlichen Wandel, die dem Menschen bei allem Spielraum, den sie ihm ließ, „vielfach zwangsläufig" (Penck, 1934b: S. 26) zeigte, was zu tun und was zu lassen war. Auf sie musste der Geograph stets alles rückbeziehen. Unter diesen Umständen spielen Fragen der Verantwortung keine Rolle, solange den Wegweisungen der Natur gefolgt wurde, denn die Natur hatte immer Recht. Verantwortungslos war es dagegen, diesen Gesetzen nicht zu folgen! Dass dies möglich war, setzt allerdings einen konflikthaften Dualismus von Natur und Geist voraus, der in Pencks naturwissenschaftlichem Weltbild nicht vorgesehen war. Tatsächlich funktioniert diese Art von politischer Geographie, wie sie Penck (und auch andere Geographen) praktizierten, nur, wenn die Erdoberfläche zuvor *normativ* aufgeladen wird, wenn in sie hineinprojiziert wird, was der Geograph als wissenschaftlich gesichertes Raumkonzept gerne verwirklicht hätte. So kehren die natürlichen Bedingungen als Vorschrift für ein bestimmtes Handeln in den politischen Diskurs zurück. Aus dem Buch der Natur wird eine Gebrauchsanweisung, die die Völker verstehen mochten oder auch nicht. Wer sie verstand,

konnte damit rechnen, dass er im Rahmen der Möglichkeiten, die ihm die Natur der Länder bot, immer das Richtige tat. So ist erklärlich, dass Penck die Gebietsgewinne, die er 1917 für das Deutsche Reich reklamierte, nicht als bewusst gewollte Siegprämie im Kräftemessen der imperialistischen Mächte um ihre Weltgeltung rechtfertigte, sondern seinen Zuhörern versicherte: „Das ist kein uferloses Sehnen nach Macht, kein imperialistisches Streben. Das ist einfach Notwendigkeit" (Penck, 1917: S. 31).

Ist Penck damit entlastet? Führt seine Gefangenschaft im naturwissenschaftlichen Denken, das sich ausschließlich auf die sinnlich wahrnehmbare Erdoberfläche beschränkte und alles ausblendete, was Staat, Wirtschaft, Politik und Gesellschaft als solche betraf, dazu, dass seine Rolle als *geistiger Lebensraumkrieger* und Wegbereiter der NS-Politik (wenn auch nicht im radikalen, vernichtungspolitischen Sinne) relativiert werden muss? Sähe man dies so und würde man ihm Absolution erteilen, so würde man allerdings jenen Zeitgenossen Unrecht tun, die sich nicht dem Druck einer vermeintlich objektiven Wissenschaft beugten und deren revisionistische Raumphantasien übernahmen, sondern auf der Basis des *Status quo* der Nachkriegsordnung ein friedliches Miteinander der Völker bei garantiertem kulturellen Minderheitenschutz propagierten und den Dialog der Gewalt vorzogen. Leider waren unter den Geographen nur wenige dazu bereit.

Literatur

Aubin, H.: Zur Erforschung der deutschen Ostbewegung, Deutsches Archiv für Landes- und Volksforschung, 1, 37–70, 309–331, 563–602, 1937.

Briesewitz, G.: Raum und Nation in der polnischen Westforschung 1918–1948, fibre, Osnabrück, Deutschland, 526 S., 2014.

Brogiato, H. P. und Schelhaas, B. (Hrsg.): „Die Feder versagt ...", Feldpostbriefe aus dem Ersten Weltkrieg an den Leipziger Geographie-Professor Joseph Partsch, Leipziger Universitätsverlag, Leipzig, Deutschland, 422 S., 2014.

Burkert, M.: Die Ostwissenschaften im Dritten Reich. Bd. I: 1933–1939, Harrassowitz, Wiesbaden, Deutschland, 771 S., 2000.

Etzemüller, T.: Suchen wir Schuld oder wollen wir Gesellschaft analysieren? Eine Anmerkung zur aktuellen Debatte um Hans Rothfels, Historisches Forum, 1, 27–33, 2004.

Fahlbusch, M.: Die verlorene Ehre der deutschen Geographie, Frankfurter Rundschau, 2. Oktober, S. 6, Druck- und Verlagshaus der Frankfurter Rundschau, Frankfurt am Main, Deutschland, 1999a.

Fahlbusch, M.: Wissenschaft im Dienst der nationalsozialistischen Politik? Die „Volksdeutschen Forschungsgemeinschaften" von 1931–1945, Nomos, Baden-Baden, Germany, 887 S., 1999b.

Haar, I.: Historiker im Nationalsozialismus. Deutsche Geschichtswissenschaft und der „Volkstumskampf" im Osten, Vandenhoeck & Ruprecht, Göttingen, Deutschland, S. 433, 2000.

Haar, I.: Leipziger Stiftung für deutsche Volks- und Kulturbodenforschung, in: Handbuch der völkischen Wissenschaften, Herausgeber: Haar, I. und Fahlbusch, M., Saur, München, Deutschland, 374–382, 2008.

Hasse, E.: Die Besiedelung des deutschen Volksbodens (= Deutsche Politik Bd. 1: Heimatpolitik H. 2), Lehmann, München, Deutschland, 156 S., 1905.

Henning, J. W. M.: Leitfaden beim methodischen Unterricht in der Geographie, Literarisches Büreau, Iferten, Schweiz, 567 S., 1812.

Henniges, N.: „Naturgesetze der Kultur": Die Wiener Geographen und die Ursprünge der „Volks- und Kulturbodentheorie", ACME: An International E-Journal for Critical Geographies, 14, 1309–1351, 2015.

Henniges, N. und Meyer, P. J.: „Das Gesamtbild des Vaterlande stets vor Augen": Hermann Haack und die Gothaer Schulkartographie vom Wilhelminischen Kaiserreich bis zum Ende des Nationalsozialismus, Zeitschrift für Geographiedidaktik, 44, 37–60, 2016.

Herb, H. G.: Under the map of Germany. Nationalism and propaganda 1918–1945, Routledge, London, UK and New York, USA, 250 S., 1997.

Herb, H. G.: Von der Grenzrevision zur Expansion: Territorialkonzepte in der Weimarer Republik, in: Welt-Räume. Geschichte, Geographie und Globalisierung seit 1900, Herausgeber: Schröder, I. und Höhler, S., Campus, Frankfurt a. M., Deutschland, 175–203, 2005.

Jureit, U.: Das Ordnen von Räumen. Territorium und Lebensraum im 19. und 20. Jahrhundert, Hamburger Edition, Hamburg, Deutschland, 445 S., 2012.

Kirchhoff, A.: Europa im Allgemeinen, in: Länderkunde des Erdteils Europa, Herausgeber: Kirchhoff, A., Temsky, Freytag, Wien, Österreich, Prag, Tschechien and Leipzig, Deutschland, 1/1, 7–87, 1887.

Kost, K.: Die Einflüsse der Geopolitik auf Forschung und Theorie der Politischen Geographie von ihren Anfängen bis 1945, Dümmler, Bonn, Deutschland, 467 S., 1988.

Mendelssohn, G. B.: Das germanische Europa, Duncker & Humblot, Berlin, Deutschland, 502 S., 1836.

Mommsen, W. J.: Interview mit W. J. Mommsen, online aufrufbar: http://hsozkult.geschichte.hu-berlin.de/BEITRAG/intervie/wmommsen.htm (letzter Zugriff: 19 November 2010), 1999.

Partsch, J.: Mitteleuropa, Perthes, Gotha, Deutschland, 463 S., 1904.

Partsch, J.: Von der deutschen Grenzwacht in Schlesien, Deutsche Erde, 5, 2–5, 1906.

Penck, A.: Physikalische Skizze von Mitteleuropa; Das Deutsche Reich, in: Länderkunde des Erdteils Europa, Herausgeber: Kirchhoff, A., Temsky, Freytag, Wien, Österreich, Prag, Tschechien and Leipzig, Deutschland, 1/1, 89–618, 1887.

Penck, A.: Morphologie der Erdoberfläche, Engelhorn, Stuttgart, Deutschland, Bd. 1: 471 S., Bd. 2: 696 S., 1894.

Penck, A.: Deutsches Volk und deutsche Erde, Die Woche, 9, 179–182, 1907.

Penck, A.: Was wir im Kriege gewonnen und was wir verloren haben, Heymann, Berlin, Deutschland, 30 S., 1915a.

Penck, A.: Politisch-geographische Lehren des Krieges, Meereskunde, 106, 1–40, 1915b.

Penck, A.: Die Ukraina, Zeitschrift der Gesellschaft für Erdkunde zu Berlin, Bd. 1916, 345–361, 458–477, 1916a.

Penck, A.: Die österreichische Alpengrenze, Engelhorns Nachf., Stuttgart, Deutschland, 79 S., 1916b.

Penck, A.: Über politische Grenzen, Norddeutsche Verlagsanstalt, Berlin, Deutschland, 32 S., 1917.

Penck, A.: Die natürlichen Grenzen Rußlands, Meereskunde, 133, 1–40, 1918a.

Penck, A.: Polen. Eine Anzeige, Zeitschrift der Gesellschaft für Erdkunde zu Berlin, Bd. 1918, 97–131, 1918b.

Penck, A.: Die Grenzen Böhmens, Deutsche Arbeit in Österreich, 18, 177–178, 1918/19.

Penck, A.: Gutachten über einen Lehrplanentwurf von H. Wagner, Geheimes Staatsarchiv PK, Akte I. HA Rep. 76 VI Sekt. 1 Gen. ff., Nr. 2, Bd. 1, Blatt 228–231, 1921.

Penck, A.: Deutscher Volks- und Kulturboden, in: Volk unter Völkern, Bücher des Deutschtums, Herausgeber: Loesch, K. C. v., Hirt, Breslau, Polen, 1, 62–73, 1925.

Penck, A.: Deutschland als geographische Gestalt, in: Leopoldina, Quelle & Meyer, Leipzig, Deutschland, 1, 72–81, 1926.

Penck, A.: Neuere Geographie, in: Sonderband zur Hundertjahrfeier der Gesellschaft für Erdkunde zu Berlin, Herausgeber: Haushofer, A., Selbstverlag der Zeitschrift für Erdkunde, Berlin, Deutschland, 30–56, 1928.

Penck, A.: Das Erwachen des Deutschtums, Velhagen & Klasings Monatshefte, 45/I, 430–433, 512–515, 1930/31.

Penck, A.: Nationale Erdkunde, Zeitschrift der Gesellschaft für Erdkunde zu Berlin, Bd. 1933, 321–335, 1933.

Penck, A.: Nationale Erdkunde als Unterrichtsgegenstand, Die Deutsche Schule, 38, 257–262, 1934a.

Penck, A.: Nationale Erdkunde, Bucholz & Weißwange, Berlin-Charlottenburg, Deutschland, 36 S., 1934b.

Penck, A.: Das deutsche Kolonialproblem, Petermanns Mitteilungen, 82, 261–263, 1936.

Philippson, A.: Ansprache des Vorsitzenden des Zentralausschusses, Verhandlungen des 21. Deutschen Geographentages zu Breslau 1925, 21, 25–30, 1926.

Philippson, A.: Europa außer Deutschland, Bibliographisches Institut, Leipzig, Deutschland, 576 S., 1928.

Ratzel, F.: Deutschland, Grunow, Leipzig, Deutschland, 332 S., 1898.

Ratzel, F.: Politische Geographie oder die Geographie des Staates, des Verkehres und des Krieges, 2. Auflage, Oldenbourg, München and Berlin, Deutschland, 838 S., 1903.

Rudnyćkyj, S.: Ukraina. Land und Volk. Eine gemeinfassliche Landeskunde, Bund zur Befreiung der Ukraina, Wien, Österreich, 416 S., 1916.

Schultz, H.-D.: „Ein wachsendes Volk braucht Raum." Albrecht Penck als politischer Geograph, in: 1810–2010: 200 Jahre Geographie in Berlin, Herausgeber: Nitz, B., Schultz, H.-D. und Schulz, M., 2. Auflage, Selbstverlag Geographisches Institut der Humboldt Universität zu Berlin, Berlin, Deutschland, 99–153, 2011.

Schultz, H.-D.: „Jedes Volk arbeitet nach seiner Art." Der „Volksgeist" im Spiegel der Kulturlandschaft, in: Visuelle Geographien,

Herausgeber: Schlottmann, A. und Miggelbrink, J., trancript, Bielefeld, Deutschland, 175–188, 2015.

Sölch, J.: Albrecht Penck, Mitteilungen der Geographischen Gesellschaft Wien, 89, 88–122, 1946.

Volz, W.: Das deutsche Land, in: Grundriß der Deutschkunde, Herausgeber: Brandt, O. H., Velhagen & Clasing, Bielefeld and Leipzig, 1–18, 1927.

von Roon, A.: Grundzüge der Erd-, Völker- und Staatenkunde 2: Physische Geographie, 2. Auflage, Duncker & Humblot, Berlin, Deutschland, 723 S., 1838.

CONTENTS